AD-A096 637 SRI INTERNATIONAL MENLO PARK CA F/G 16/1
LABORATORY INVESTIGATION OF EXPANSION AND VENTING AND PLUG RESP--ETC(U)
FEB 79 J R BRUCE, J K GRAN DNA001-77-C-0232
UNCLASSIFIED DNA-5235F NL

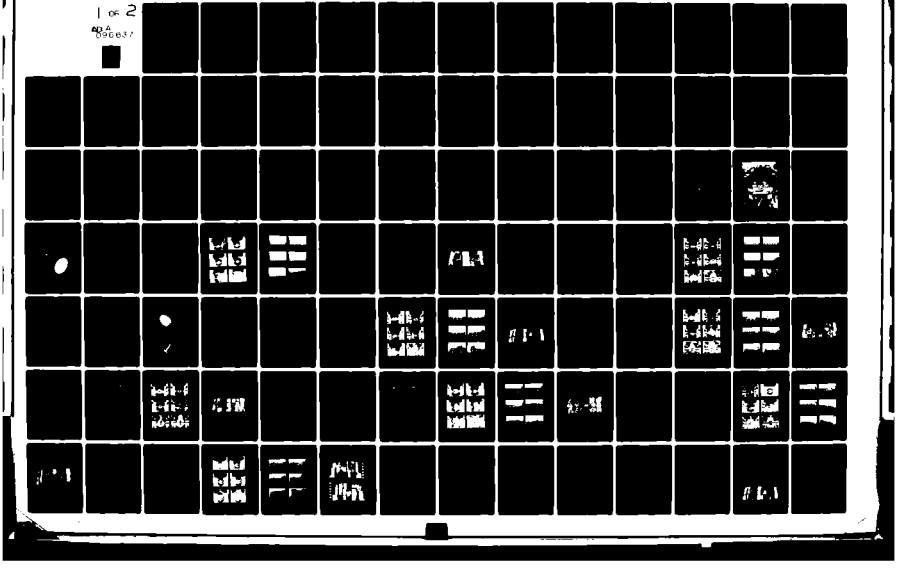

DNA 5235F

LABORATORY INVESTIGATION OF EXPANSION AND VENTING AND PLUG RESPONSE IN THE MX TRENCH

John R. Bruce
James K. Gran
SRI International
333 Ravenswood Avenue
Menlo Park, California 94025

1 February 1979

Final Report for Period 1 March 1977—1 February 1979

CONTRACT No. DNA 001-77-C-0232

THIS WORK SPONSORED BY THE DEFENSE NUCLEAR AGENCY
UNDER RDT&E RMSS CODE B344077462 H35HAXSX35533 H2590D.

Prepared for
Director
DEFENSE NUCLEAR AGENCY
Washington, D. C. 20305

Destroy this report when it is no longer needed. Do not return to sender.

PLEASE NOTIFY THE DEFENSE NUCLEAR AGENCY, ATTN: STTI, WASHINGTON, D.C. 20305, IF YOUR ADDRESS IS INCORRECT, IF YOU WISH TO BE DELETED FROM THE DISTRIBUTION LIST, OR IF THE ADDRESSEE IS NO LONGER EMPLOYED BY YOUR ORGANIZATION.

UNCLASSIFIED

SECURITY CLASSIFICATION OF THIS PAGE (When Data Entered)

REPORT DOCUMENTATION PAGE

READ INSTRUCTIONS BEFORE COMPLETING FORM

1 REPORT NUMBER: DNA 5235F	2 GOVT ACCESSION NO.: AD-A096637
3 RECIPIENT'S CATALOG NUMBER:	
4 TITLE (and Subtitle): LABORATORY INVESTIGATION OF EXPANSION AND VENTING AND PLUG RESPONSE IN THE MX TRENCH	5 TYPE OF REPORT & PERIOD COVERED: Final Report for period 1 Mar 77—1 Feb 79
	6 PERFORMING ORG. REPORT NUMBER: SRI PYU-6307
7 AUTHOR(s): John R. Bruce, James K. Gran	8 CONTRACT OR GRANT NUMBER(s): DNA 001-77-C-0232
9 PERFORMING ORGANIZATION NAME AND ADDRESS: SRI International, 333 Ravenswood Avenue, Menlo Park, California 94025	10 PROGRAM ELEMENT, PROJECT, TASK AREA & WORK UNIT NUMBERS: Subtask B35HAXSX355-33
11 CONTROLLING OFFICE NAME AND ADDRESS: Director, Defense Nuclear Agency, Washington, D.C. 20305	12 REPORT DATE: 1 February 1979
	13 NUMBER OF PAGES: 184
14 MONITORING AGENCY NAME & ADDRESS (if different from Controlling Office)	15 SECURITY CLASS (of this report): UNCLASSIFIED
	15a DECLASSIFICATION DOWNGRADING SCHEDULE

16 DISTRIBUTION STATEMENT (of this Report)

Approved for public release; distribution unlimited.

17 DISTRIBUTION STATEMENT (of the abstract entered in Block 20, if different from Report)

18 SUPPLEMENTARY NOTES

This work sponsored by the Defense Nuclear Agency under RDT&E RMSS Code B344077462 H35HAXSX35533 H2590D.

19 KEY WORDS (Continue on reverse side if necessary and identify by block number)

MX Trench	Structures
Scale Model Experiments	Soil
Fiber-Reinforced Concrete	Dynamic
Shock Tubes	Blast Simulation
Explosively Driven Shock Tubes	

20 ABSTRACT (Continue on reverse side if necessary and identify by block number)

An experimental investigation using small-scale models of the MX trench was conducted to study the effects of internal pressure on the expansion and venting of the trench and on the plug/trench interaction. The 1/26-scale fiber-reinforced concrete trench models were two diameters long for the expansion and venting tests and six diameters long for the plug/trench response tests. The models were buried to scaled depth. In-trench pressures ranging from 400 psi (2.8 MPa) to 3600 psi (24.8 MPa) were generated using an explosively driven shock tube. →

DD FORM 1 JAN 73 1473 EDITION OF 1 NOV 65 IS OBSOLETE

UNCLASSIFIED

SECURITY CLASSIFICATION OF THIS PAGE (When Data Entered)

410 281

20. Abstract (continued)

For the expansion and venting experiments, high-speed movies show that several cracks form in the trench wall almost immediately after the shock wave arrives at the test section. The expansion of the trench is cylindrically symmetrical until the rarefaction wave returns from the free soil surface. The roof then moves off at a greater velocity than the lower portion of the trench. Typically, venting to the atmosphere begins at a roof crack near the crown when the trench roof has moved approximately to the level of the original soil surface. Once venting has begun the trench unzips from one end to the other in about the same time as required for the shock wave reflected from the end of the trench to travel the length of the test section. For the trench and soil properties used, it was found that, for a given pressure, the roof motion depends only on the densities of trench and soil and not on their strengths; however, the expansion of the lower portion of the trench depends on the strength of the soil. Trench strength and trench geometry were found to affect roof cracking and initiation of venting. Also, with higher pressure, venting starts sooner and with less roof displacement.

Three plug/trench interaction experiments were performed. First, a simple 4-inch-long steel plug in a nonribbed trench was tested to provide data on leakage and crack propagation past a stationary plug. In this experiment, the portion of the trench surrounding the plug cracked and expanded, providing an open path for the high pressure gas to the back of the plug. Second, two simple plug models incorporating features of realistic plugs were tested. The realistic plugs are designed as two-section plugs whose first section restricts a portion of the flow ("leaky plug") before the flow impinges on a section that seals the trench ("solid plug"). The simple plug models were designed to study each section separately. It was found that a solid plug can seal the trench at at least 200 psi (1.3 MPa) incident pressure, one-third the design load of 600 psi (4 MPa), and that a leaky plug coupled to a solid plug could be designed to reduce the load on the solid plug so that it can seal the trench.

SUMMARY*

As part of the DNA MX program, SRI International conducted experiments to examine two effects: the expansion and venting response of the MX trench to internal loading, and plug/trench interaction. The specific objectives of the first experiments were to determine the trench expansion dynamics and the time of venting for a range of pressure levels, soil properties, and trench properties and to provide data that could be used to validate existing calculational models for expansion and venting. The specific objectives of the second experiments were to study plug/trench interaction using simple plug models, identifying key areas for further study.

The approach was to perform several 1/26-scale experiments using 6-inch-diameter trench models a few diameters long. The pressure pulses were generated with an explosively driven shock tube by reflecting the shock from a rigid wall at the end of the model trench test section. Loads from the shock tube were calibrated using a rigid steel tube in place of the model trench. The shock tube and model trench assembly was mounted in a soil bin large enough to eliminate soil boundary effects, and soil was packed around the model trench to a scaled depth. A Lucite window, supported by a steel frame, was used for the reflecting wall so that the trench and soil response could be photographed from the end. One high-speed movie camera photographed the end view through the Lucite window and another photographed the soil surface from the side. Pressure gages were mounted in the reflecting wall and in the shock tube run-up section to measure pressure at both ends of the model trench test section. Force, acceleration, and strain were measured in the plug tests.

In-trench pressures ranging from 400 to 3600 psi (2.8 to 24.8 MPa) were obtained. Initial tests were performed with simple clay drain pipe trench models. The main series of expansion and venting tests and the

*A more detailed description of the conclusions is given in Section 5.

plug/trench interaction tests were performed using steel-fiber-reinforced concrete trench models and soil obtained from the HAVE HOST site on Luke Air Force Range, Arizona. The soil was used at representative compactions and moisture contents.

Eleven expansion and venting tests were performed. Along with these tests, some basic analyses were performed to verify the consistency of the data. Individual response features were treated separately; that is, in each analysis certain data were used as input and another part of the response was calculated. The response features analyzed were:

(1) Trench roof displacement calculated from the pressure measured at the reflecting wall.

(2) Trench expansion at the springlines and invert calculated from the pressure measured at the reflecting wall.

(3) Calibration pressure at the reflecting wall calculated from the pressure measured in the run-up section of the shock tube.

(4) Expansion and venting test pressure at the reflecting wall calculated from the corresponding calibration pressure and the expansion data.

The scale model experiments and basic analyses showed the following general features of the expansion and venting response of the MX trench to internal pressure to be independent of loading, geometry, and material properties for the range of variables studied:

(1) Several longitudinal cracks form in a circumferentially symmetric distribution in the trench wall almost immediately after the arrival of the shock wave (Figure 52).

(2) The expansion of the trench into the soil is cylindrically symmetric until the rarefaction wave returns from the free soil surface to the trench roof (Figure 53).

(3) After the symmetric expansion phase, the slug of roof fragments moves off in the vertical direction with little or no change of shape until venting occurs. The soil above the crown mounds up without much lateral flow. The expansion of the trench at the springlines and floor continues to be approximately symmetric (Figure 54).

(4) Venting begins at the roof crack nearest the crown, when the trench roof has moved to about the level of the original soil surface. In cases where the roof did not crack, no venting was observed (Figure 55).

(5) Venting, even at late times, occurs only directly above the roof. The soil mounds up very steeply, forming a large opening for venting, but the surface is not broken anywhere else (Figure 56).

(6) Once venting begins (near the reflecting wall), the soil surface unzips along the length of the trench at about the same rate as the propagation of the reflected shock wave (Figure 57).

The following effects of pressure level, soil properties, and trench strength and geometry were determined for the range of variables studied:

(1) A higher pressure causes venting to occur sooner and with less roof displacement. Also, more trench cracking occurs at higher pressures (Figures 58, Table 5).

(2) Soil strength, which is related to soil compaction, significantly affects the expansion of the trench below the springlines. For a given pressure, the motion of the roof depends primarily on soil density. The moisture content of the soil is not thought to have an effect on venting (Figure 59).

(3) Differences in trench strength and geometry have only a small effect on trench expansion, but a significant effect on trench cracking and initiation of venting.

Three plug/trench interaction tests were performed. The first test, performed with a simple 4-inch-long steel plug in a nonribbed model trench, provided some initial data on leakage and crack propagation past a stationary plug. The results of the test showed that the portion of the trench surrounding the plug cracked in the longitudinal direction and expanded with the rest of the trench, providing an open path for the high pressure gas to the back of the plug and suggesting the importance of longitudinal cracking of the trench wall.

The second and third plug tests examined the concept of a leaky plug that allows blow-by, located upstream of a solid plug that seals the trench. The idea behind this concept is that the leaky plug reflects a portion of the air shock, thereby lowering the load on the solid plug. Our approach was to test a simple leaky plug and a simple solid plug separately. The results of the test of the solid plug showed that a solid plug can seal the trench for a load of 200 psi (1.3 MPa) incident pressure, or one-third the design load. The results of the test with a leaky plug suggested that a leaky plug connected to a solid plug using a load-limiting, energy-absorbing material could be designed to seal the trench at the 600-psi (4-MPa) design load.

PREFACE

The program described in this report was performed for the Defense Nuclear Agency during the period from March 1977 to February 1979 under Contract DNA 001-77-C-0232. The technical monitor was Dr. George Ullrich.

The authors wish to thank LTC James Neal, Capt. Robert Elsberry, Capt. Tim Webster, and Lt. James Shinn of the Air Force Weapons Laboratory for providing details on trench designs and on fiber-reinforced concrete mixes, for their help in obtaining soil from the Luke Air Force Range, and for their overall assistance throughout the program.

The program was supervised by George Abrahamson. Herbert Lindberg provided valuable counsel in formulating the program. Carl Blahnik made the detailed designs for the mechanical hardware. John Busma supervised the hardware fabrication. Terry Henry and Curt Benson performed the setup for the experiments. Terry Henry also fabricated the model trenches and conceived and executed many improvements in the experimental technique. Robert Gates provided guidance in fabricating the model trenches. Hugh Hanna was responsible for making and detonating the explosive charges, and Edward Eckert and William Heckman performed the electronic measurements. The photography was done by Kenneth Stepleton and Henry Rudnicki. Betty Bain and Cheryl Stout reduced the data.

Conversion factors for U.S. customary to metric (SI) units of measurement

To Convert From	To	Multiply By
angstrom	meters (m)	1.000 000 X E -10
atmosphere (normal)	kilo pascal (kPa)	1.013 25 X E +2
bar	kilo pascal (kPa)	1.000 000 X E +2
barn	meter^2 (m^2)	1.000 000 X E -28
British thermal unit (thermochemical)	joule (J)	1.054 350 X E +3
calorie (thermochemical)	joule (J)	4.184 000
cal (thermochemical)/cm^2	mega joule/m^2 (MJ/m^2)	4.184 000 X E -2
curie	*giga becquerel (GBq)	3.700 000 X E +1
degree (angle)	radian (rad)	1.745 329 X E -2
degree Fahrenheit	degree kelvin (K)	$t_K = (t°f + 459.67)/1.8$
electron volt	joule (J)	1.602 19 X E -19
erg	joule (J)	1.000 000 X E -7
erg/second	watt (W)	1.000 000 X E -7
foot	meter (m)	3.048 000 X E -1
foot-pound-force	joule (J)	1.355 818
gallon (U.S. liquid)	meter^3 (m^3)	3.785 412 X E -3
inch	meter (m)	2.540 000 X E -2
jerk	joule (J)	1.000 000 X E +9
joule/kilogram (J/kg) (radiation dose absorbed)	Gray (Gy)	1.000 000
kilotons	terajoules	4.183
kip (1000 lbf)	newton (N)	4.448 222 X E +3
kip/inch^2 (ksi)	kilo pascal (kPa)	6.894 757 X E +3
ktap	newton-second/m^2 (N-s/m^2)	1.000 000 X E +2
micron	meter (m)	1.000 000 X E -6
mil	meter (m)	2.540 000 X E -5
mile (international)	meter (m)	1.609 344 X E +3
ounce	kilogram (kg)	2.834 952 X E -2
pound-force (lbs avoirdupois)	newton (N)	4.448 222
pound-force inch	newton-meter (N-m)	1.129 848 X E -1
pound-force/inch	newton/meter (N/m)	1.751 268 X E +2
pound-force/foot^2	kilo pascal (kPa)	4.788 026 X E -2
pound-force/inch^2 (psi)	kilo pascal (kPa)	6.894 757
pound-mass (lbm avoirdupois)	kilogram (kg)	4.535 924 X E -1
pound-mass-foot^2 (moment of inertia)	kilogram-meter^2 (kg-m^2)	4.214 011 X E -2
pound-mass/foot^3	kilogram/meter^3 (kg/m^3)	1.601 846 X E +1
rad (radiation dose absorbed)	**Gray (Gy)	1.000 000 X E -2
roentgen	coulomb/kilogram (C/kg)	2.579 760 X E -4
shake	*second (s)*	1.000 000 X E -8
slug	kilogram (kg)	1.459 390 X E +1
torr (mm Hg, 0° C)	kilo pascal (kPa)	1.333 22 X E -1

*The becquerel (Bq) is the SI unit of radioactivity; 1 Bq = 1 event/s.
**The Gray (Gy) is the SI unit of absorbed radiation.

TABLE OF CONTENTS

TABLE OF CONTENTS (Cont'd)

LIST OF ILLUSTRATIONS

LIST OF ILLUSTRATIONS (Cont'd)

LIST OF ILLUSTRATIONS (Cont'd)

LIST OF ILLUSTRATIONS (Cont'd)

LIST OF ILLUSTRATIONS (Cont't)

LIST OF TABLES

1. INTRODUCTION

The MX trench concept is a mobile missile launch facility stored in a long buried concrete trench. As part of the DNA MX program, SRI International (formerly Stanford Research Institute) conducted a 1-year experimental study of expansion and venting response and of plug/trench interaction for the MX trench under internal loading. The three main objectives of the program were to

- Determine the trench expansion dynamics and time of venting for an appropriate range of pressure histories, structural properties, and soil properties.
- Provide data to validate existing calculational models for expansion and venting for an appropriate range of pressure histories and soil properties.
- Study the phenomenology of plug/trench interaction using simple plug models.

Our approach was to perform 1/26-scale experiments using 6-inch-diameter trench models. The expansion and venting tests were conducted with trench models two diameters long. The plug/trench interaction tests were conducted with trench models six diameters long. Internal pressure was applied by an explosively driven shock tube. The response was photographed with two high-speed cameras, one viewing the end of the trench through a Lucite window and one viewing the soil surface from the side. Internal pressure was measured at each end of the test section. In addition, for the plug/trench interaction tests, acceleration and force were measured in the plug, pressure was measured on the plug face, and strain was measured in the concrete trench.

Loads from the explosively driven shock tube were calibrated using a rigid steel tube (allowing no expansion or venting) in place of the model trench. The first expansion and venting tests were performed with

simple (nonreinforced) clay drain pipe trench models. Here, the objectives were mainly to test and refine instrumentation, improve hardware, and obtain bounds on trench response. The main series of expansion and venting experiments and the plug/trench interaction experiments were performed using fiber-reinforced concrete trench models and soil obtained from the HAVE HOST site on the Luke Air Force Range (Arizona). This soil was used at a representative compaction and moisture content.

Section 2 of this report describes the load simulation method for the expansion and venting tests, including the shock tube experimental assembly and the load calibration tests. An account of the expansion and venting experiments with clay and fiber-reinforced concrete trench models is presented in Section 3, along with a brief comparison of our small-scale test data with data from the Air Force Weapons Laboratory (AFWL) 1/2-scale HAVE HOST Test T-1. Section 4 presents some basic analyses of trench dynamics and pressure histories and compares the analytical results with the experimental data. Section 5 discusses our conclusions, based on the experimental and analytical results from the expansion and venting tests. Section 6 describes the plug/trench interaction experiments.

Appendix A lists all the tests performed and the pertinent parameters of each. Appendix B lists the displacement data for the crown, invert, and springlines of the trench and of the soil surface for the expansion and venting tests. Appendix C describes the fabrication of the trench models.

2. LOAD SIMULATION METHOD FOR EXPANSION AND VENTING TESTS

An explosively driven shock tube was used to simulate the in-trench pressure history. The experimental assembly used for the load calibration and the expansion and venting experiments was designed under a previous contract (DNA001-76-C-0393). Under the current contract (DNA001-77-C-0232), we fabricated the experimental assembly and designed and built a soil bin for mounting the assembly. The soil bin and assembly were set up at SRI's Corral Hollow Experimental Site (CHES) near Tracy, California.

2.1 EXPERIMENTAL ASSEMBLY

As shown in Figure 1, the shock tube assembly with a rigid test section that allowed no expansion or venting was used for load calibration tests. Pressure pulses in the 400 to 2600 psi range were generated by reflecting the shock from the rigid wall at the end of the test section. The shock tube was designed so that reflected rarefaction waves from the end of the explosive driver would not reach the test section during the time of interest. Reference 1 describes the theroy of explosively driven shock tubes used to estimate the magnitude and duration of the pressure produced in the test section.

The assembly shown in Figure 1 centered around a 12-foot-long steel tube (6 inches ID, 9 inches OD) used previously by SRI as an explosively driven shock tube. A 30-inch-long steel tube with the same diameter (6 inches ID, 9 inches OD) was used as a run-up section. A 12-inch-long steel test section was located between the run-up section and the rigid end wall. A gasket was fitted between the 12-foot steel tube and the 30-inch-long run-up section to isolate the pressure gages from the tube ringing induced by the explosive. The entire experimental assembly was anchored in a 16-foot-long soil bin, 3 feet high by 4 feet wide.

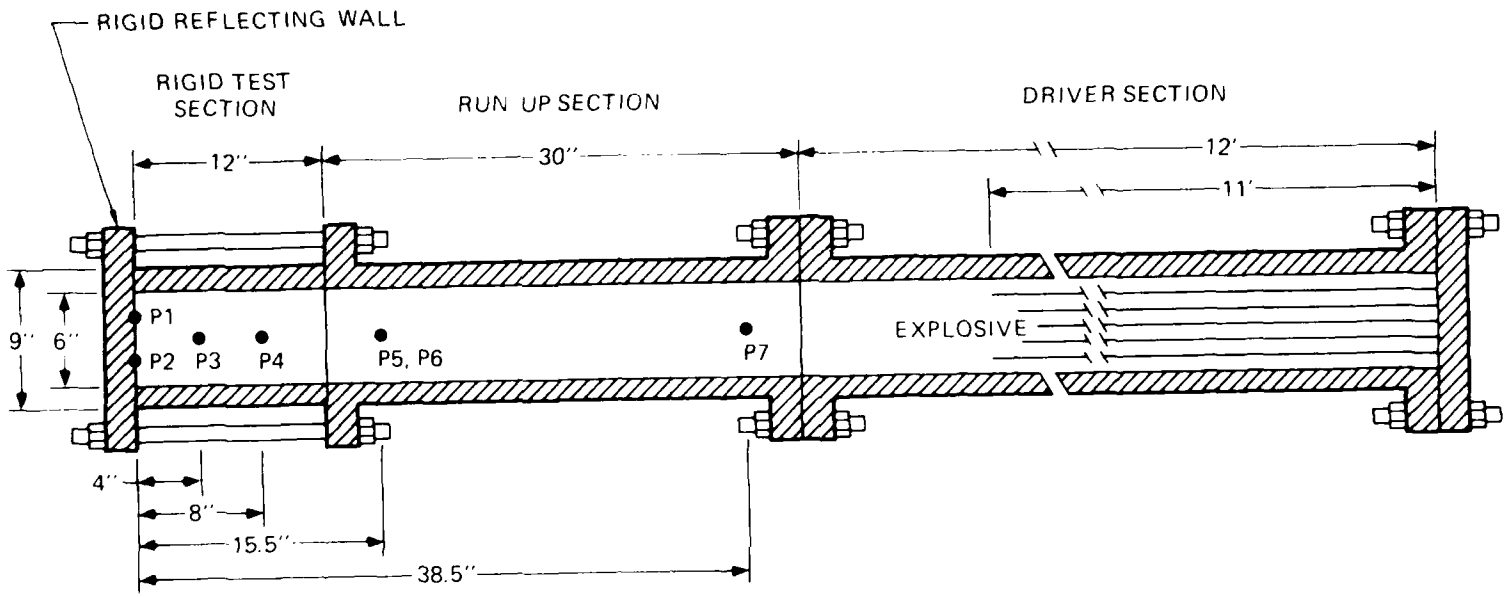

MA 6307 39

FIGURE 1 SHOCK TUBE ASSEMBLY FOR EXPANSION AND VENTING CALIBRATION TESTS

The 12-foot-long tube was loaded from the end away from the test section with strands of Primacord,* a convenient and inexpensive form of PETN explosive. On detonation, an air shock is generated in the tube. This air shock propagates through the run-up and test sections. When it reflects from the rigid wall at the end of the test section, the reflected pressure increases 6 to 8 times the initial shock pressure.

Dynamic pressure was measured at the reflecting wall, in the test section, and in the run-up section using PCB quartz pressure transducers (Model 113A03). The gages were located as shown in Figure 1 and listed in Table 1. The pressures registered by the gages were recorded on oscilloscopes and on magnetic tape.

2.2 LOAD CALIBRATION TESTS

A square shock wave and a load duration that would be long with respect to the response time for the model trench were desired. We tested various Primacord distributions and lengths to determine a suitable configuration. Many smaller strands of Primacord, uniformly distributed in the driver section, gave a better pressure pulse than a centered group of strands. We ultimately chose as standard for all tests a configuration using eight strands of Primacord, one strand down the center of the tube and seven spaced evenly around a 4-inch-diameter circle. The Primacord strands were held in place with cardboard spacers and a central steel rod and were detonated simultaneously from the end away from the test section. A Primacord length of 11 feet was found to provide adequate load duration.

Figures 2 through 6 show the pressure records from five load calibration tests (Tests 12, 13, 14, 23, and 26). Time t = 0 is defined by the initiation of detonation of the explosive. The tape recorded signals were electronically digitized to make these plots and the plots for the expansion and venting tests (Section 3). A standard format was used in

*Produced by the Ensign-Bickford Co., Simsberg, Connecticut.

Table 1

PRESSURE GAGE LOCATIONS

Pressure Gage	Location
P1	At reflecting wall, 1.25 inches above tube centerline
P2	At reflecting wall, 1.25 inches below tube centerline
P3*	In test section, 4 inches from reflecting wall
P4*	In test section, 8 inches from reflecting wall
P5	In run-up section, 15.5 inches from reflecting wall
P6	In run-up section, 15.5 inches from reflecting wall, and 180° from P5
P7†	In run-up section 38.5 inches from reflecting wall

*Used for load calibration test only

†Used for Tests 15, 17, 18, 19, 20, 21, 22, and 23 only

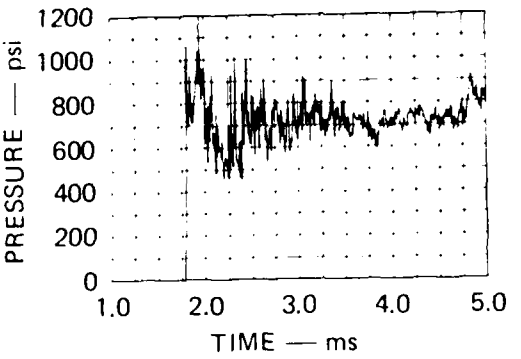

(a) P1 (AT REFLECTING WALL)

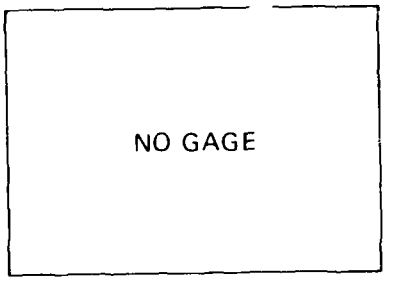

(b) P2 (AT REFLECTING WALL)

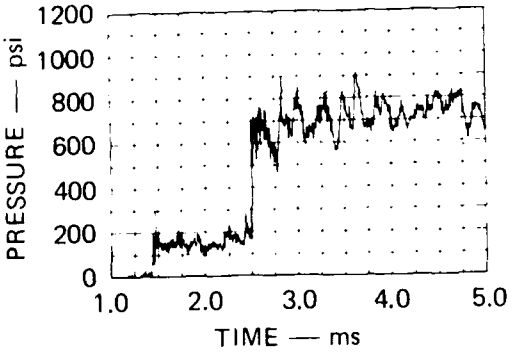

(c) P5 (15.5 in. FROM REFLECTING WALL)

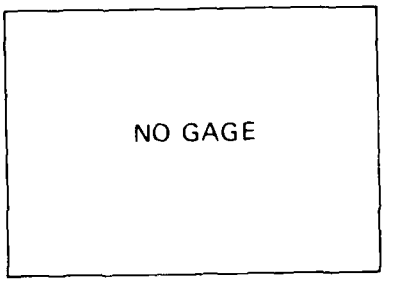

(d) P6 (15.5 in. FROM REFLECTING WALL)

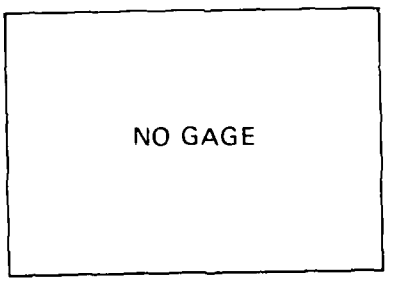

(e) P7 (38.5 in. FROM REFLECTING WALL)

MA-6307-18

FIGURE 2 PRESSURE RECORDS FROM LOAD CALIBRATION TEST 12
Explosive charge 400 gr/ft

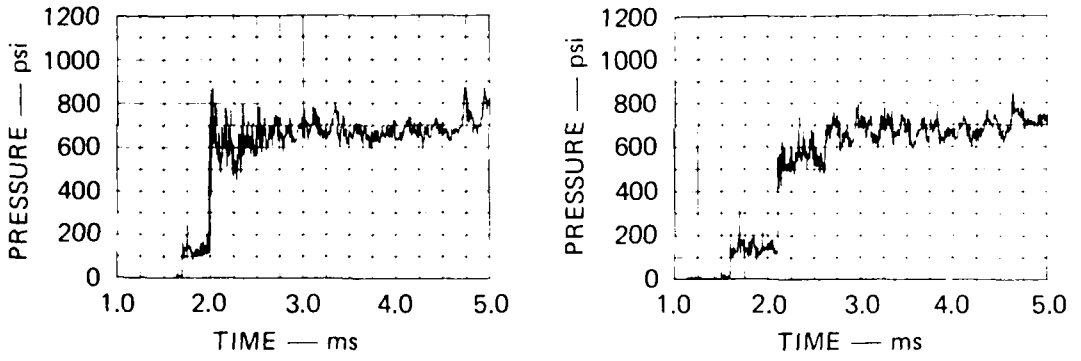

(a) P3 (4 in. FROM REFLECTING WALL) (b) P4 (8 in. FROM REFLECTING WALL)

MA-6307-19

FIGURE 2 PRESSURE RECORDS FROM LOAD CALIBRATION TEST 12 (Concluded)

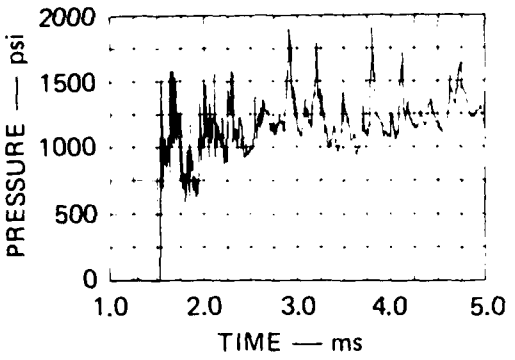

(a) P1 (AT REFLECTING WALL)

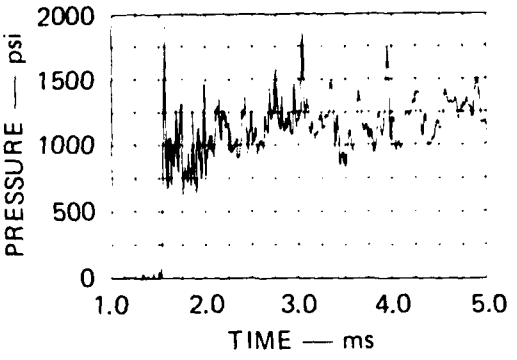

(b) P2 (AT REFLECTING WALL)

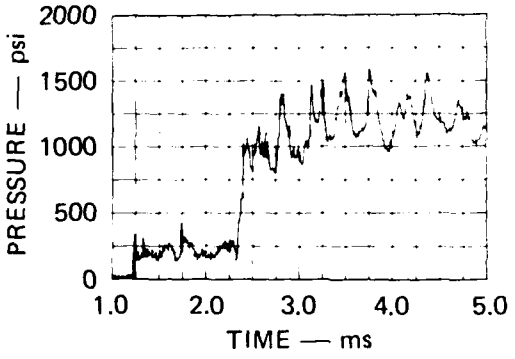

(c) P5 (15.5 in. FROM REFLECTING WALL)

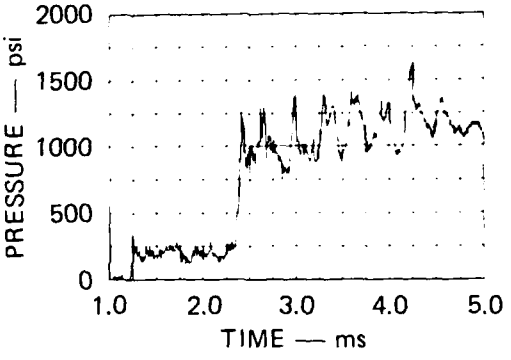

(d) P6 (15.5 in. FROM REFLECTING WALL)

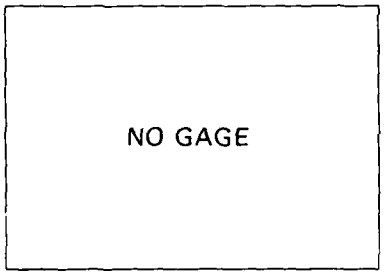

(e) P7 (38.5 in. FROM REFLECTING WALL)

MA-6307-20

FIGURE 3 PRESSURE RECORDS FROM LOAD CALIBRATION TEST 13
Explosive charge 800 gr/ft

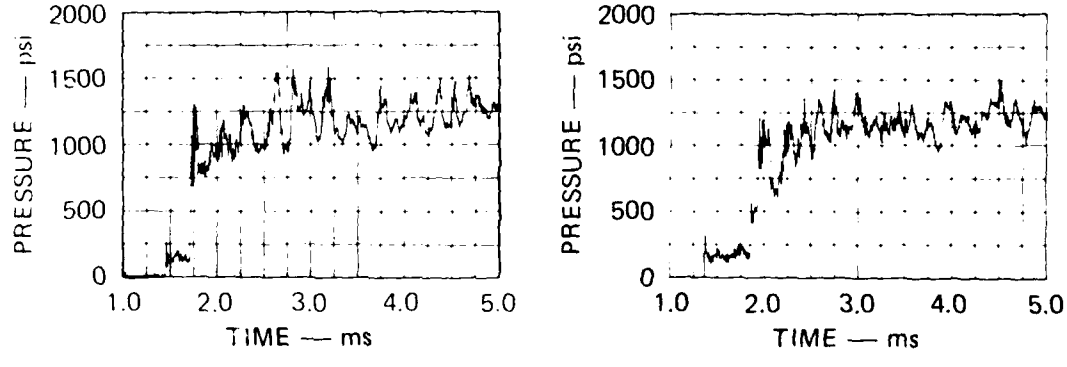

FIGURE 3 PRESSURE RECORDS FROM LOAD CALIBRATION TEST 13 (Concluded)

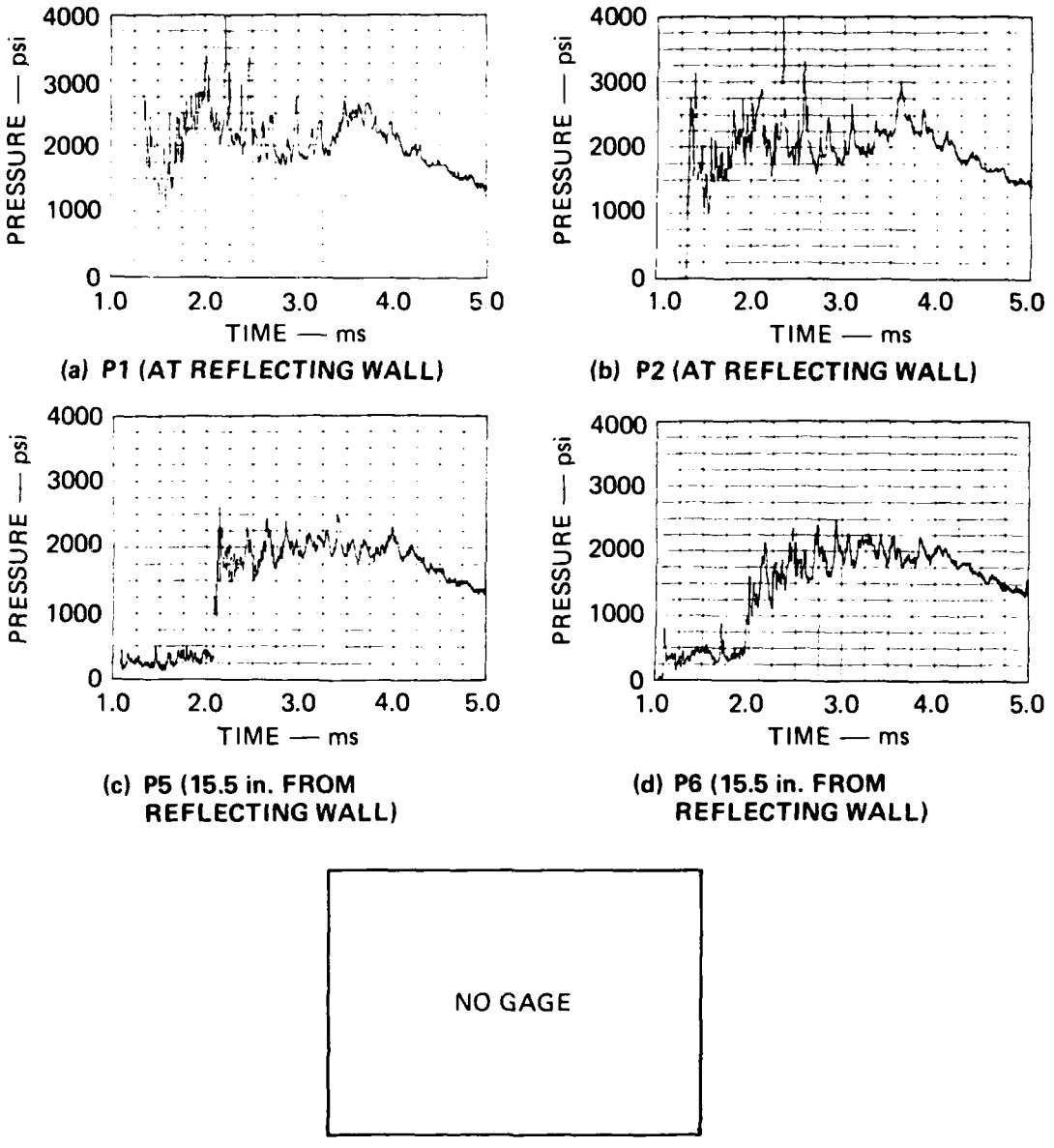

FIGURE 4 PRESSURE RECORDS FROM LOAD CALIBRATION TEST 14

Explosive charge 1200 gr/ft

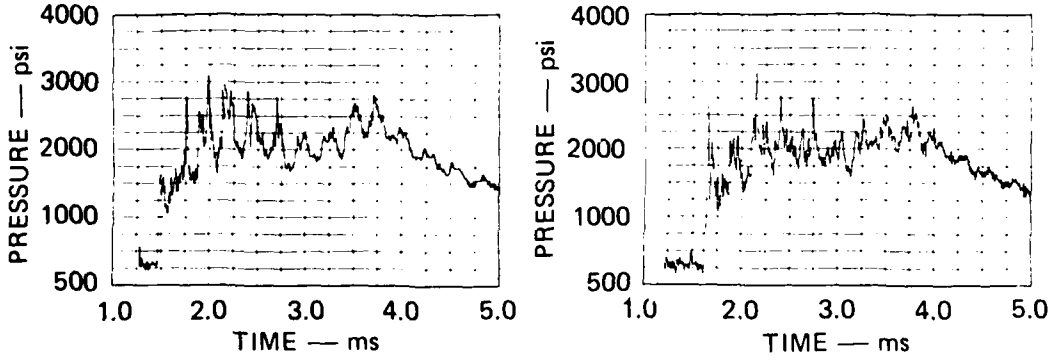

FIGURE 4 PRESSURE RECORDS FROM LOAD CALIBRATION TEST 14 (Concluded)

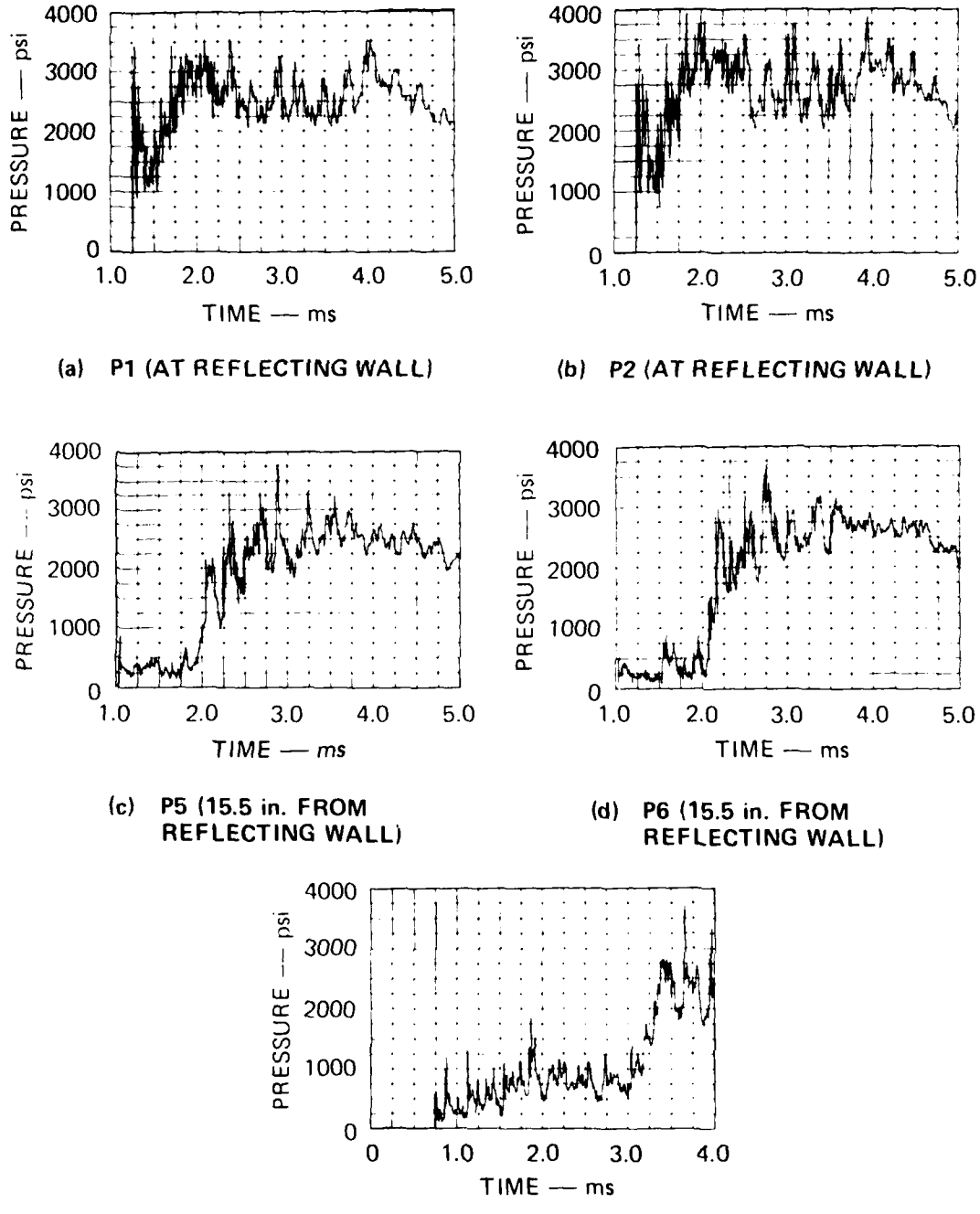

FIGURE 5 PRESSURE RECORDS FROM LOAD CALIBRATION TEST 23

Explosive charge 1600 gr/ft

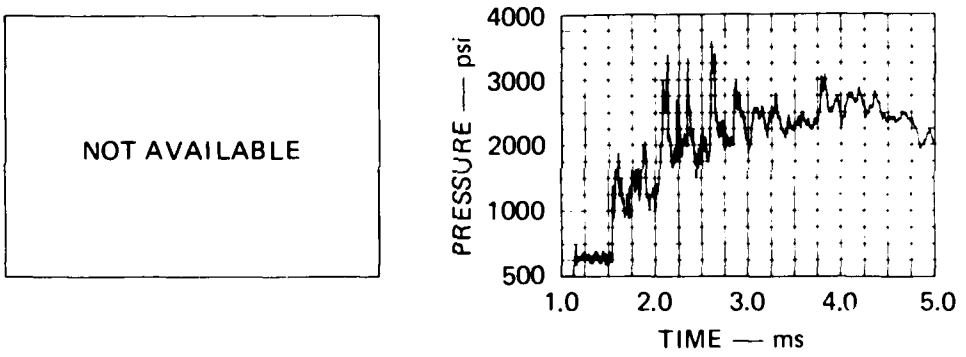

(a) P3 (4 in. FROM REFLECTING WALL) (b) P4 (8 in. FROM REFLECTING WALL)

MA-6307-23

FIGURE 5 PRESSURE RECORDS FROM LOAD CALIBRATION TEST 23 (Concluded)

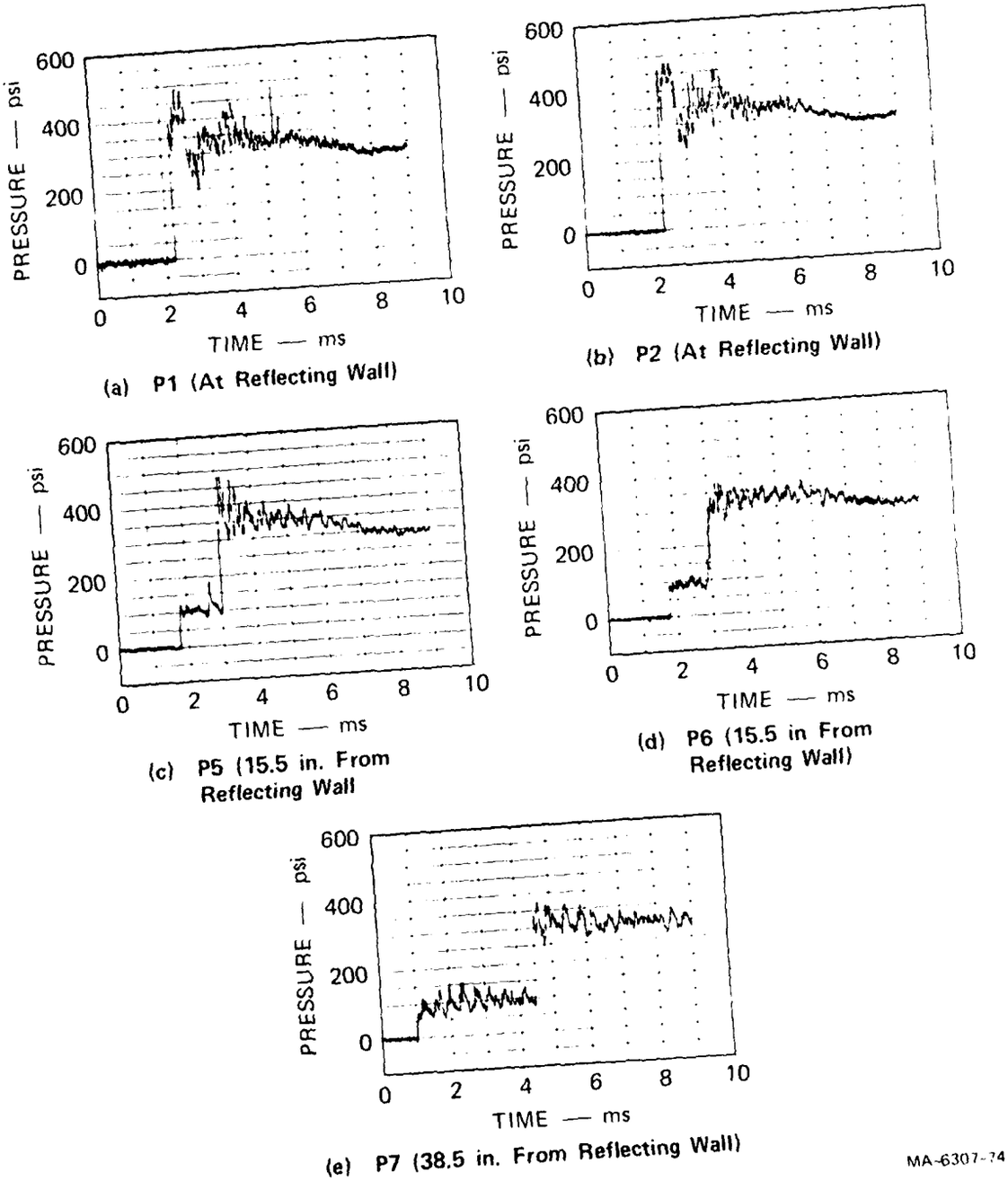

FIGURE 6 PRESSURE RECORDS FROM LOAD CALIBRATION TEST 26

Explosive charge 200 gr/ft

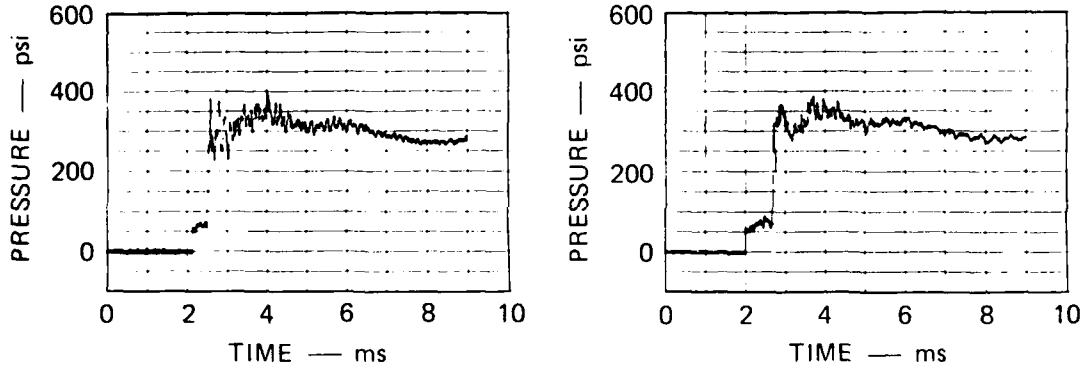

(f) P3 (4 in. From Reflecting Wall)

(g) P4 (8 in. From Reflecting Wall)

MA-6307-75

FIGURE 6 PRESSURE RECORDS FROM LOAD CALIBRATION TEST 26 (Concluded)

the figures. In cases where a particular gage was not used in a test, the blank space is marked "no gage." In cases where the digitized records were not available due to electronic difficulties, the blank space is marked "not available." In most of these cases, oscilloscope records are available, but were not included in this report.

In Test 12 we used eight strands of 50 grain-per-foot (gr/ft) Primacord in the driver, giving a nominal reflected pressure of 700 psi. In Test 13, we used eight strands of 100 gr/ft, giving a nominal reflected pressure of 1100 psi. In Test 14, we used eight strands of 150 gr/ft, giving a nominal reflected pressure of 2100 psi. In Test 23, we used sixteen strands of 100 gr/ft, giving a nominal reflected pressure of 2600 psi. The sixteen strands were arranged in pairs, in a configuration similar to the eight singles, with two pairs down the center of the tube and seven pairs spaced evenly around a 4-inch-diameter circle. Although we might have obtained a cleaner pressure pulse by further refining the Primacord arrangement, we decided that at this stage more could be gained by proceeding with the expansion and venting experiments.

The Primacord loading densities given in this report are nominal values. The Primacord manufacturer indicated that nominal and actual loading densities could vary up to 10%. Careful laboratory measurements were performed on the Primacord used to determine the actual loading densities of PETN and of the plastic cover. Table 2 gives the results of these measurements.

Table 2

ACTUAL PRIMACORD LOADING DENSITIES

Nominal Loading Density (gr/ft)	Loading Density of PETN (gr/ft)	Loading Density of Cover (gr/ft)
50	47	45
100	92	61
150	136	66

1 grain (gr) = 0.0648 gram

3. EXPANSION AND VENTING EXPERIMENTS

Several small-scale experiments were performed to determine the trench expansion dynamics and the time of venting for an appropriate range of pressure histories, structural properties, and soil properties.

3.1 EXPERIMENTAL ASSEMBLY

The sketch in Figure 7 shows the expansion and venting experimental assembly. The 12-foot-long explosively driven shock tube and the 30-inch-long run-up section are the same as used for the load calibration tests. For the expansion and venting tests, we used a 12-inch-long, 6-inch-ID model trench as the test section. The assembly was placed in a soil bin that provided two feet of soil to each side and below the model trench to eliminate soil boundary effects. For the reflecting wall, we used a 2-inch-thick Lucite view window, supported by a steel frame, so that we could photograph the response of the trench from the end.

Pressure gages P1, P2, P5, P6, and P7, were installed in the reflecting wall and in the run-up section. The pressure gage locations are the same as indicated in Figure 1 and Table 1 (Section 2.1). Pressure gages P3 and P4, in the test section, were not used for the expansion and venting tests. The pressure readings were recorded on oscilloscopes and magnetic tape.

The response was photographed with two high-speed (Hycam) cameras. One viewed the end of the trench through the Lucite window, the other viewed the soil surface from the side. A photograph of the setup is shown in Figure 8.

The soil was packed around the trench model manually, and samples were taken to measure the soil density and moisture content. A thin layer of dolomite, usually about 1/4-inch-thick, was spread over the soil to provide a white surface for the high-speed photography. The soil

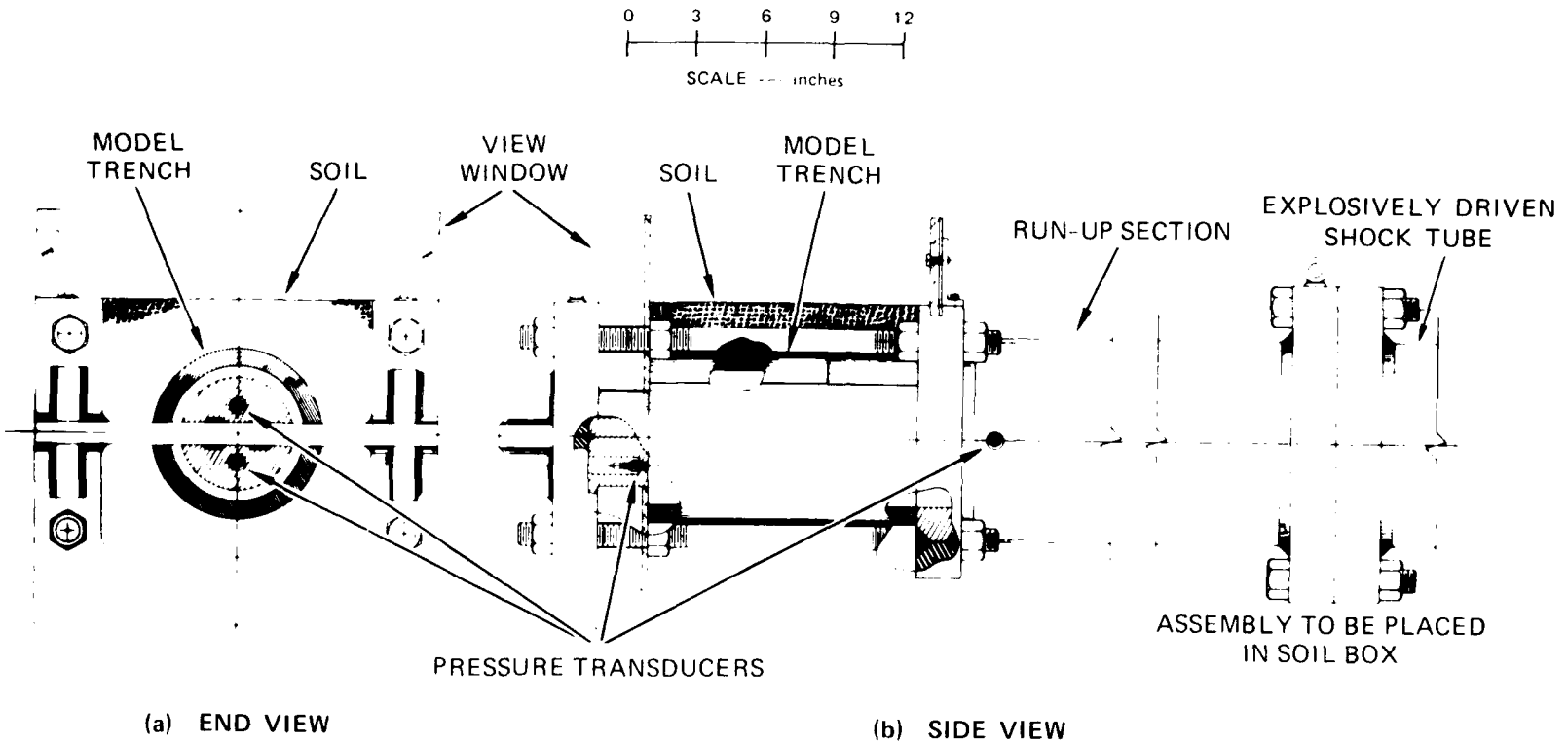

FIGURE 7 MX TRENCH EXPANSION AND VENTING EXPERIMENT ASSEMBLY

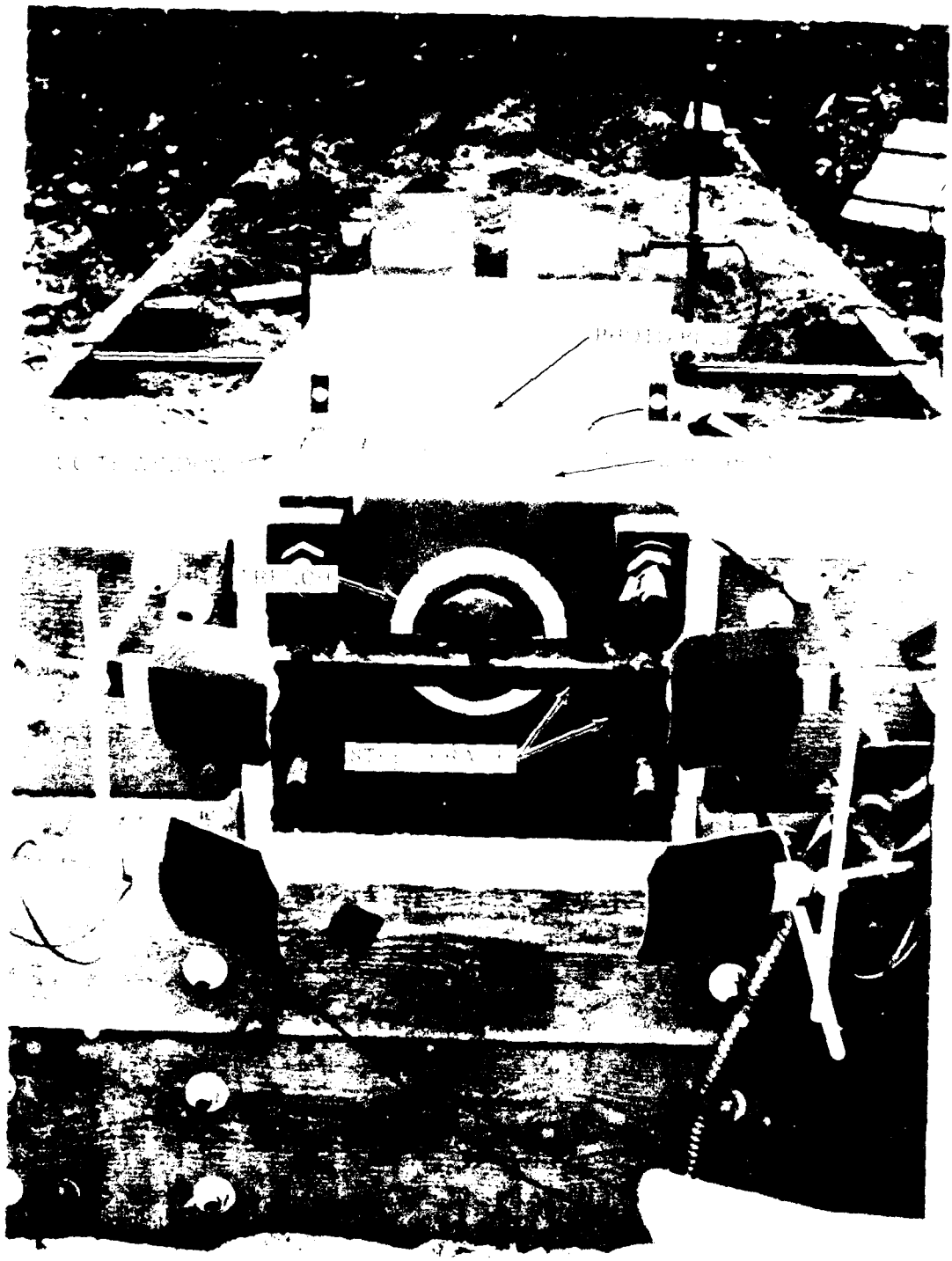

FIGURE 8 EXPERIMENTAL SETUP

surface was marked with a grid consisting of 1/4-inch-wide black lines, 3 inches center to center, running parallel and perpendicular to the trench axis. These grid lines provide contours for determining surface motion.

In most of the tests, we used six photo pins to determine the roof displacement at the crown. These pins were located 1, 3, 5, 7, 9, and 11 inches back from the reflecting wall. When three photo pins were used, they were located 3, 6, and 9 inches back from the reflecting wall (Test 30). The pins rested on the trench roof and protruded through the soil surface. Each pin was striped with a 3/4-inch white and 1/4-inch black pattern. At the top of each pin, a nut from a large bolt was supported by a thin tape that covered the hole in the nut and rested on the point of the pin. As each pin accelerated upward it punctured the tape, and the nut then went into free fall, providing a "fixed" reference point during the few milliseconds of test time.

3.2 PRELIMINARY TESTS WITH CLAY TRENCH MODELS

Five expansion and venting tests were performed using clay trench models (Appendix A) summarizes the tests). The primary objectives of these tests were to refine the instrumentation, improve the hardware, and obtain approximate bounds on trench response. Data from three of these tests (Tests 11, 15, and 16) are included in this section. The expansion data are tabulated in Appendix B.

Figure 9 shows a 12-inch-long clay drain pipe that was used as a model for the trench. The clay trench model had a 6-inch ID and a 1-inch wall thickness. Two longitudinal 0.9-inch-deep saw cuts offset 90 degrees from each other and two transverse 0.9-inch-deep saw cuts at the third points were used to separate the roof blocks. The clay had a density of 120 lb/ft^3.

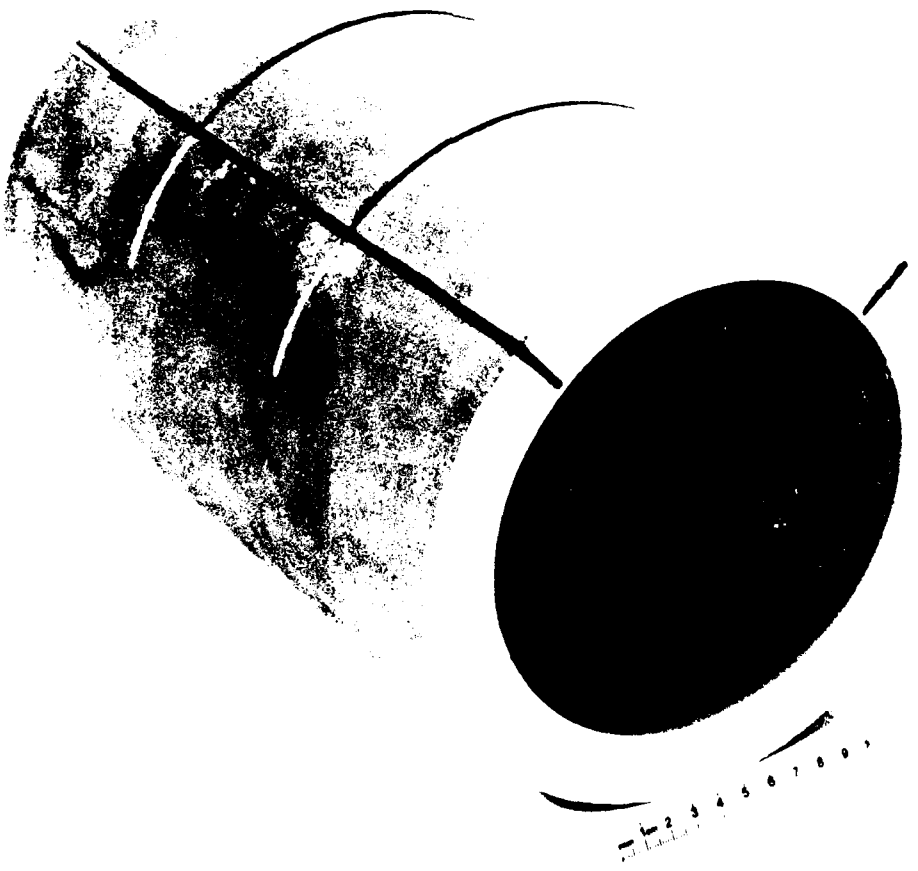

FIGURE 9 CLAY TRENCH MODEL

Test 11

Test 11 was conducted at a nominal reflected pressure of 700 psi. Dry Monterey sand was packed around the trench model to a cover depth of 2.0 inches. Another 0.5 inch of dolomite was added, giving a total cover depth of 2.5 inches. The density of the Monterey sand was 99 lb/ft^3; the density of the dolomite was 100 lb/ft^3.

The digitized pressure records for Test 11 are plotted in Figure 10. Time t = 0 is the time when detonation begins. The corresponding load calibration pressure records from Test 12 were shown in Figure 2. A comparison of the records from pressure gage P1 at the reflecting wall for Tests 11 and 12 shows that the pressures are the same for the first 0.40 ms after shock arrival. For Test 11 there is a gradual decay in the pressure at the wall after the first 0.40 ms (compared with the load calibration test) resulting from expansion of the clay trench.

Figures 11 and 12 show representative frames from the Hycam films for Test 11. In the end view, the film speed was 9,990 frames per second. In the side view, the film speed was 9,610 frames per second. Eleven 1000-watt PAR64 quartz-iodide sealed-beam lights were used to supply illumination. In the end view, the light layer at the soil surface is the dolomite. In the side view, the reflecting wall is on the right.

The shock arrived at the reflecting wall at t = 1.80 ms. The first cracks in the model trench are seen at t = 2.10 ms(Figure 11). In addition to the two saw cuts that separate the roof, four cracks in the model trench can be seen in the end view. No trench-to-surface venting was observed, even when the trench roof had lifted above the original ground surface.

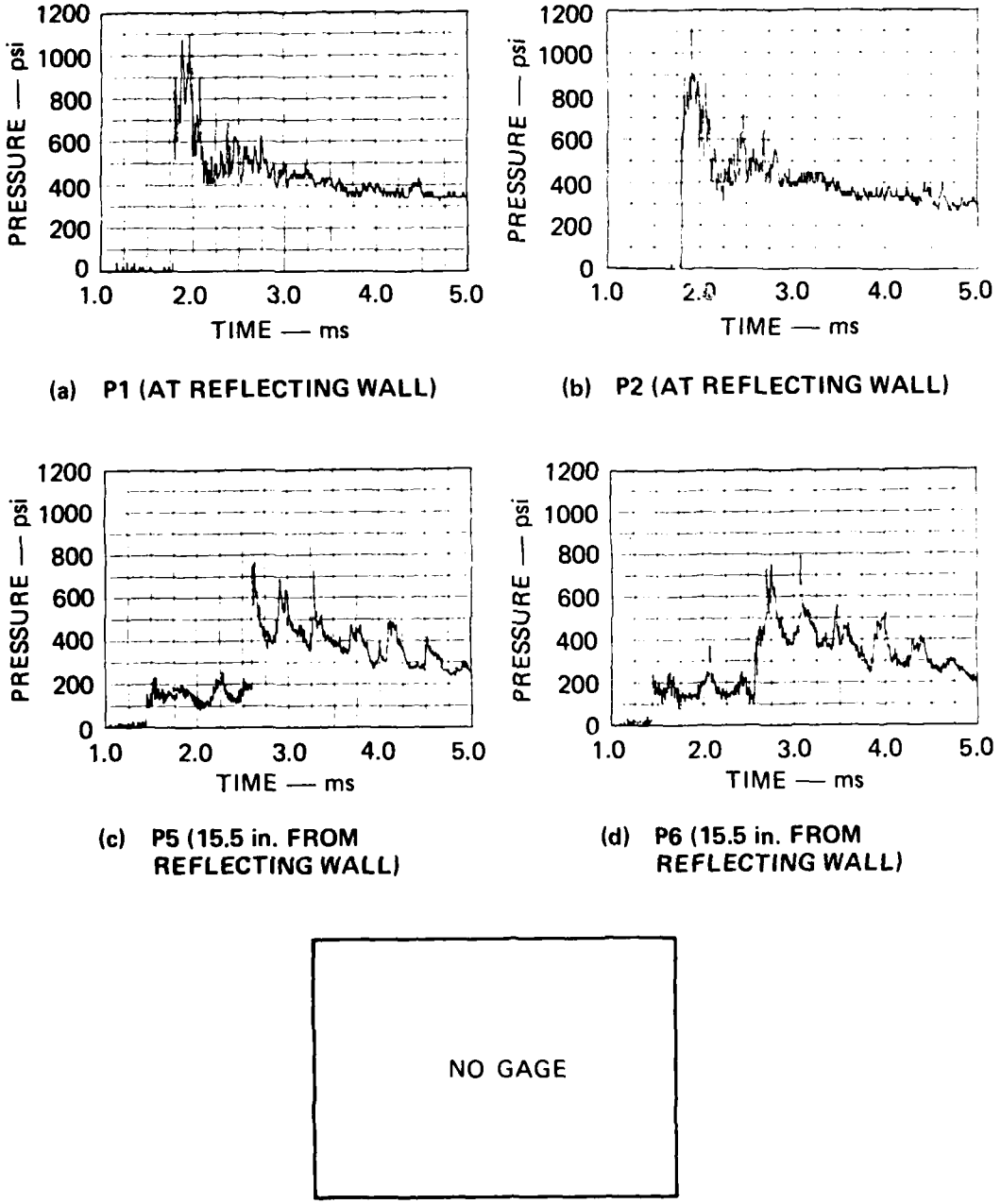

FIGURE 10 PRESSURE RECORDS FROM EXPANSION AND VENTING TEST 11
Explosive charge 400 gr/ft

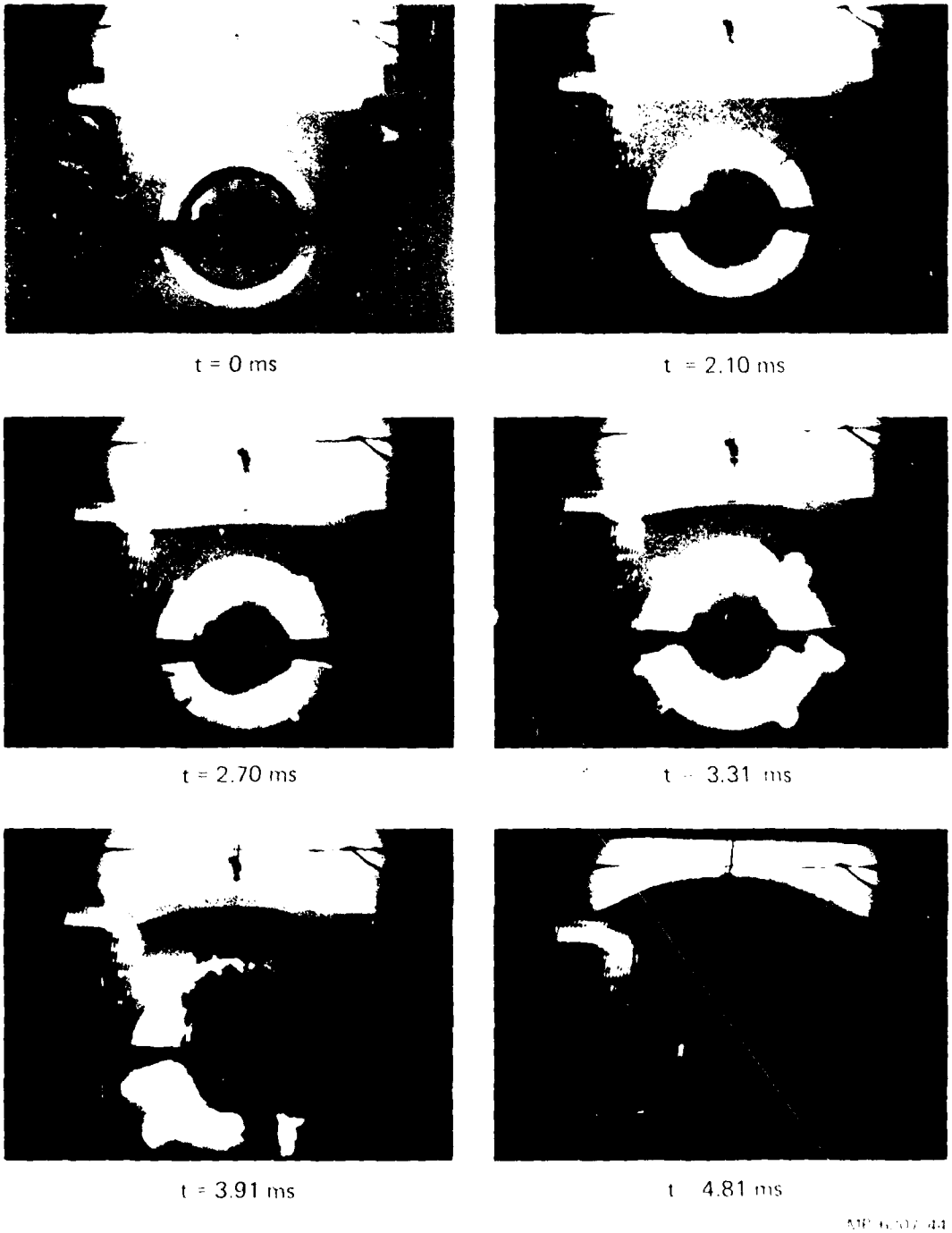

FIGURE 11 HYCAM PICTURES (End Views, Test 11)

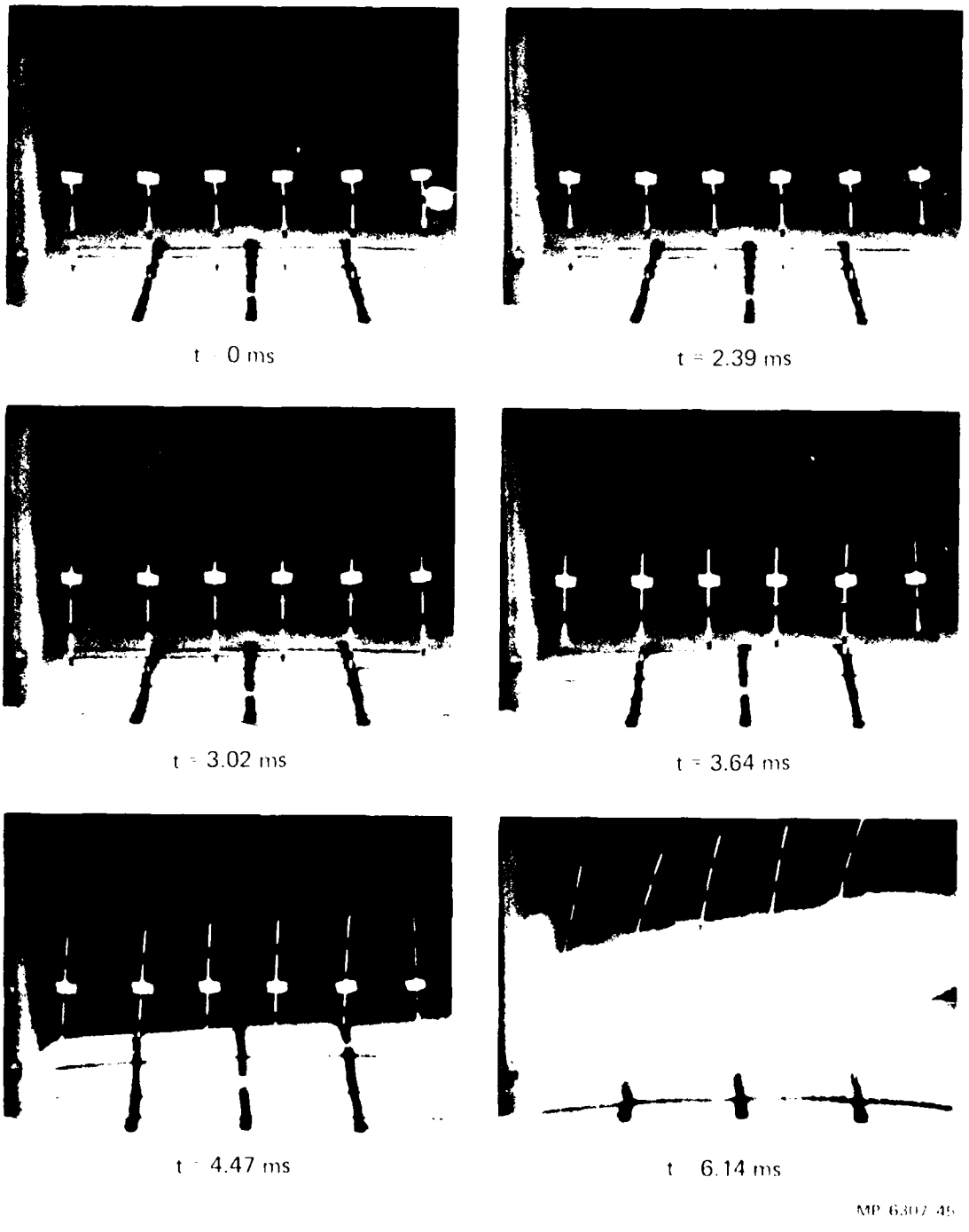

FIGURE 12 HYCAM PICTURES (Side View, Test 11)

Test 15

Test 15 was also conducted for a nominal reflected pressure of 700 psi. Soil from the HAVE HOST site waw used instead of the Monterey sand used for Test 11. The soil was compacted to a measured density of 118 lb/ft^3, at a moisture content of 3.9%. Again, the trench was covered with 2.5 inches of soil.

The digitized pressure records are plotted in Figure 13. Test 12 is the corresponding load calibration test (Figure 2).

The flashbulbs did not trigger during this test, but the high temperature of the in-trench gases provided enough light to yield some expansion data. The trench roof sections did not crack, and only three longitudinal cracks formed in the lower portion of the trench. No venting was observed.

Figure 14 shows the recovered trench fragments from Test 15. In this test, as in Test 11, the trench roof failed only along the precut saw lines. The roof sections were found within a 100-foot radius of the test setup. The lower portion of the trench fractured into about a dozen major pieces and a few smaller fragments.

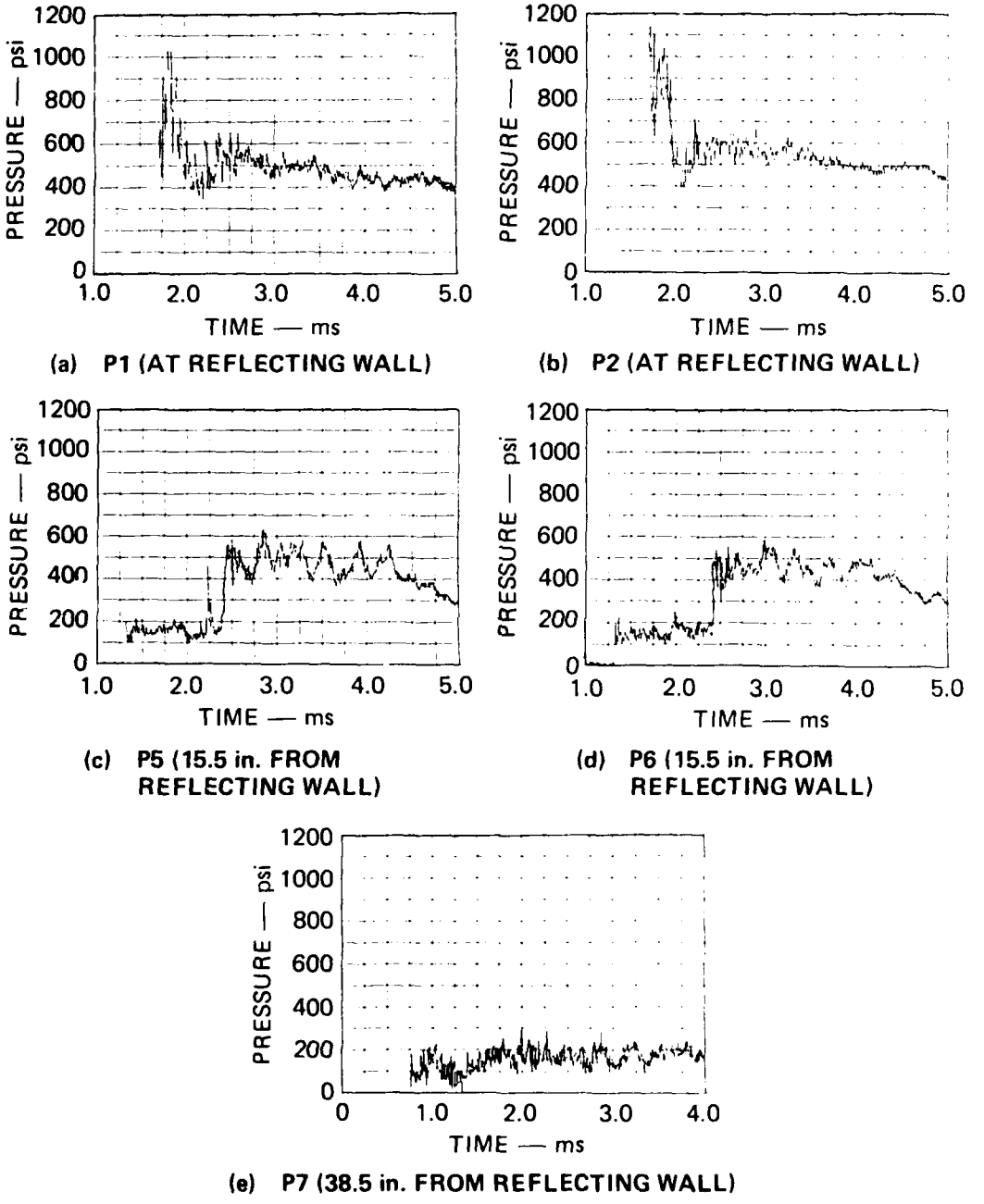

FIGURE 13 PRESSURE RECORDS FROM EXPANSION AND VENTING TEST 15

Explosive charge 400 gr/ft

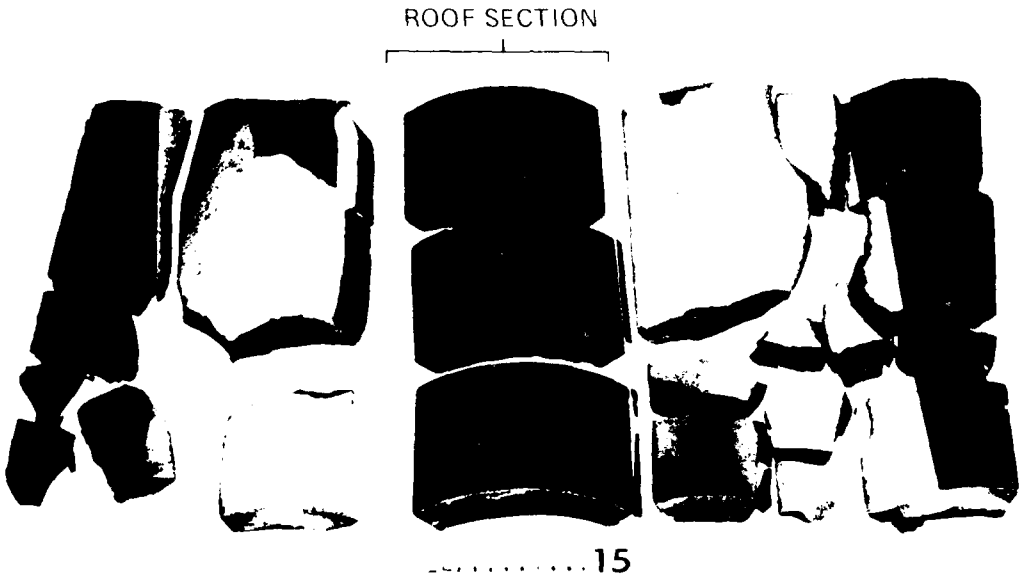

MP 6307-47

FIGURE 14 TRENCH FRAGMENTS RECOVERED FROM TEST 15

Front of trench is at bottom.

Test 16

Test 16 was conducted for a nominal reflected pressure of 2100 psi. Soil from the HAVE HOST site was used with a cover depth of 2.5 inches. It was compacted to a measured density of 118 lb/ft^3, at a moisture content of 3.9 .

The digitized pressure records are plotted in Figure 15. Test 14 is the corresponding load calibration test (Figure 4). A comparison of pressure records at the reflecting wall (P1 and P2) for Tests 16 and 14 shows the pressures to be the same for the first 0.3 ms after shock arrival. For Test 16, the pressure decayed gradually at the wall after the first 0.3 ms (compared with the load calibration test) as a result of the expansion and venting of the model trench.

Figures 16 and 17 show representative frames from the Hycam films for Test 16. In the end view, the film speed was 10,870 frames per second. In the side view, the film speed was 10,380 frames per second. No. 3 flashbulbs were used. As in Test 11, the soil surface was marked with a 3-inch square grid.

The shock arrived at the reflecting wall at t = 1.40 ms. The first cracks in the model trench appeared at t = 1.56 ms (Figure 16). In addition to the two saw cuts that separate the roof, ten cracks in the model trench can be seen in the end view. The trench roof cracked at the crown, and trench-to-surface venting began through this crack at the roof crown at t = 2.41 ms (Figure 17). At this time, the roof had lifted 1.2 inches above its original position.

Six photo pins show the roof position in the side view. The first indication of venting appeared at the pin closest to the reflecting wall (Figure 17). The pin probably provided a path of least resistance for the gases. By t = 2.89 ms, venting appeared over a large area (Figure 17). We conclude that the pin, at most, only speeded up the venting process. Later test results shown below verify this conclusion.

Another important result in Test 16 was the measurement of the speed of the pressure wave in the soil. The cylindrical wave front is clearly distinguishable in the first two frames of Figure 16. In the complete film, a sequence of five frames shows that the wave front moved at a constant speed from the roof to the soil surface. The speed calculated from the movie data is 465 ft/s ±5 ft/s.

The fractured trench showed that the trench roof not only failed along the precut saw lines, but each roof section cracked into many small pieces. Four small sections of roof constituting less than one-third of the total roof were found within a 300-foot radius of the test setup. The remainder of the roof was not found. We estimate that the trench fractured into approximately thirty small pieces.

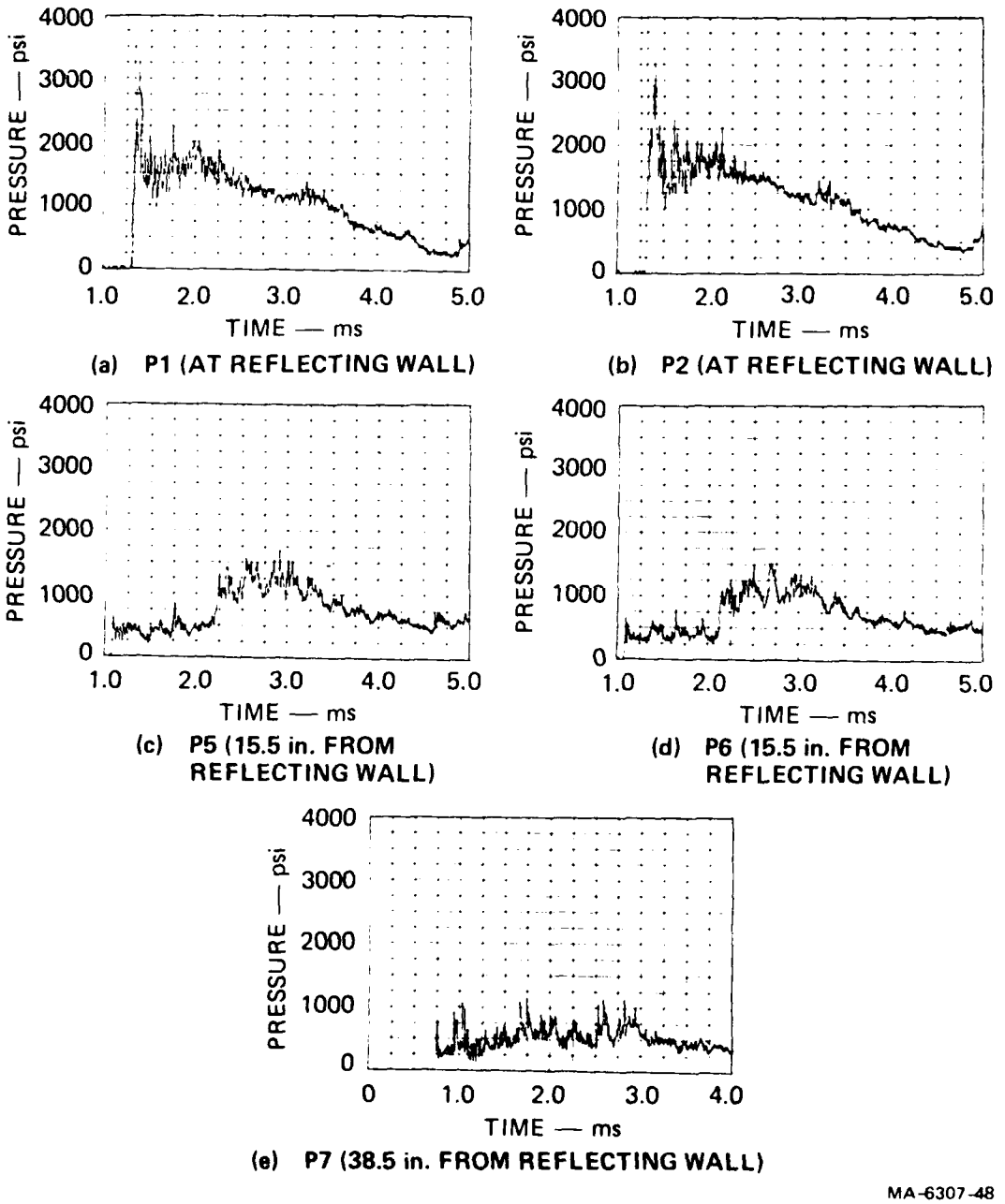

FIGURE 15 PRESSURE RECORDS FROM EXPANSION AND VENTING TEST 16
Explosive charge 1200 gr/ft.

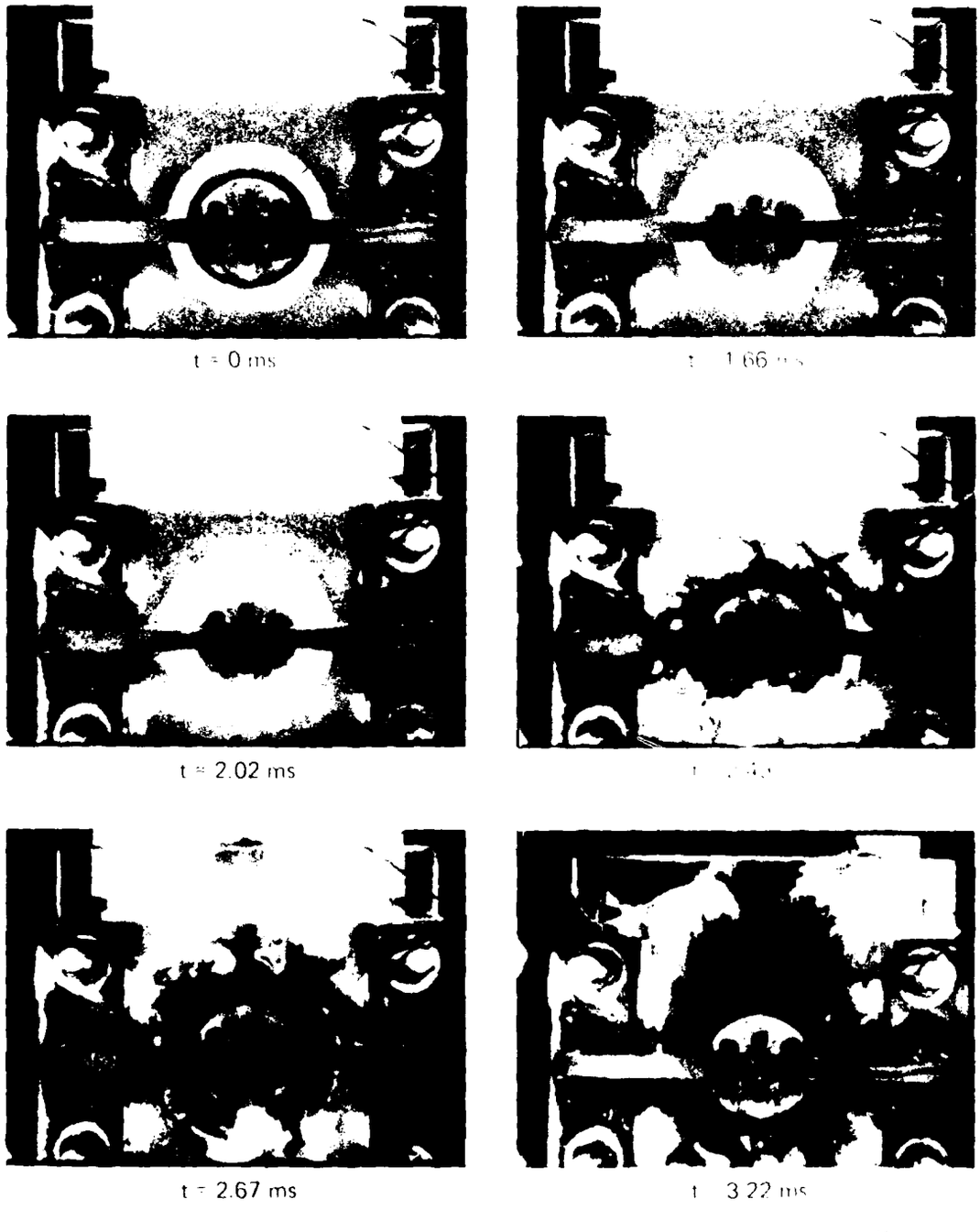

FIGURE 16 HYCAM PICTURES (End View, Test 16)

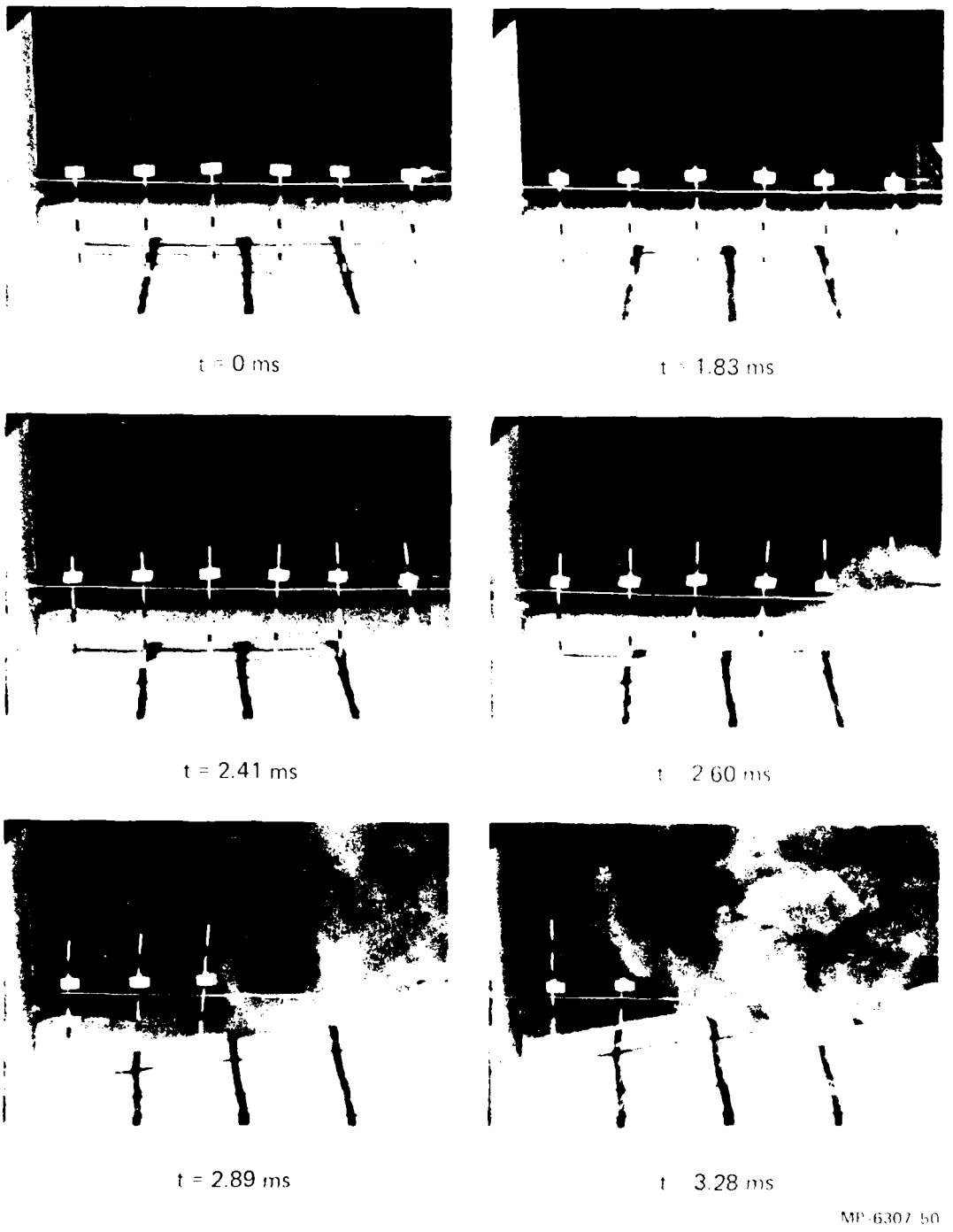

FIGURE 17 HYCAM PICTURES (Side View, Test 16)

3.3 TESTS WITH FIBER-REINFORCED TRENCH MODELS

Six expansion and venting tests were performed with fiber-reinforced concrete trench models to study the expansion dynamics and venting phenomena for a range of pressure histories with typical soil and concrete properties. The concrete trench models, discussed below, were fabricated at SRI. Soil from the HAVE HOST test site was used in all the tests. The expansion data are tabulated in Appendix B.

Fiber-Reinforced Concrete Trench Models

The Air Force Weapons Laboratory (AFWL) provided drawings of the current half-scale AFWL models, from which dimensions for the 6-inch-ID model trench were determined. Tests 17, 18, 19, 20, and 22 were performed using 6-inch-ID, 12-inch-long trench models fabricated without internal ribs and having a wall thickness of 0.75 inch (scaled from the AFWL models by smearing out the ribs). For these trench models two longitudinal 0.56-inch-deep saw cuts offset 110 degrees from each other and two transverse 0.56-inch-deep saw cuts at the third points were used to separate the roof blocks. A typical trench model is shown in Figure 18.

A single test (Test 30) was performed on a 6-inch-diameter 12-inch-long, thin-walled ribbed trench. The thin wall (10-inch wall, full-scale) is an alternative design from the baseline MX trench design (17-inch wall, full-scale). The rib dimensions were scaled from the full-size MX trench design. The trench wall thickness was 0.375 inch and the rib height was 0.25 inch. The rib spacing was 2.31 inch, the rib width was 0.77 at the inner radius, and the rib face had an 18-degree cant. The roof was separated with simple longitudinal saw cuts spaced 100 degrees apart.

The formula used for the fiber-reinforced concrete was similar to that used by AFWL for 13-inch-diameter models. The steel fibers are U.S. Steel Fibercon, 0.010 inch in diameter and 0.5 inch long. They represent about 1.7% of the concrete mix by weight (0.5% by volume). A Type III cement was used to give a 14-day cure time. The trenches were poured under vacuum to minimize the number of air bubbles in the trench walls.

Eight unconfined compression tests (ASTM C39-64) and five split-cylinder tension tests (ASTM C496-71) were performed on 3-inch-diameter, 6-inch-long samples of the fiber-reinforced concrete after 14 days. These tests were performed by Testing Engineers of Santa Clara, California. The compression strength varied from 6590 psi to 8420 psi and averaged 7430 psi. The split-cylinder tension strength varied from 820 psi to 1010 psi and averaged 900 psi. A failed compression specimen and a tension specimen are shown in Figure 19.

Test 17

Test 17 was conducted for a nominal reflected pressure of 700 psi. The trench was covered with 2.3 inches of HAVE HOST soil, compacted to a measured density of 122 lb/ft , at a moisture content of 3.3 .

Figure 20 shows the digitized pressure records for Test 17. Test 12 is the corresponding load calibration test (Figure 2). For about 0.4 ms after the shock reaches the reflecting wall, the pressure at P1 in Test 17 is the same as in the calibration test. After the first 0.4 ms, the pressure at P1 in Test 17 decays more rapidly than in the calibration test, first because of the expansion and later because of both expansion and venting of the trench.

The end-view Hycam film illustrates the important features of the response. Selected frames are shown in Figure 21. The film speed was 9,980 frames per second. As seen in the film, when the shock wave reached the reflecting wall at t = 1.70 ms, the longitudinal saw cuts forming the roof blocks began to open up. Several additional cracks formed almost immediately. (They can be seen easily at t = 2.20 ms.) The roof cracked in two places, about 10 degrees from the crown on one side and about 15 degrees on the other. The walls and floor cracked in five fairly uniformly distributed locations. At t = 3.01 ms, each fragment had moved principally in the radial direction, but at t = 3.71 ms, the roof section had clearly begun lifting off vertically without changing its curvature significantly. The soil above the trench mounded up but did not compress noticeably. Gas jets formed in the sand at each crack location, and venting to the surface first occurred at the crack nearest the crown at about 4.10 ms. By that time, the roof had moved vertically about 2.5 inches. Venting in the form of jetting near the crown continued for an additional 1.0 ms. As late as t = 6.31 ms, venting was still apparent only near the crown, although the soil was very steeply mounded and the roof was well above the original soil surface.

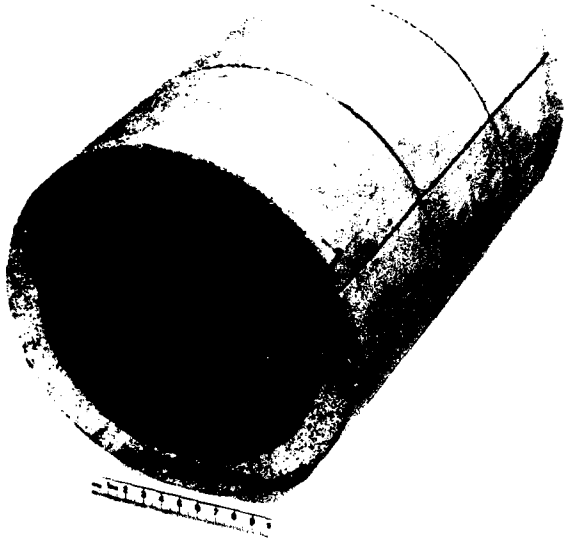

MP-6307-51

FIGURE 18 FIBER-REINFORCED CONCRETE TRENCH MODEL WITH SAW-CUT ROOF BLOCKS

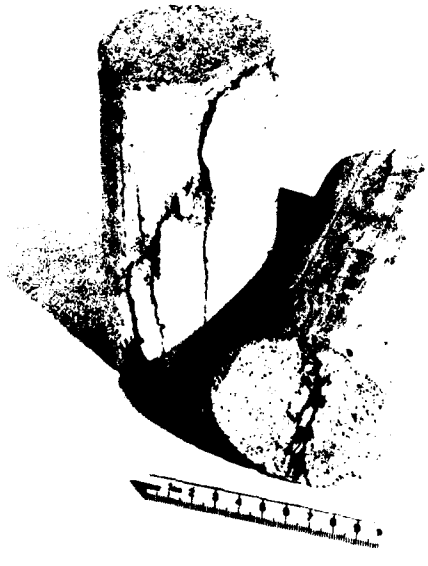

MP-6307-52

FIGURE 19 SPECIMENS FROM UNCONFINED COMPRESSION AND SPLIT-CYLINDER TENSION TESTS

Test 17

Test 17 was conducted for a nominal reflected pressure of 700 psi. The trench was covered with 2.3 inches of HAVE HOST soil, compacted to a measured density of 122 lb/ft^3, at a moisture content of 3.3%.

Figure 20 shows the digitized pressure records for Test 17. Test 12 is the corresponding load calibration test (Figure 2). For about 0.4 ms after the shock reaches the reflecting wall, the pressure at P1 in Test 17 is the same as in the calibration test. After the first 0.4 ms, the pressure at P1 in Test 17 decays more rapidly than in the calibration test, first because of the expansion and later because of both expansion and venting of the trench.

The end-view Hycam film illustrates the important features of the response. Selected frames are shown in Figure 21. The film speed was 9,980 frames per second. As seen in the film, when the shock wave reached the reflecting wall at t = 1.70 ms, the longitudinal saw cuts forming the roof blocks began to open up. Several additional cracks formed almost immediately. (They can be seen easily at t = 2.20 ms.) The roof cracked in two places, about 10 degrees from the crown on one side and about 15 degrees on the other. The walls and floor cracked in five fairly uniformly distributed locations. At t = 3.01 ms, each fragment had moved principally in the radial direction, but at t = 3.71 ms, the roof section had clearly begun lifting off vertically without changing its curvature significantly. The soil above the trench mounded up but did not compress noticeably. Gas jets formed in the sand at each crack location, and venting to the surface first occurred at the crack nearest the crown at about 4.10 ms. By that time, the roof had moved vertically about 2.5 inches. Venting in the form of jetting near the crown continued for an additional 1.0 ms. As late as t = 6.31 ms, venting was still apparent only near the crown, although the soil was very steeply mounded and the roof was well above the original soil surface.

Selected frames from the side-view Hycam film are shown in Figure 22. The film speed was 10,500 frames per second. In this view, both the photo pins and the soil surface show that the expansion of the trench was fairly uniform but was slightly greater near the reflecting wall. This illustrates that the expansion was due primarily to the reflected shock wave. Venting occurred first at the reflecting wall; then the soil surface appeared to "unzip" toward the shock tube. The elapsed time from the initiation of venting at the reflecting wall until venting occurred along the entire 12-inch trench length was about 1.0 ms. (The time required for the reflected shock wave to travel 12 inches is about 0.67 ms.)

The Test 17 trench fragments that were recovered within a 300-foot radius are shown in Figure 23. The fragments were placed in their original relative positions to illustrate the locations of the cracks. Generally, the cracks run longitudinally and extend over the entire length of the test section. At the cracks, the steel fibers pulled out of the concrete but did not break.

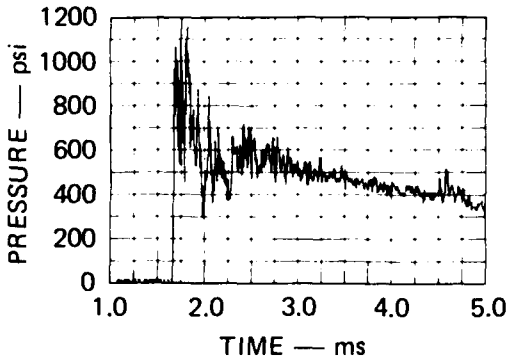

(a) P1 (AT REFLECTING WALL)

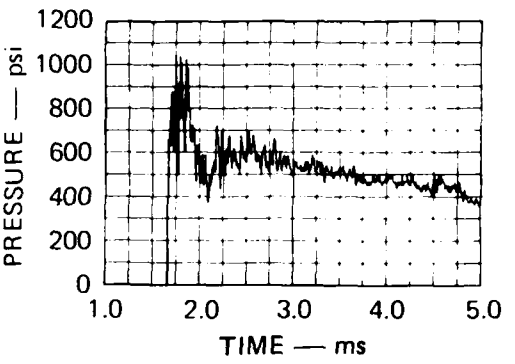

(b) P2 (AT REFLECTING WALL)

NOT AVAILABLE

(c) P5 (15.5 in. FROM REFLECTING WALL)

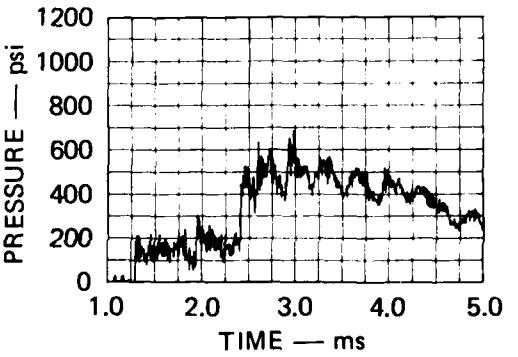

(d) P6 (15.5 in. FROM REFLECTING WALL)

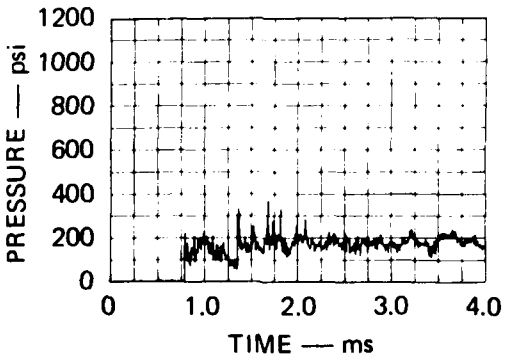

(e) P7 (38.5 in. FROM REFLECTING WALL)

MA-6307-24

FIGURE 20 PRESSURE RECORDS FROM EXPANSION AND VENTING TEST 17
Explosive charge 400 gr/ft

FIGURE 21 HYCAM PICTURES (End View, Test 17)

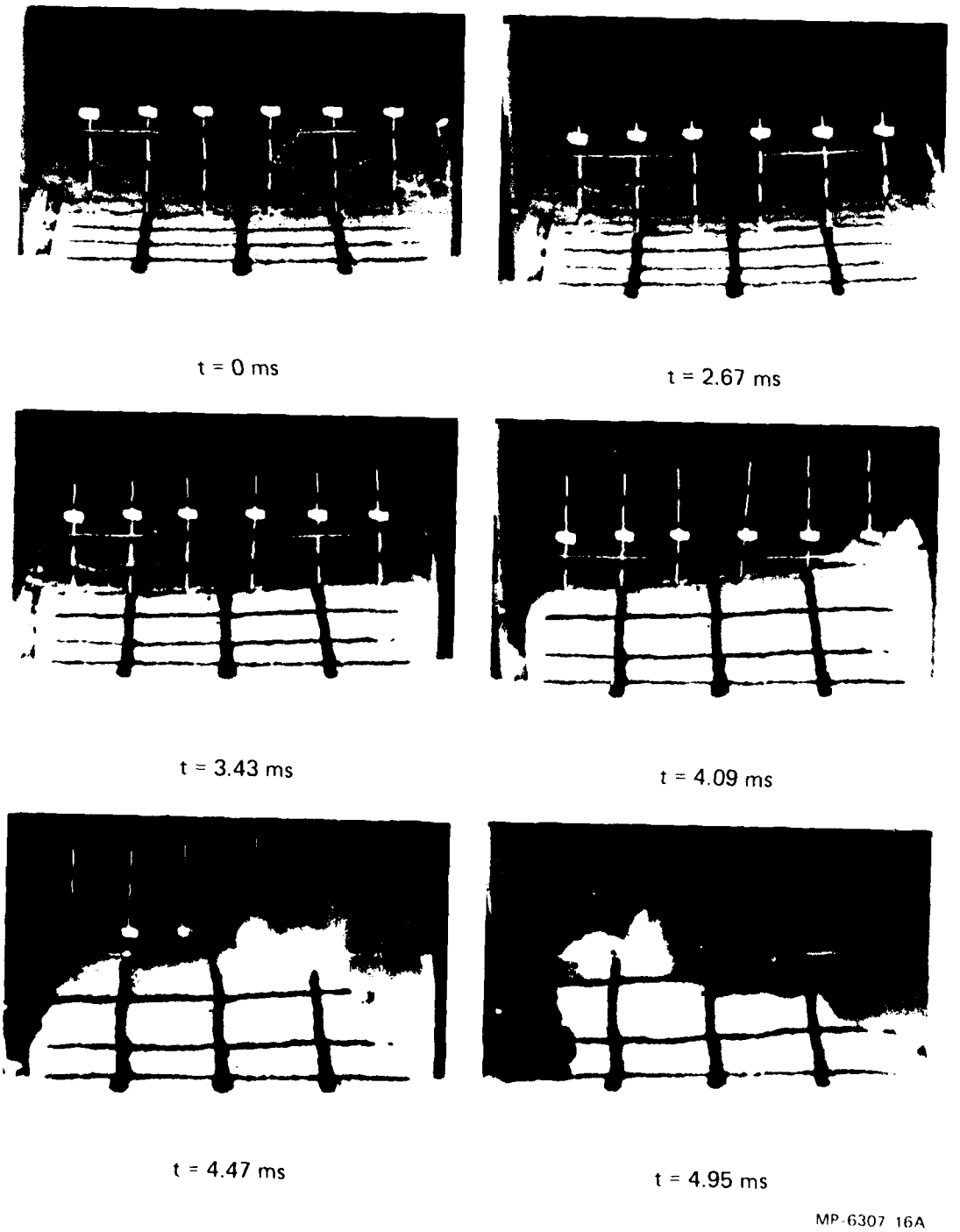

FIGURE 22 HYCAM PICTURES (Side View, Test 17)

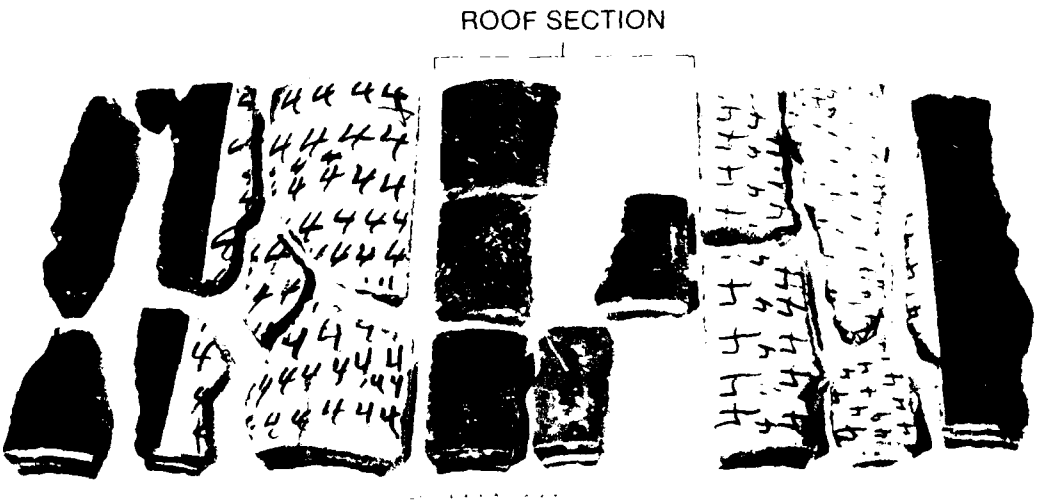

MP 6307 17

FIGURE 23 TRENCH FRAGMENTS RECOVERED FROM TEST 17

Front of trench is at bottom.

Test 18

Test 18 was conducted for a nominal reflected pressure of 1100 psi. The trench was covered with 2.3 inches of HAVE HOST soil compacted to a measured density of 122 lb/ft^3, at a moisture content of 2.6%. The digitized pressure records are plotted in Figure 24, corresponding to the calibration pressure records from Test 13 (Figure 3).

Selected frames from the Hycam films are shown in Figures 25 and 26. In the end view the film speed was 10,180 frames per second. In the side view the film speed was 10,370 frames per second. The results of Test 18 were qualitatively similar to the results of Test 17 (Figure 20), with the exception that the roof section in Test 18 cracked in three places--at the crown and on each side. After initial cracking and symmetrical expansion of the trench, the entire roof section moved vertically. Venting first occurred at 2.7 ms, initiating at the photo pin nearest the reflecting wall. Relative to the incidence of the wave at the reflecting wall, venting in Test 18 occurred about 1.0 ms earlier than in Test 17, where the pressure was 700 psi. At this time the roof position is obscured in the film but its displacement is estimated to be about 1.1 inch. Following venting initiation, the soil surface unzipped entirely along the crown in about 0.70 ms. (The reflected shock wave transit time is about 0.63 ms.) The vent area at the crown became very large as the soil mounded up steeply. The recovered trench fragments are shown in Figure 27. Again, the recovered trench fragments showed that the cracks generally ran longitudinally along the entire length of the trench model.

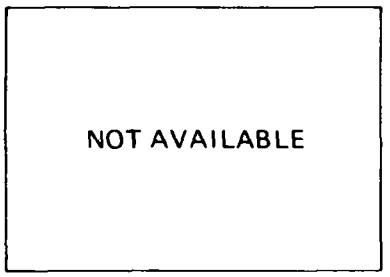

(a) P1 (AT REFLECTING WALL)

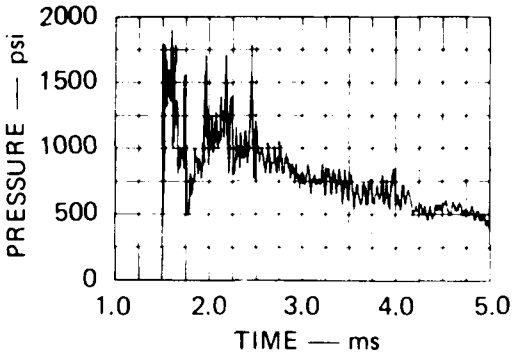

(b) P2 (AT REFLECTING WALL)

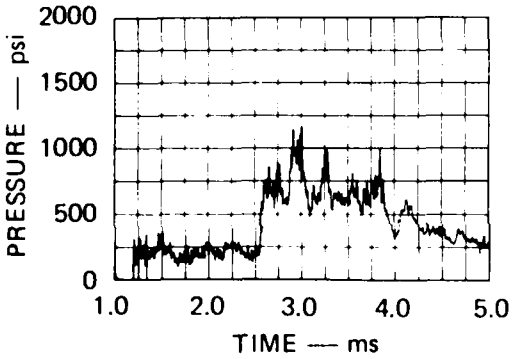

(c) P5 (15.5 in. FROM REFLECTING WALL)

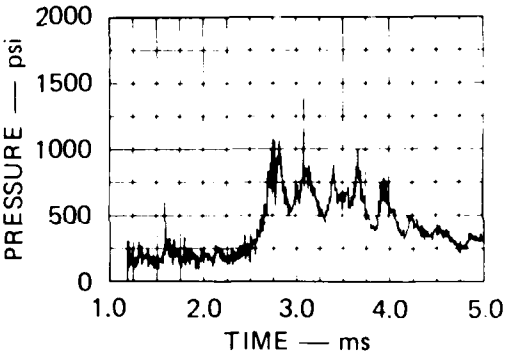

(d) P6 (15.5 in. FROM REFLECTING WALL)

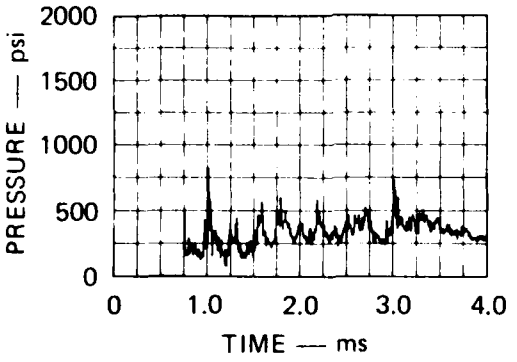

(e) P7 (38.5 in. FROM REFLECTING WALL)

MA-6307-25

FIGURE 24 PRESSURE RECORDS FROM EXPANSION AND VENTING TEST 18
Explosive charge 800 gr/ft

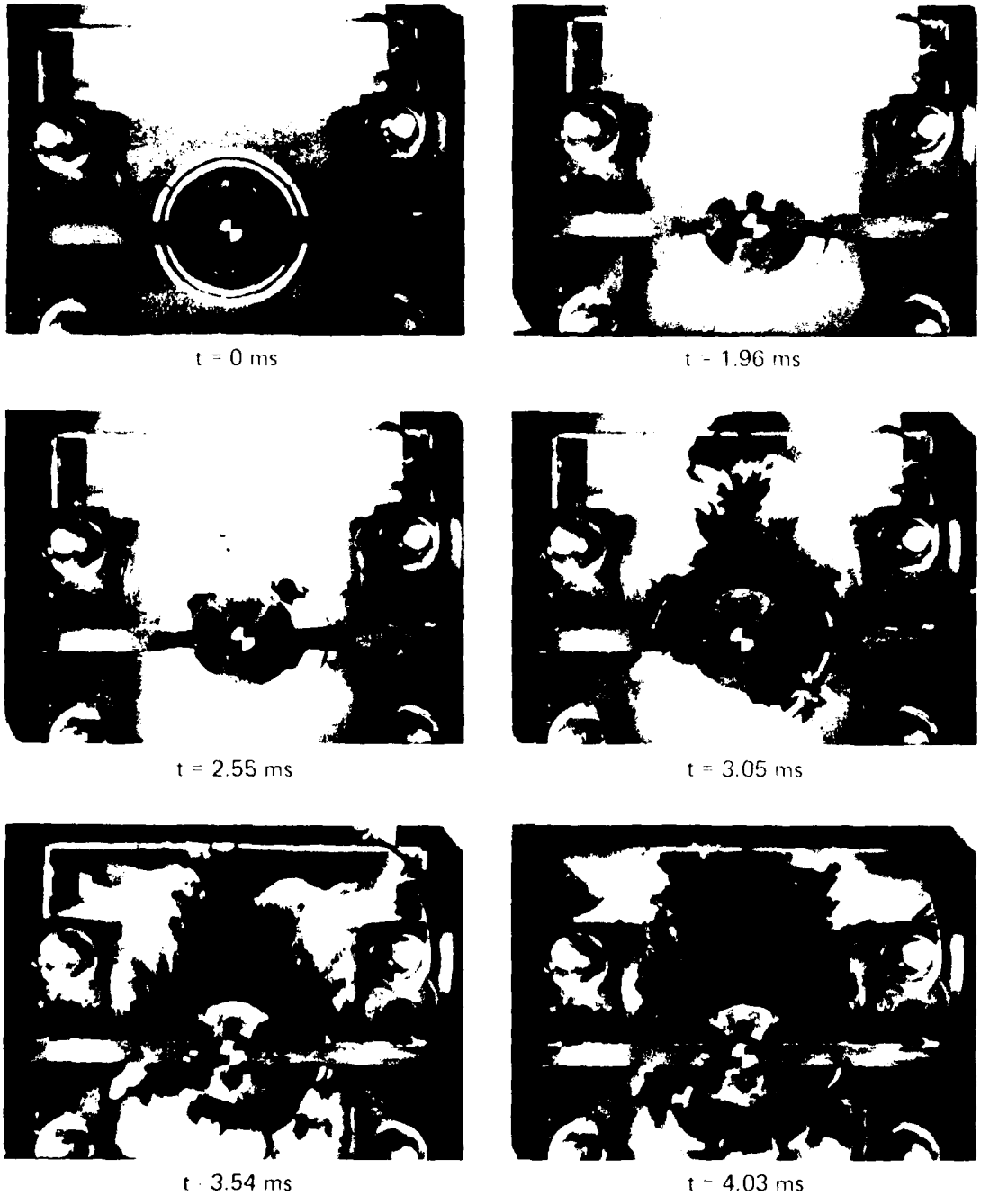

FIGURE 25 HYCAM PICTURES (End View, Test 18)

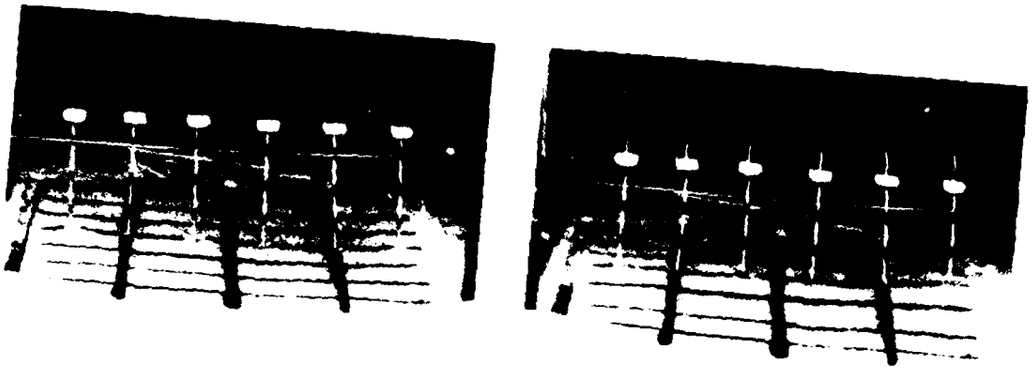

t = 0 ms

t = 2.51 ms

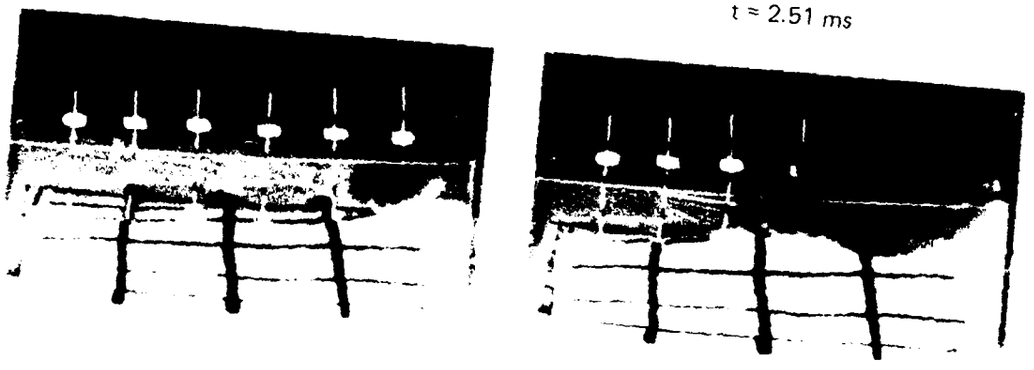

t = 2.80 ms

t = 3.09 ms

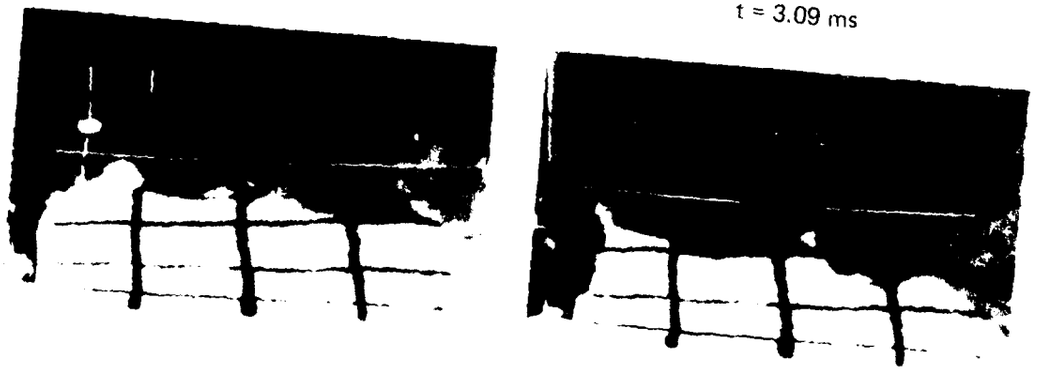

t = 3.38 ms

t = 3.66 ms

MP-6307-31A

FIGURE 26 HYCAM PICTURES (Side View, Test 18)

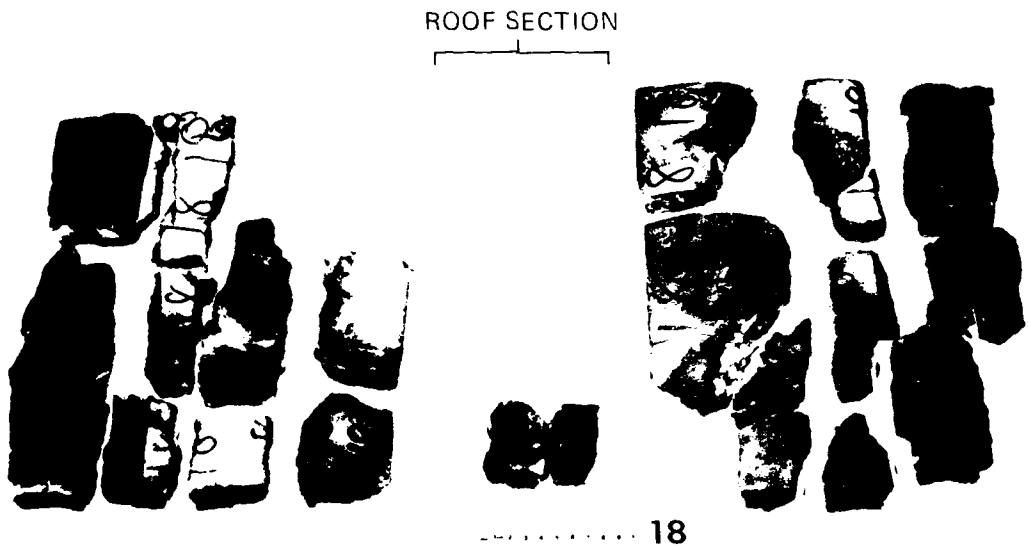

MP-6307-53

FIGURE 27 TRENCH FRAGMENTS RECOVERED FROM TEST 18
Front of trench is at bottom.

Test 19

The purpose of Test 19 was to demonstrate repetability. The explosive charge and soil preparation were the same as in Test 18. The measured soil density was 122 lb/ft^3, with a moisture content of 2.8%. The Hycam movies were taken with color film to see if any additional response features were distinguishable in color.

Generally, the pressure and the expansion and the venting response showed good repeatability. The digitized pressure records for this test are plotted in Figure 28. When compared with the records for Test 18 (Figure 24), they show that the pressure at the reflecting wall in Test 19 was slightly higher. Selected frames from the end view Hycam for Test 19 are shown in Figure 29. The film speed was 10,130 frames per second. When these are compared with the frames from Test 18 (Figure 25), good repeatability of the response is apparent. One difference is that, in Test 19, the roof cracked only at the crown. Venting, again initiating at the photo pin nearest the reflecting wall, is apparent one frame earlier (0.1 ms) in Test 19. The color movies showed that the venting jets are a combination of hot gas, soot, and sand. The recovered trench fragments are shown in Figure 30.

Table 3 compares pertinent measurements for Tests 18 and 19. The times of arrival were determined from the records of pressure gage P2 at the reflecting wall (Figures 24 and 28). The average pressures up to the time of venting in each test were also calculated from the records of P2. The time of first venting was determined from the movies and is accurate only to ±0.05 ms. Since the roof position was obscured in the end view movies, the roof displacements at the reflecting wall at the time of first venting were estimated by extrapolating the photo pin data to the reflecting wall. In each test, one springline was in clear view in the movies at the time of venting.

NOT AVAILABLE

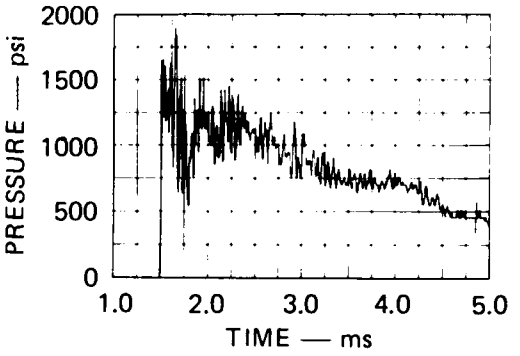

(a) P1 (AT REFLECTING WALL)

(b) P2 (AT REFLECTING WALL)

NOT AVAILABLE

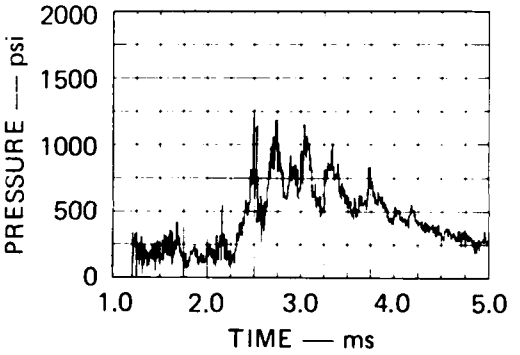

(c) P5 (15.5 in. FROM REFLECTING WALL)

(d) P6 (15.5 in. FROM REFLECTING WALL)

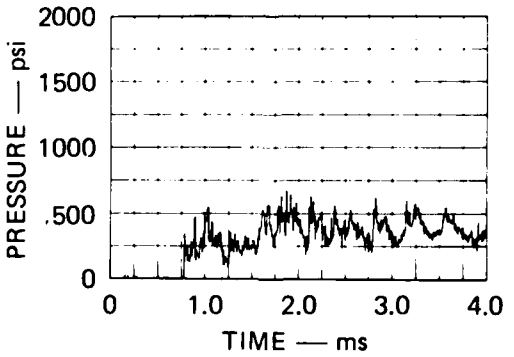

(e) P7 (38.5 in. FROM REFLECTING WALL)

MA-6307-26

FIGURE 28 PRESSURE RECORDS FROM EXPANSION AND VENTING TEST 19
Explosive charge 800 gr/ft

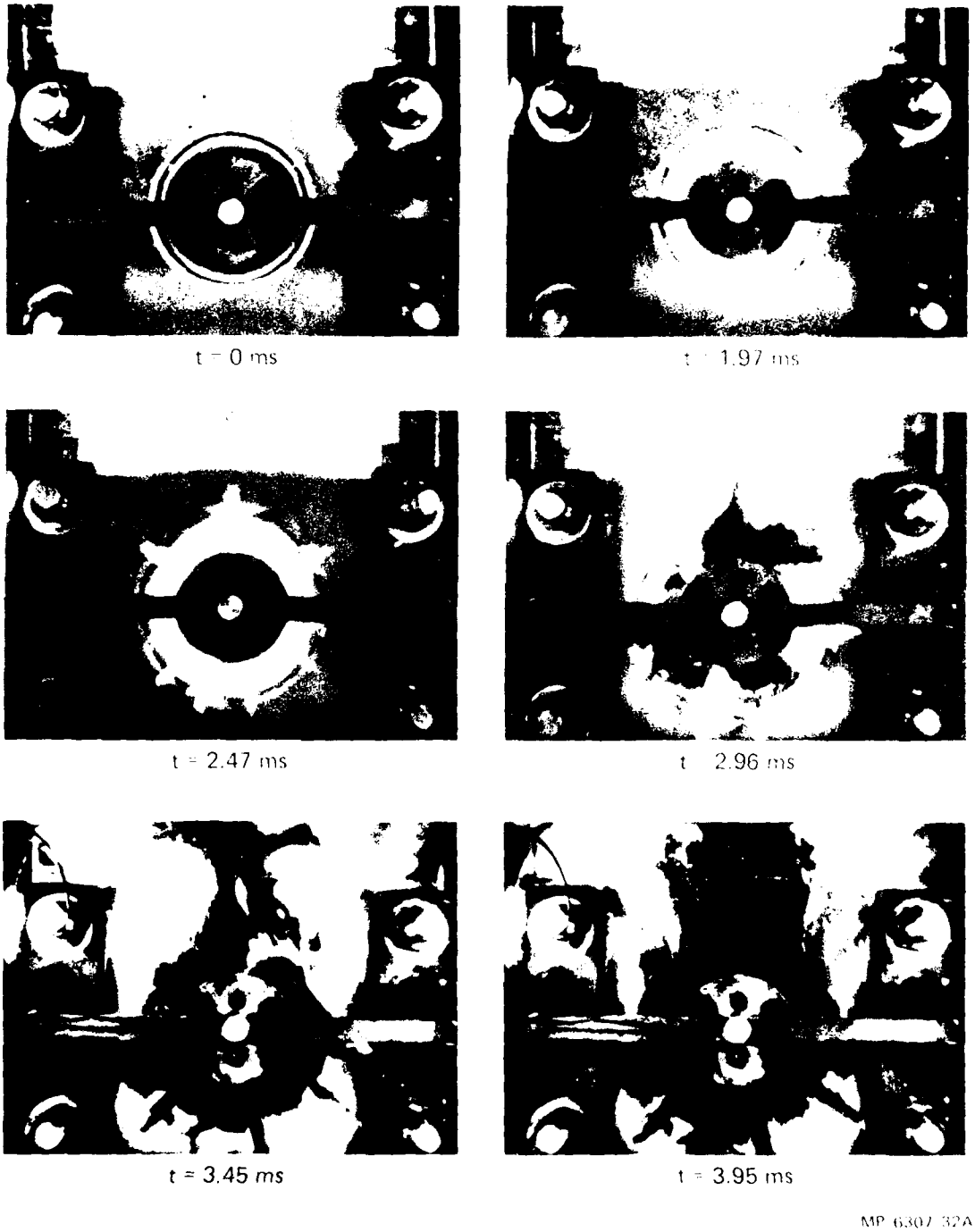

FIGURE 29 HYCAM PICTURES (End View, Test 19)

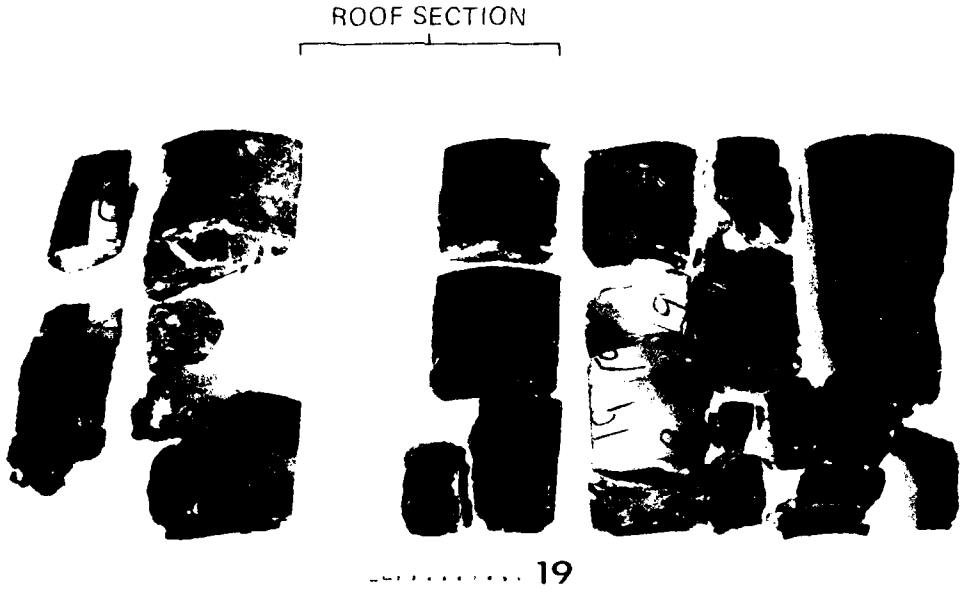

MP 6307 54

FIGURE 30 TRENCH FRAGMENTS RECOVERED FROM TEST 19

Front of trench is at bottom.

Table 3

REPEATABILITY OF RESULTS
IN TESTS 18 AND 19

Measurement	Test No. 18	Test No. 19
Time of shock arrival (ms)	1.50	1.50
Average pressure up to first venting (psi)	1090	1150
Number of longitudinal cracks (including saw cuts)	10	9
Time of first venting (ms)	2.70	2.60
Estimated roof displacement at first venting (in.)	1.11	1.13
Measured springline displacement at first venting (in.)	0.82	0.89

Test 20

The purpose of Test 20 was to determine the effect of dry soil on venting. As in Tests 18 and 19, the nominal reflected pressure was 1100 psi. The trench was covered with 2.3 inches of HAVE HOST soil, compacted to a density of 124 lb/ft^3 at a moisture content of 3.1%. The soil was then allowed to dry in the sun for 5 days. At the time of the test, the top 2 inches of soil had only 0.3% moisture; at a depth of 4 inches the moisture content was 1.9%. In this test we also attempted to determine the extent to which the photo pins affect the venting process. The photo pins normally used to measure roof displacement were not driven down to the trench roof but rested on plastic supports on the soil surface.

The digitized pressure records from Test 20 are plotted in Figure 31. Test 13 is the corresponding load calibration (Figure 3). The records in Figure 31 are essentially the same as those seen in the previous tests with wetter soil (Tests 18 and 19, Figures 24 and 28).

Selected Hycam frames are shown in Figures 32 and 33. In the end view the film speed was 10,280 frames per second. In the side view the film speed was 10,580 frames per second. The films show that the roof cracked in two places and that first venting occurred about 10 degrees from the crown and about 2 inches from the reflecting wall. Venting began about 0.50 ms later than in Tests 18 and 19, but the time required to unzip the full length of the trench was the same, leading to the conclusion that the pins affect the time of venting initiation but do not affect the rest of the features of the venting response. The roof position at the time of first venting is obscured in the film, but the displacement is estimated at about 2.3 inches. The recovered trench fragments are shown in Figure 34.

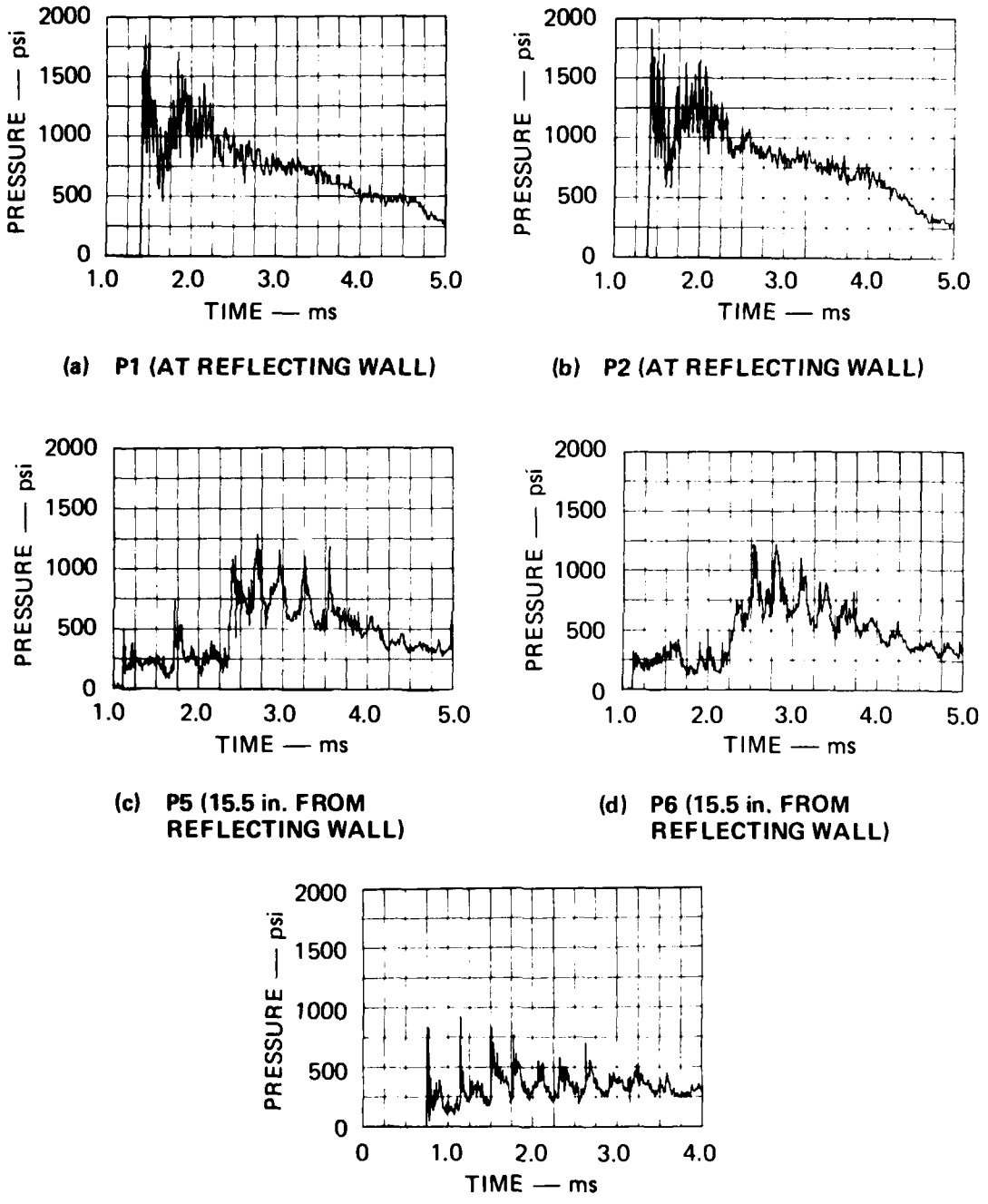

FIGURE 31 PRESSURE RECORDS FROM EXPANSION AND VENTING TEST 20

Explosive charge 800 gr/ft

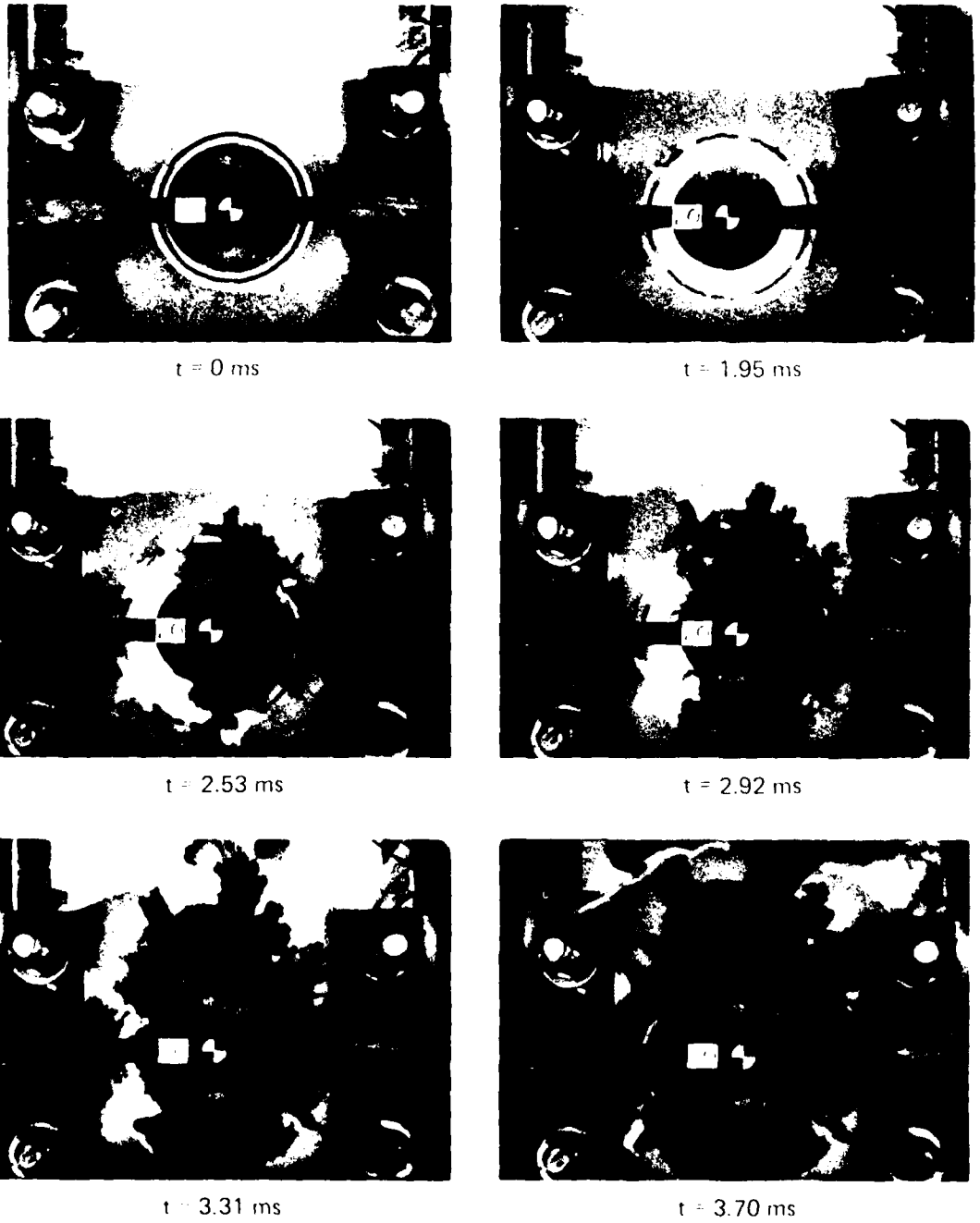

MP 6307-34A

FIGURE 32 HYCAM PICTURES (End View, Test 20)

t = 0 ms

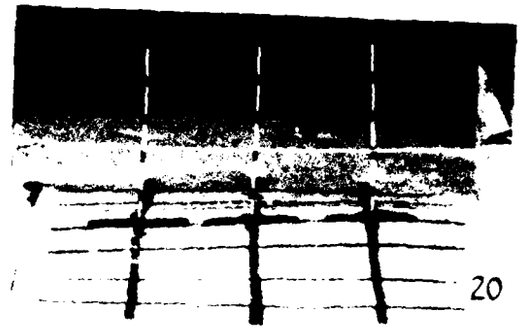

t = 2.46 ms

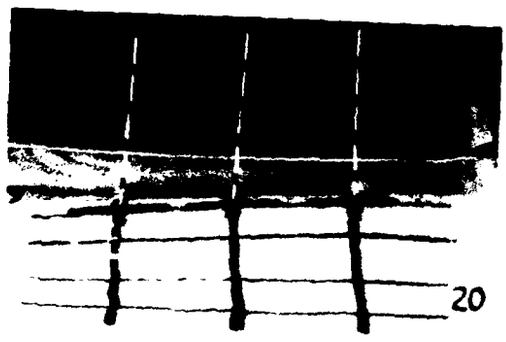

t = 2.84 ms

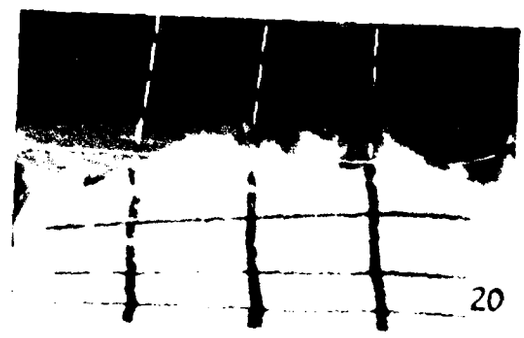

t = 3.22 ms

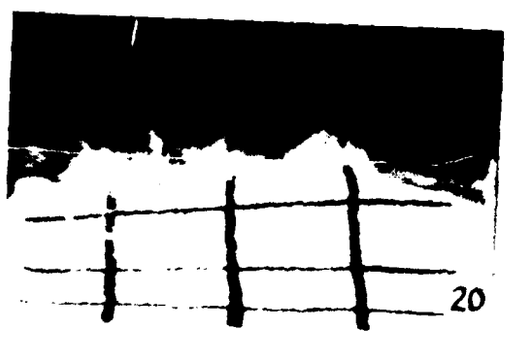

t = 3.41 ms

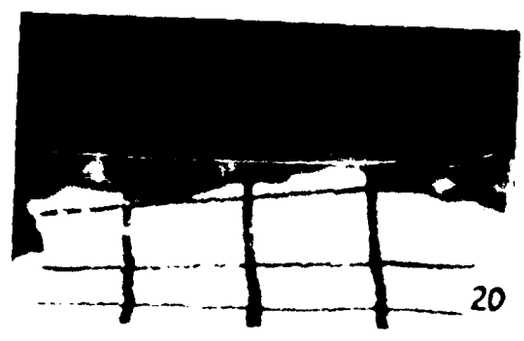

t = 3.60 ms

MP-6307-33A

FIGURE 33 HYCAM PICTURES (Side View, Test 20)

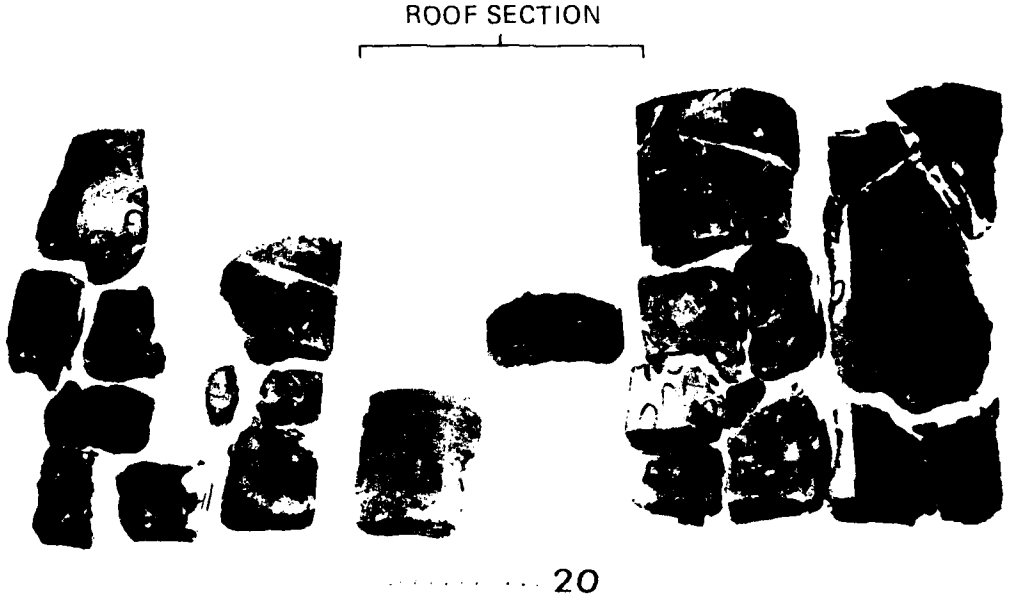

MP-6307 55

FIGURE 34 TRENCH FRAGMENTS RECOVERED FROM TEST 20

Front of trench is at bottom.

Test 22

Test 22 was conducted for a nominal reflected pressure of 2600 psi. The trench was covered with 2.3 inches of HAVE HOST soil compacted to a measured density of 118 lb/ft^3 at a moisture content of 3.6%. The digitized pressure records from Test 22 are shown in Figure 35. Test 23 is the load calibration test (Figure 5). As in previous tests, the pressure records agree with the calibration records until expansion causes the pressure to drop.

Selected frames from the Hycam movies are shown in Figures 36 and 37. In the end view the film speed was 10,500 frames per second. In the side view the film speed was 10,700 frames per second. The trench response was similar to that seen in lower pressure tests, but the expansion was faster and venting occurred at t = 2.43 ms, only 1.10 ms after the wave arrived at the reflecting wall. The roof had moved about 1.9 inches when venting initiated. The recovered trench fragments are shown in Figure 38.

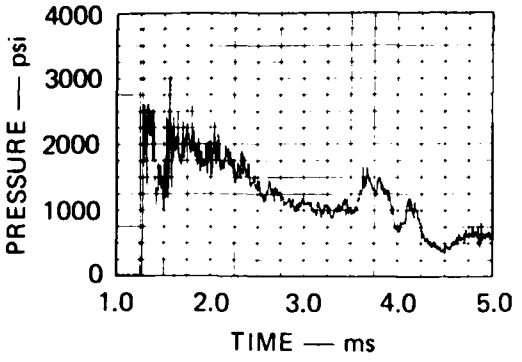

(a) P1 (AT REFLECTING WALL)

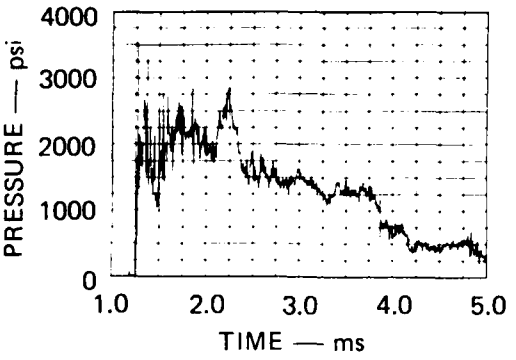

(b) P2 (AT REFLECTING WALL)

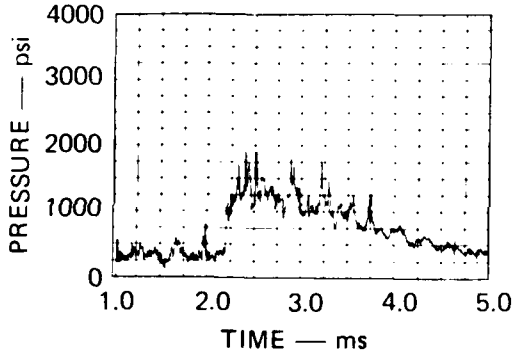

(c) P5 (15.5 in. FROM REFLECTING WALL)

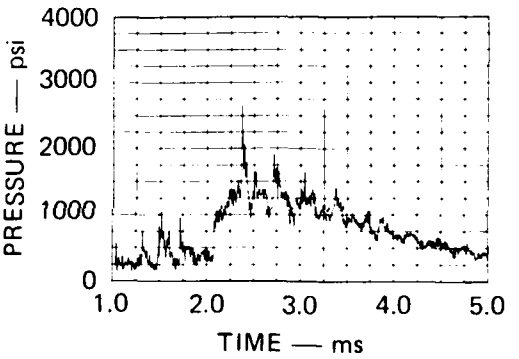

(d) P6 (15.5 in. FROM REFLECTING WALL)

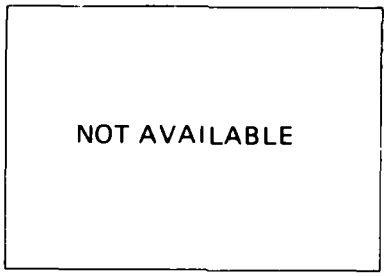

(e) P7 (38.5 in. FROM REFLECTING WALL)

MA-6307-29

FIGURE 35 PRESSURE RECORDS FROM EXPANSION AND VENTING TEST 22
Explosive charge 1600 gr/ft

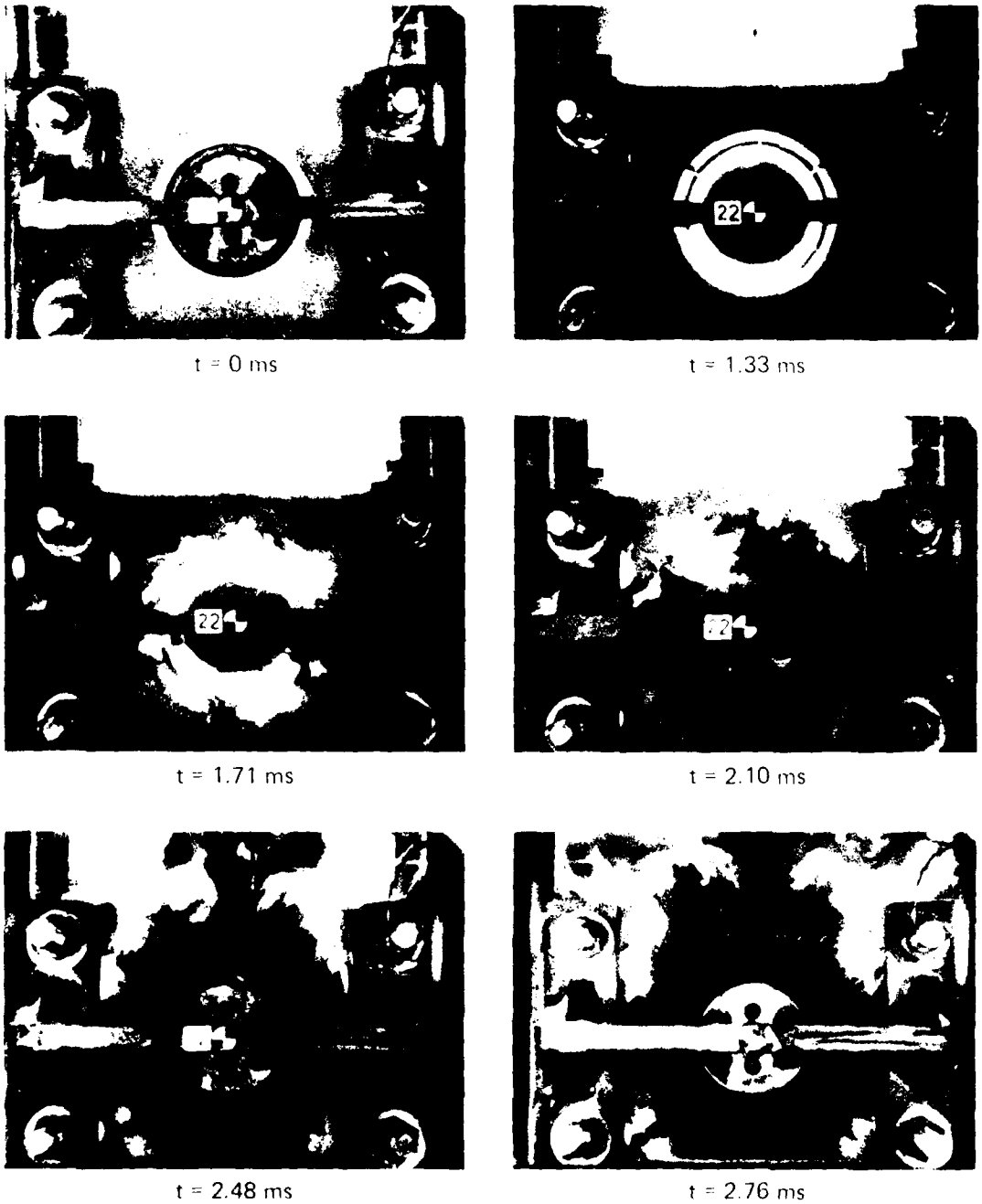

FIGURE 36 HYCAM PICTURES (End View, Test 22)

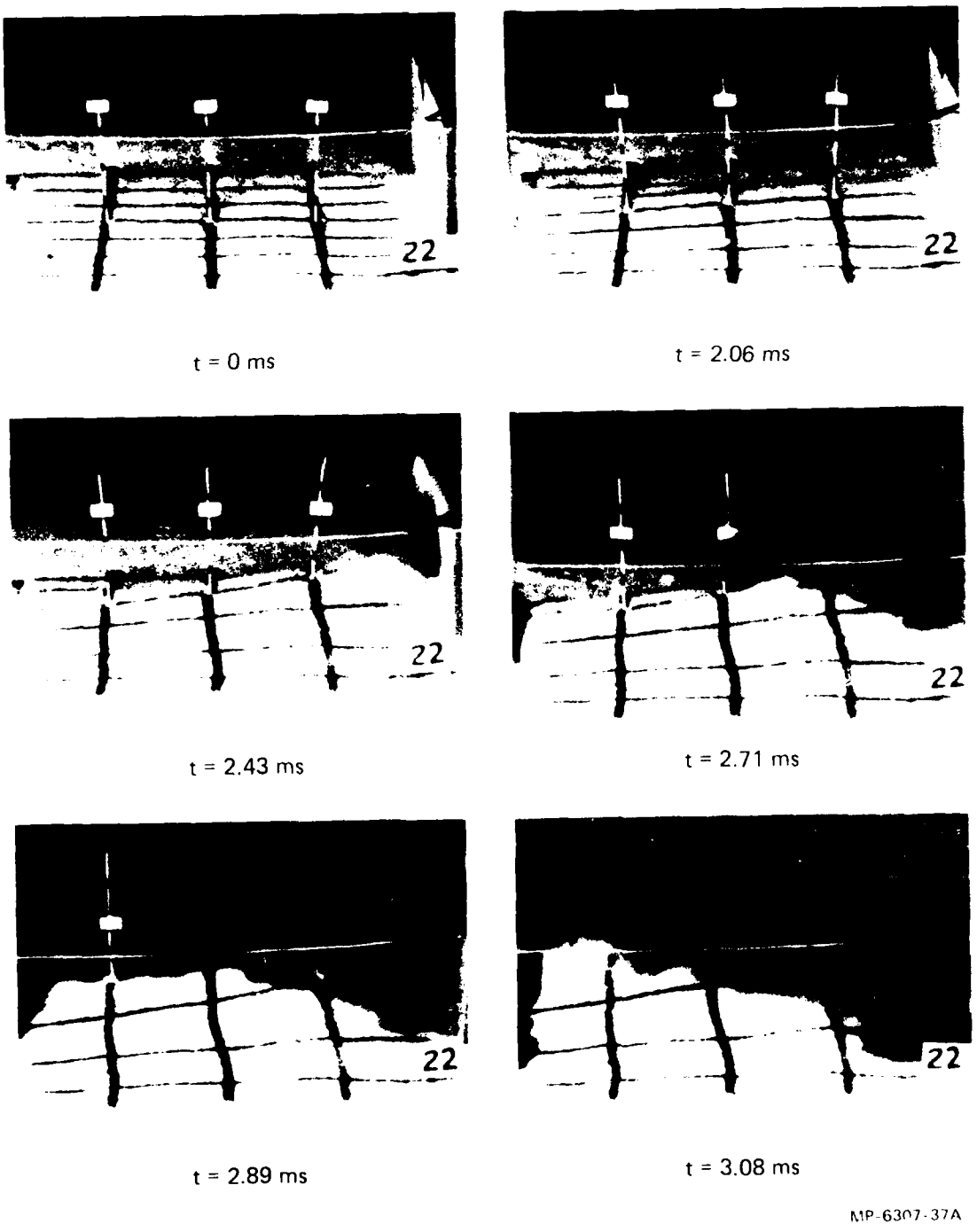

FIGURE 37 HYCAM PICTURES (Side View, Test 22)

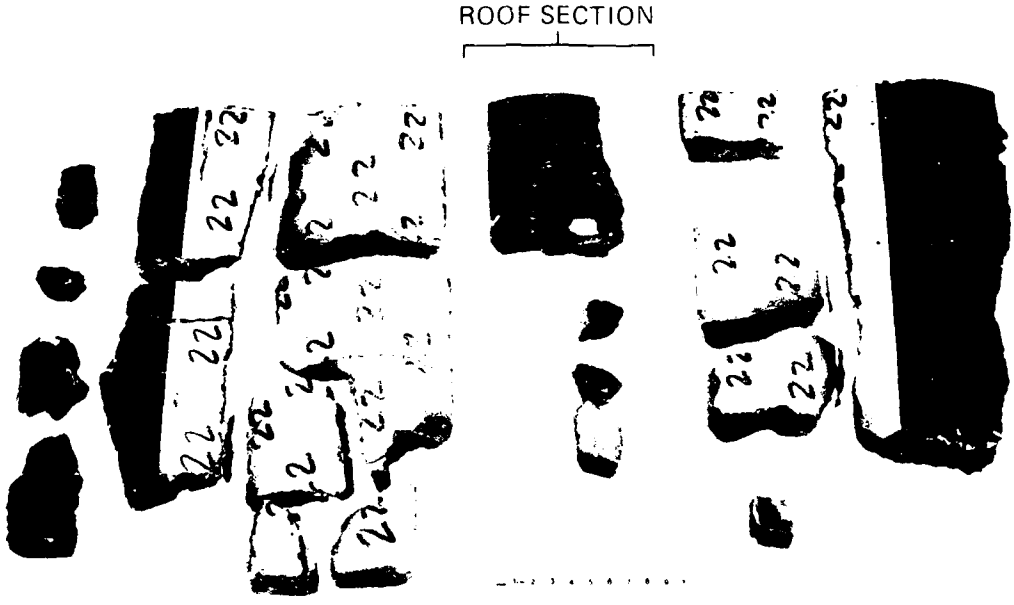

FIGURE 38 TRENCH FRAGMENTS RECOVERED FROM TEST 22
Front of trench is at bottom.

Test 30

Test 30 was conducted at a nominal reflected pressure of 400 psi with a thin-wall ribbed trench section. This ribbed model trench design was described at the beginning of this section.

In this test we attempted to pack the Yuma soil to a wet density of 132 lb/ft^3 at a moisture content of 6%. This value corresponds to the higher soil density specified for the thin-walled trench. We packed the test section in layers about 3 inches deep by successively dropping an 8-pound weight (about 10 $in.^2$) from a height of about 1 foot. The weight was dropped five or six times on each spot; after three or four blows no additional compaction was noticeable. The measured wet density was about 126 lb/ft^3 at 6% water, compared with 132 lb/ft^3 obtained previously in a Modified Proctor test at the same moisture content. (In the Modified Proctor test the soil is confined in a 4-inch-diameter cylinder and is compacted in 1-inch layers by dropping a 10-pound weight twenty-five times from a height of 18 inches.)

Figure 39 shows the digitized pressure records from Test 30. Test 26 is the load calibration test (Figure 6). As observed in our earlier tests, expansion and venting produce a noticeable decay in pressure.

Selected Hycam frames are shown in Figures 40 and 41. In the end view the film speed was 10,840 frames per second, whereas in the side view the film speed was 10,140 frames per second. The films show that the roof cracked near the crown and that the first venting occurred through this crack at t = 5.35 ms. The roof displacement at the time of first venting was 2.0 inches, which again is consistent with the results of earlier tests.

Figure 42 shows the trench fragments recovered from Test 30. In addition to the longitudinal cracks observed in earlier tests with smooth wall trenches, there were a number of circumferential cracks at the ribs.

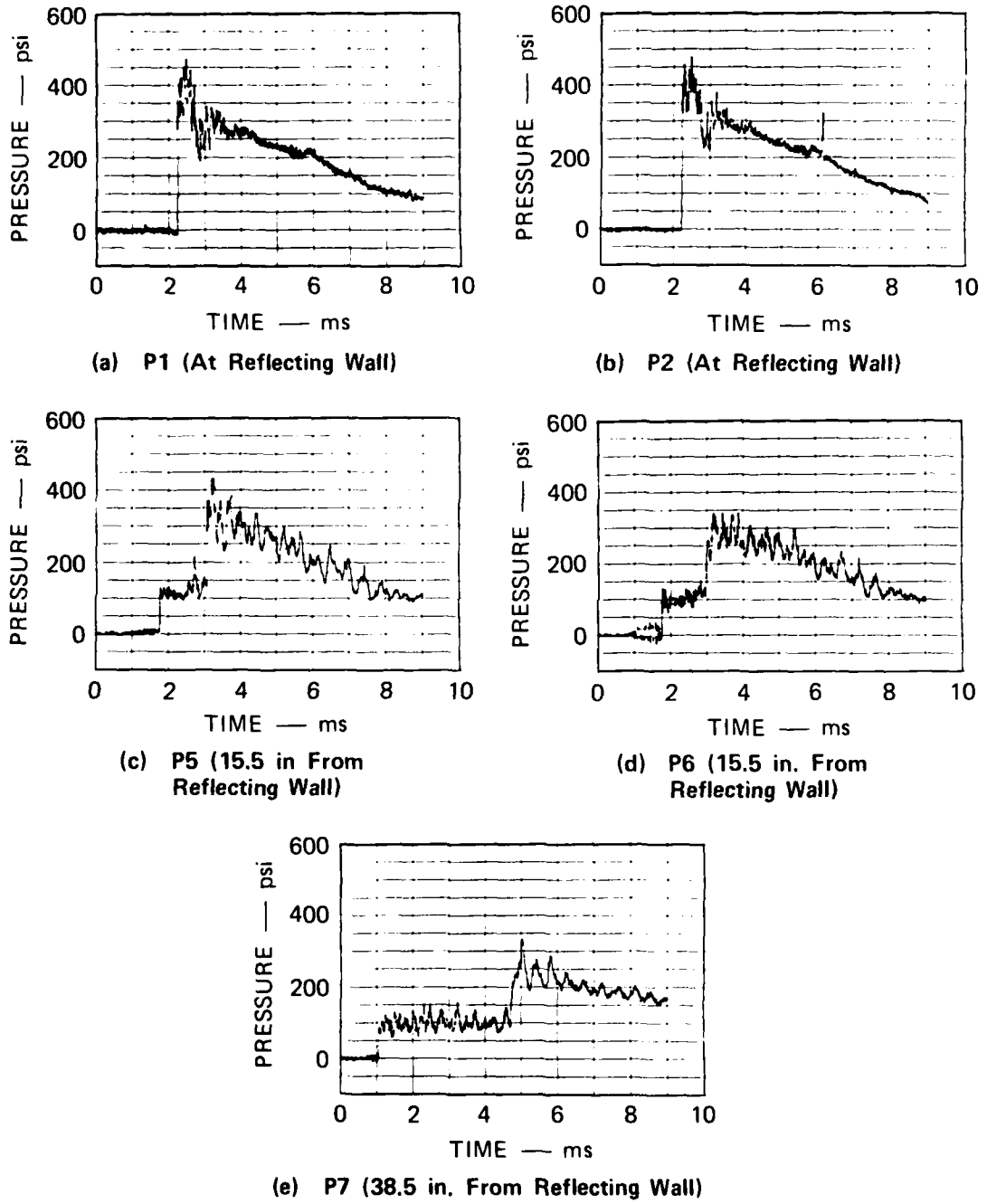

FIGURE 39 PRESSURE RECORDS FROM EXPANSION AND VENTING TEST 30

Explosive charge 200 gr/ft

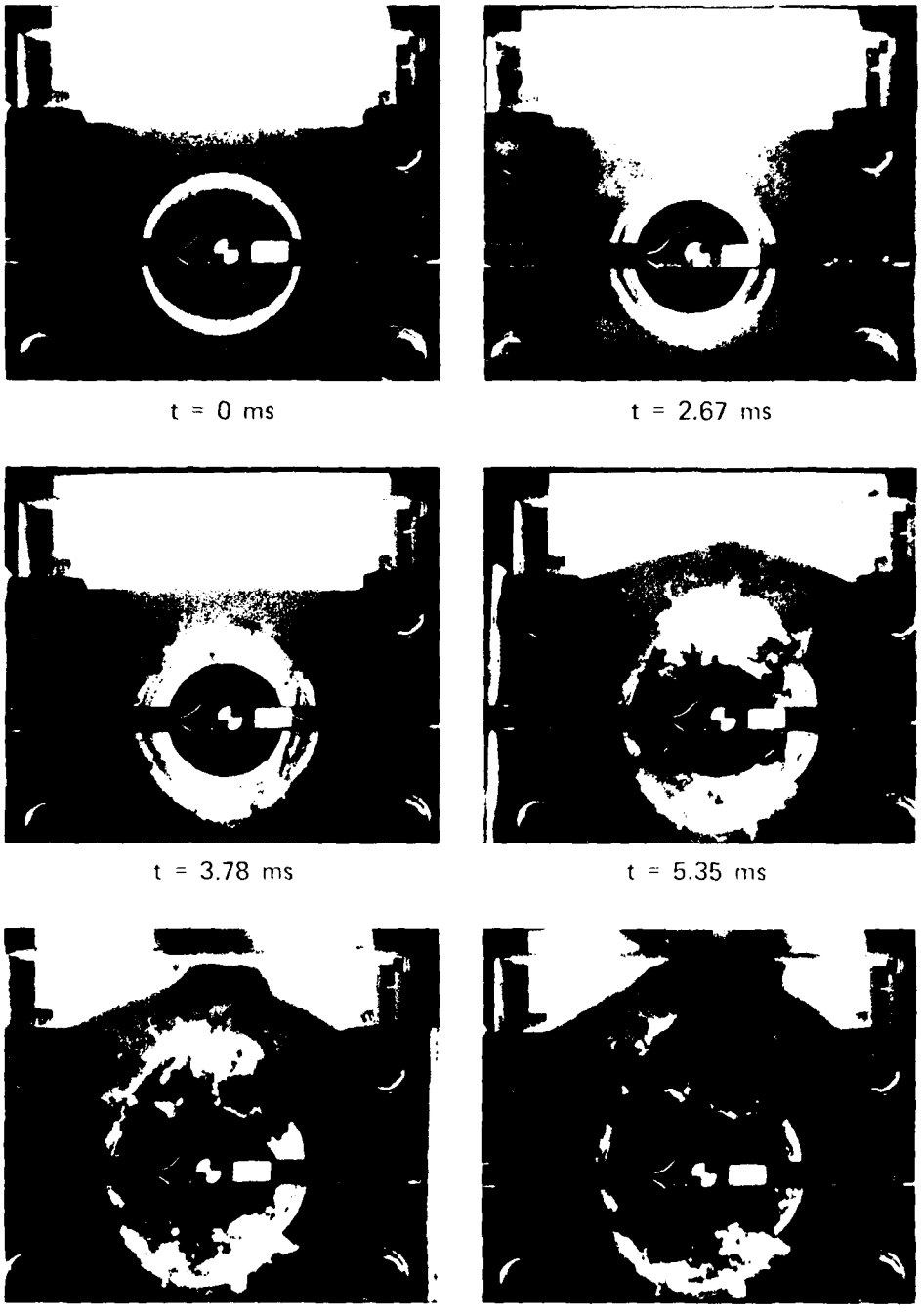

FIGURE 40 HYCAM PICTURES (End View, Test 30)

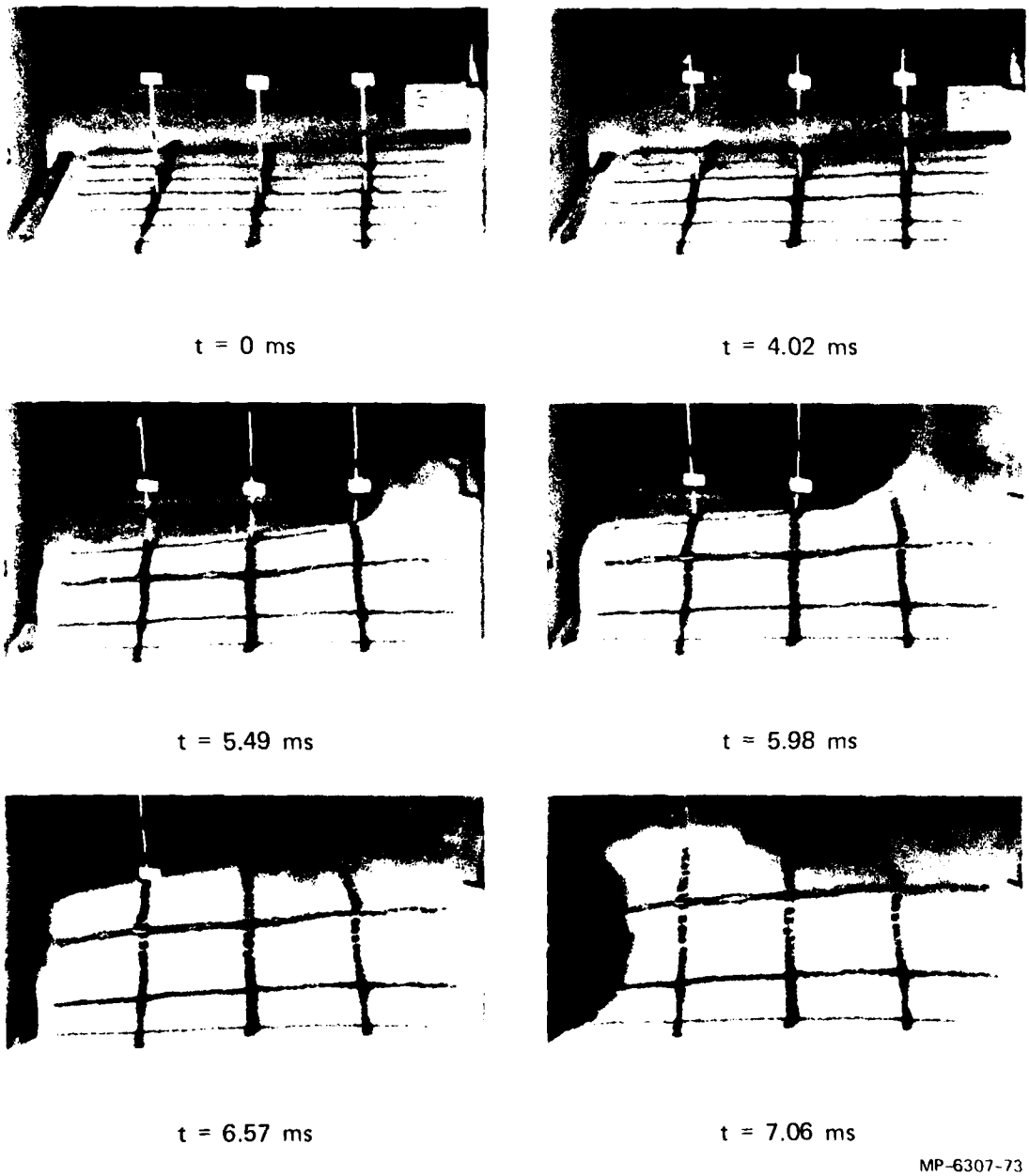

FIGURE 41 HYCAM PICTURES (Side View, Test 30)

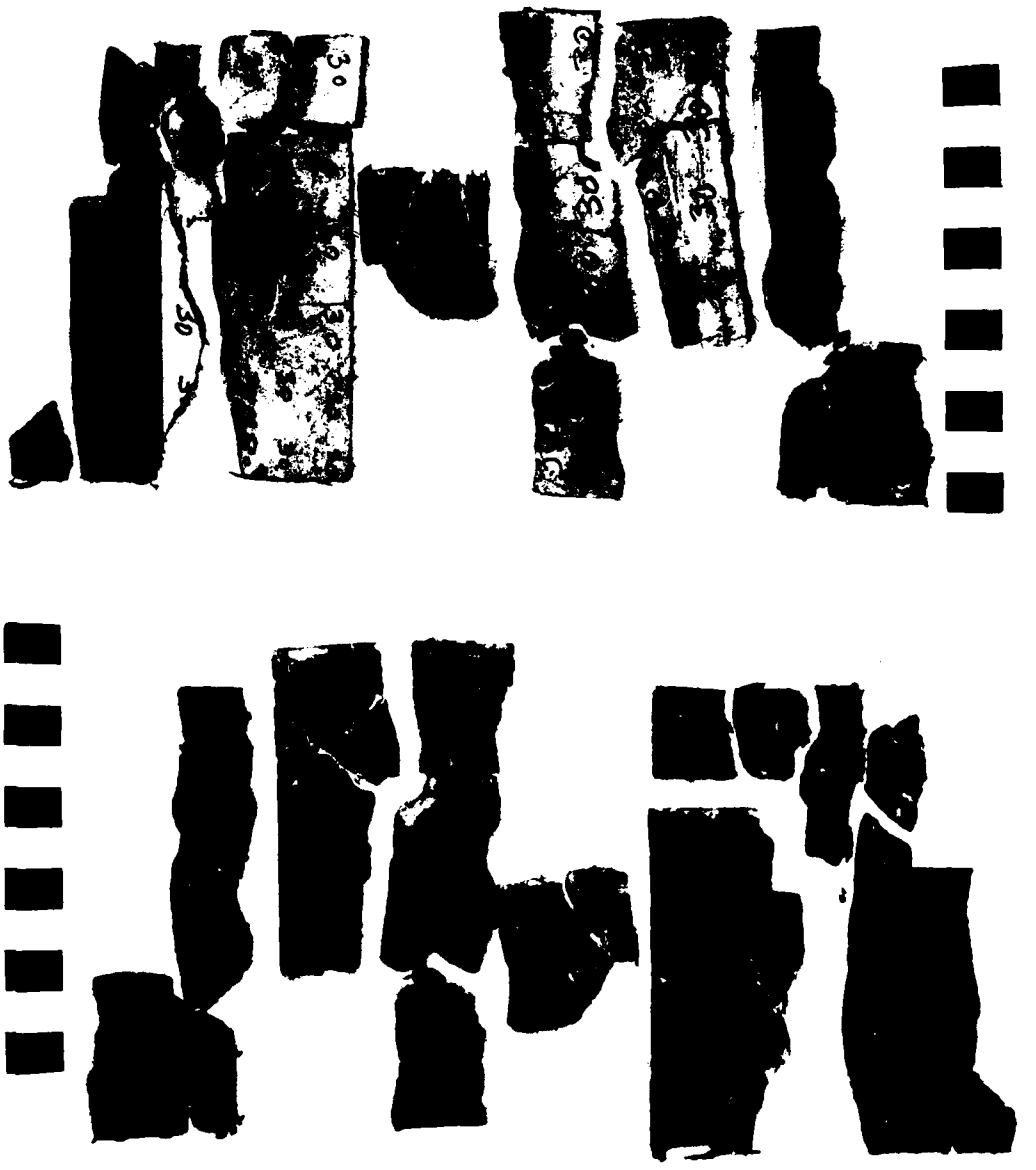

MA-6307-78

FIGURE 42 TRENCH FRAGMENTS RECOVERED FROM TEST 30

3.4 COMPARISON WITH HAVE HOST TEST T-1

The T-1 event of the HAVE HOST Test Program was a 1/2-scale test conducted by the Air Force Weapons Laboratory (AFWL) at the Luke Air Force Range (Arizona). Below we compare some relevant results of the 1/2-scale T-1 with the SRI 1/26-scale expansion and venting tests. The data for T-1 are taken from the HAVE HOST T-1 Quick Look Report (Reference 2).

None of the 1/26-scale model experiments performed by SRI were designed to be an exact scale model of the T-1 test, so the results cannot be expected to be identical. However, several important parameters, such as soil properties, trench properties, and pressure levels were approximately the same for the cases discussed below. Our comparisons show that the AFWL and SRI tests produce qualitatively similar results, and we found no quantitative inconsistencies.

Backfill Soil Properties

The soil used for the SRI experiments was obtained from a designated location at the HAVE HOST site. Grain size distribution and compaction tests were performed on this soil.* A series of soil property tests were also performed on soil samples from the HAVE HOST site by the U.S. Army Waterways Experiment Station (WES). As shown in Figures 43 and 44, our test results agreed well with WES data.

Backfill densities measured for T-1 ranged from 106 to 115 lb/ft^3 with moisture contents from 1.0 to 2.6%. Densities for the SRI tests (except Test 20, the dry soil test) ranged from 117 to 122 lb/ft^3 with moisture contents from 2.6 to 3.9%. The soil cover depth of 2.3 inches in the SRI tests was a 1/13-scale of the cover depth of 0.75 meters for T-1.

*The soil tests were performed for SRI by Testing Engineers, Incorporated, Santa Clara, Califonria.

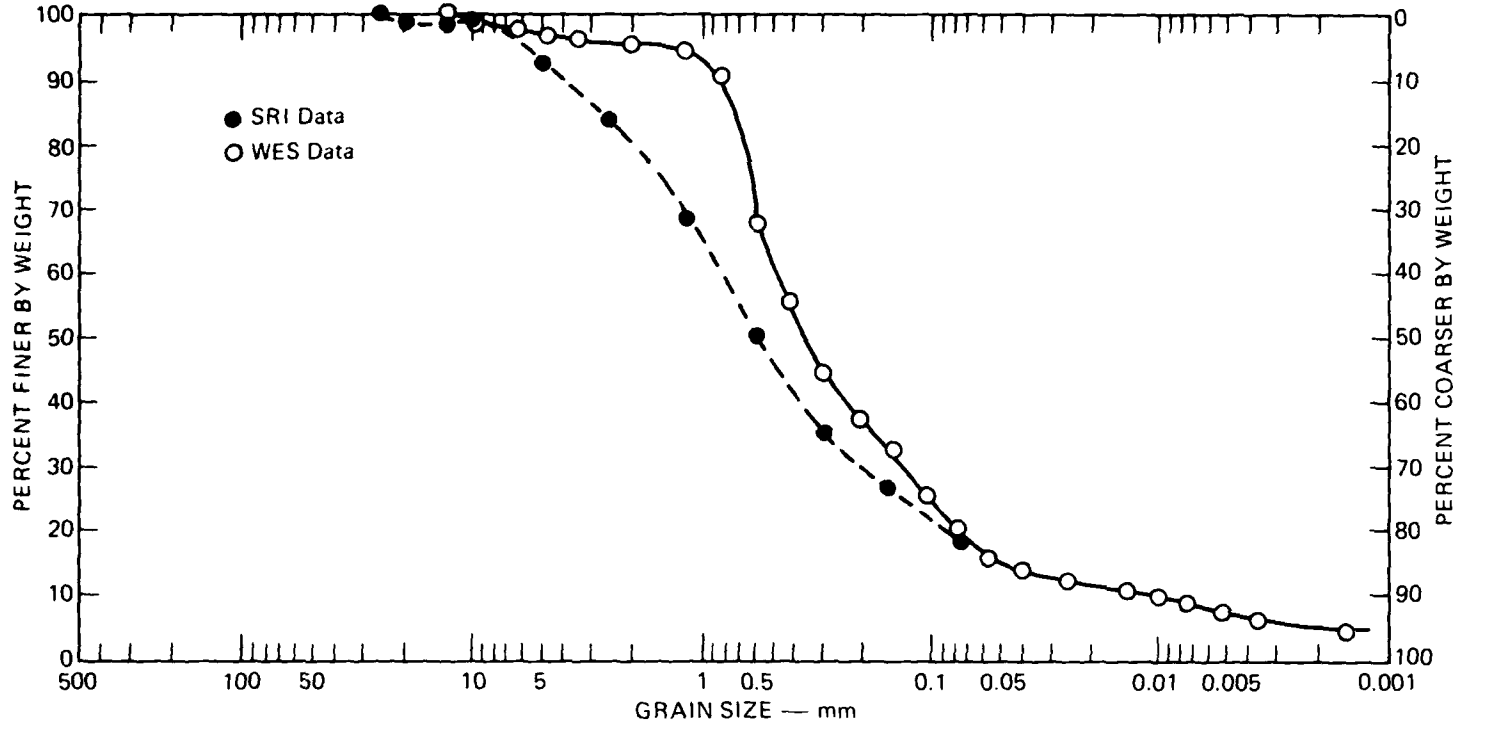

FIGURE 43 COMPARISON OF GRAIN SIZE DISTRIBUTION TESTS FOR HAVE-HOST BACKFILL SOIL

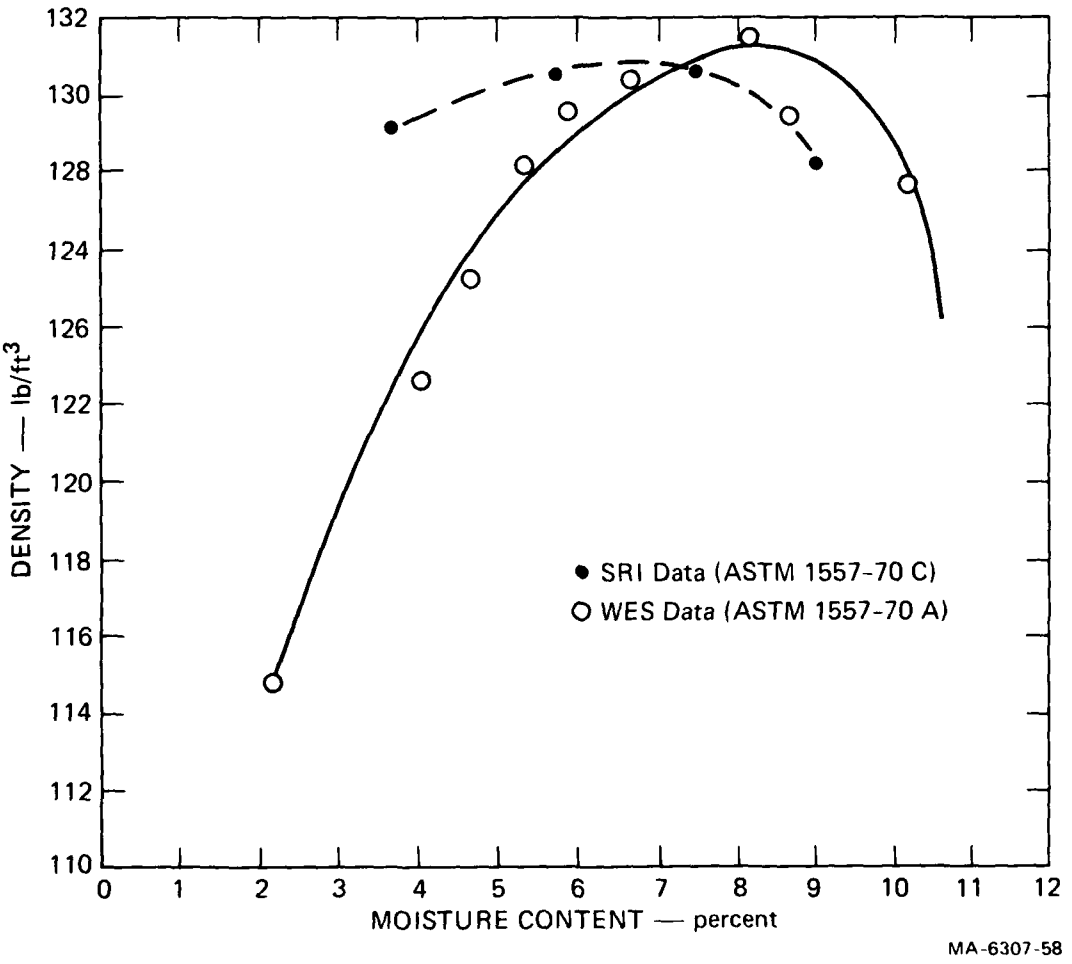

FIGURE 44 COMPARISON OF COMPACTION TESTS FOR HAVE-HOST BACKFILL SOIL

Time of arrival data for T-1 showed seismic velocities between 125 m/s and 172 m/s in the backfill. The observed wave from the end view film for SRI Test 16 showed a velocity of 142 m/s. (This wave is not clearly discernible in all the SRI tests.)

Trench and Concrete Properties

The trenches in both T-1 and the SRI tests (Tests 17 through 22) were constructed of steel-fiber-reinforced concrete. Dimensions for the SRI trenches were scaled by a factor of 13 from the T-1 dimensions. The scaled average wall thickness of the ribbed T-1 trench was used in the straight-walled trenches fabricated for the SRI tests.

Unconfined compression tests were performed for the T-1 concrete after 28 days of curing and on the test day. Cylinder strengths varied from 5200 to 6900 psi. For the SRI concrete, unconfined compression tests were performed after 14 days of curing (a 14-day Type III cement was used in the SRI concrete). Cylinder strengths varied from 6590 to 8420 psi.

Wall Expansion

The wall expansions at the springlines were compared for SRI Test 17 and a T-1 station having a similar in-trench pressure history. Figure 45(a) shows the pressure history, with time scaled by a factor of 13, for T-1 at a range of 48.5 meters. Figure 45(b) shows the pressure history for Test 17 measured at the reflecting wall. The scaled pressure for T-1 is similar, averaging 10 to 20% lower than Test 17 during the first millisecond after shock arrival.

Figure 45(c) shows the displacement at the springline for T-1 at a range of 49.3 meters, with both displacement and time scaled by a factor of 13. Figure 45(d) shows the displacement at the springline for Test 17. (The T-1 displacement data were developed by twice integrating accelerometer records, while the Test 17 displacement data were read from frames of the end-view Hycam film.) The T-1 data are 10% to 20% lower

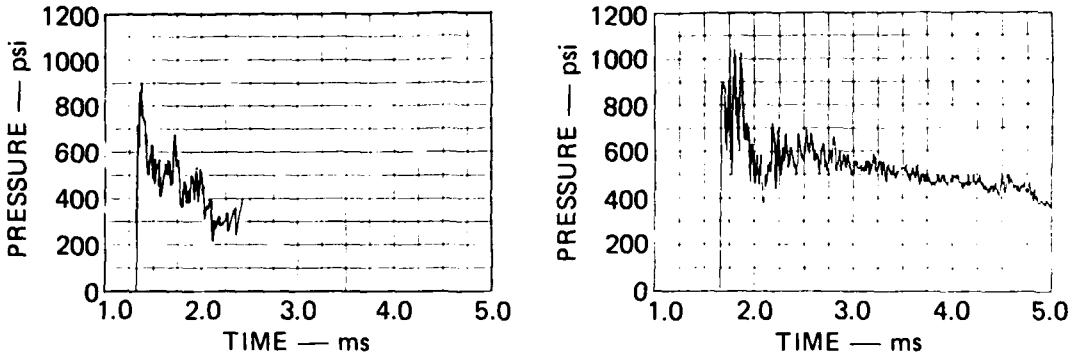

(a) PRESSURE AT RANGE 48.5 m T-1 (SCALED BY FACTOR OF 13)

(b) PRESSURE AT REFLECTING WALL TEST 17

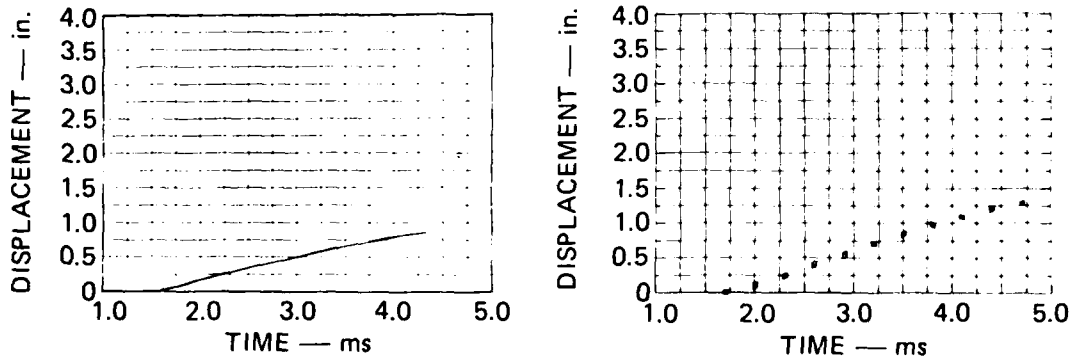

(c) SPRINGLINE DISPLACEMENT AT RANGE 49.3 m T-1 (SCALED BY FACTOR OF 13)

(d) SPRINGLINE DISPLACEMENT AT REFLECTING WALL TEST 17

MA-6307-59

FIGURE 45 COMPARISON OF WALL EXPANSION BETWEEN AFWL HAVE HOST TEST T-1 AND SRI TEST 17

than those from Test 17. Since the pressure at this location in the T-1 test was also about 10% to 20% lower, the displacement data in the two tests are consistent.

Venting

In Test T-1, venting began near the plug 15 ms after shock arrival. Photo pole data 1.5 meters in front of the plug (photo pole 17) suggest that the roof had lifted 0.34 meter at that time, a distance of about one-half the soil cover depth. This is consistent with the results from SRI Tests 18 and 19, where venting began at a photo pin after the roof had lifted 1.1 inches, also about one-half the soil cover depth. It was not confirmed for T-1 that venting started at a photo pin. In the SRI tests where venting did not start at a photo pin, venting occurred when the trench roof had moved to about the level of the original soil surface.

Trench Failure

Figure 46(a) shows the crack pattern for an upstream trench section from Test T-1, and Figure 46(b) shows the trench fragments recovered from Test 17. Both failed trenches show longitudinal cracking near the trench crown with five to six longitudinal cracks in the lower portion of the trench. These longitudinal cracks run the entire length of the trench section in both cases. Moderate circumferential cracking is also seen in the lower portion of the trench in both cases.

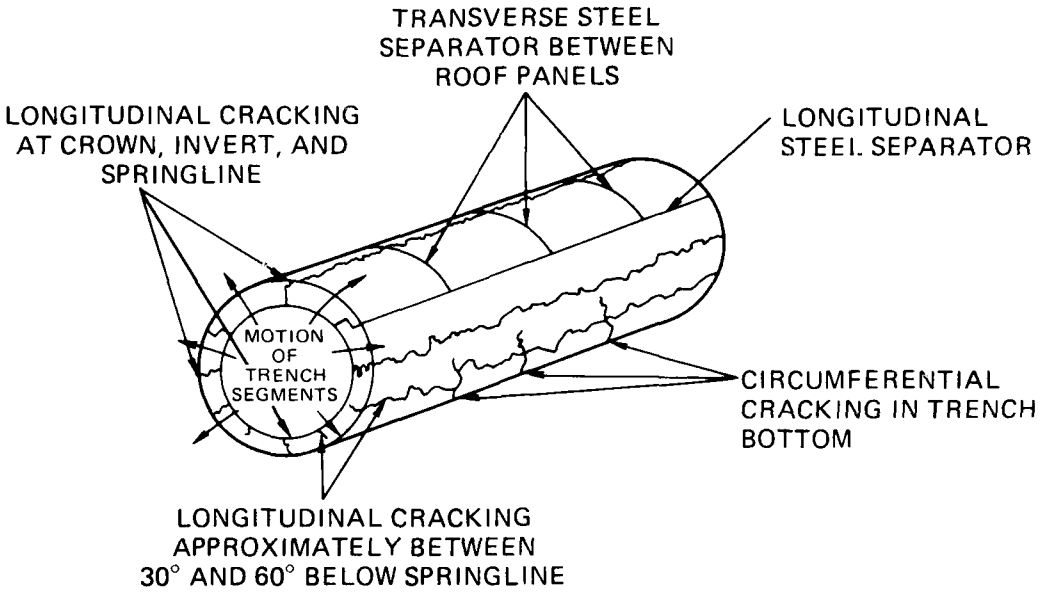

(a) CRACK PATTERN FOR UPSTREAM TRENCH SECTIONS, TEST T-1

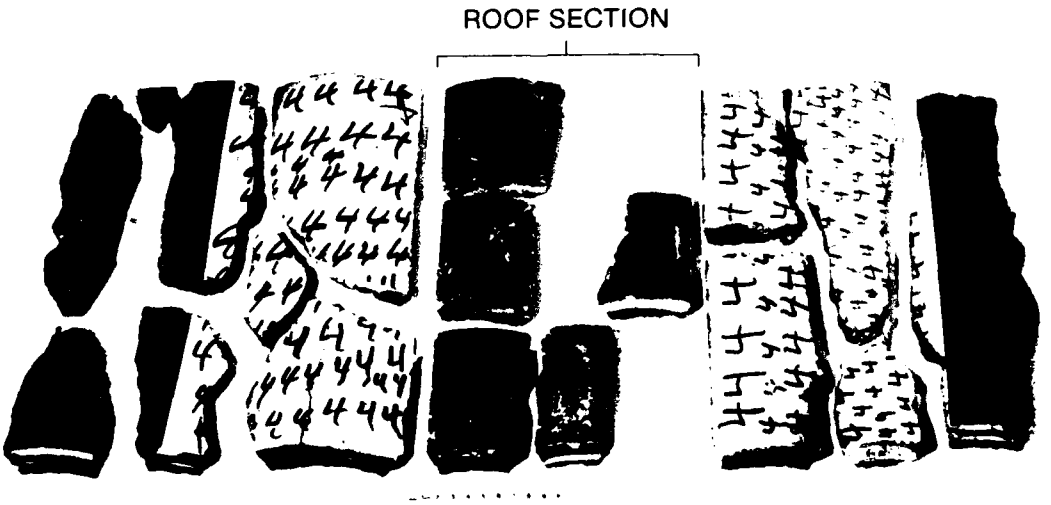

(b) RECOVERED TRENCH FRAGMENTS FROM TEST 17

MP-6307-17A

FIGURE 46 COMPARISON OF TRENCH CRACK PATTERN BETWEEN AFWL HAVE HOST TEST T-1 AND SRI TEST 17

4. ANALYTICAL INTERPRETATION OF THE EXPANSION AND VENTING DATA

To assure the consistency of the data, we performed some basic analyses, in which we treated response features separately and did not attempt to calculate the entire response in a single analysis. That is, in each analysis certain data were used as input and another part of the response was calculated. The response features analyzed were:

(1) Roof displacement calculated from the pressure measured at the reflecting wall

(2) Trench expansion at the springlines and invert calculated from the pressure measured at the reflecting wall

(3) Calibration pressure at the reflecting wall calculated from the pressure measured in the run-up section

(4) Expansion test pressure at the reflecting wall calculated from the corresponding calibration pressure and the expansion data.

This section describes the mathematical models used in these analyses and compares predicted and measured response.

4.1 ROOF DISPLACEMENT

The motion of the roof was calculated to verify the consistency of the pressure measurements and the roof displacement measurements. A one-dimensional model was found to be adequate to calculate the displacement of the roof up to the original soil surface level.

The mathematical model used to predict the roof displacement is shown in Figure 47. It consists of a partial ring of roof material and cover soil loaded by internal pressure. Inertial effects are dominant over the effects of soil strength. The roof/soil ring is assumed to

AD-A096 637 SRI INTERNATIONAL MENLO PARK CA F/G 16/1
LABORATORY INVESTIGATION OF EXPANSION AND VENTING AND PLUG RESP--ETC(U)
FEB 79 J R BRUCE, J K GRAN DNA001-77-C-0232
UNCLASSIFIED DNA-5235F NL

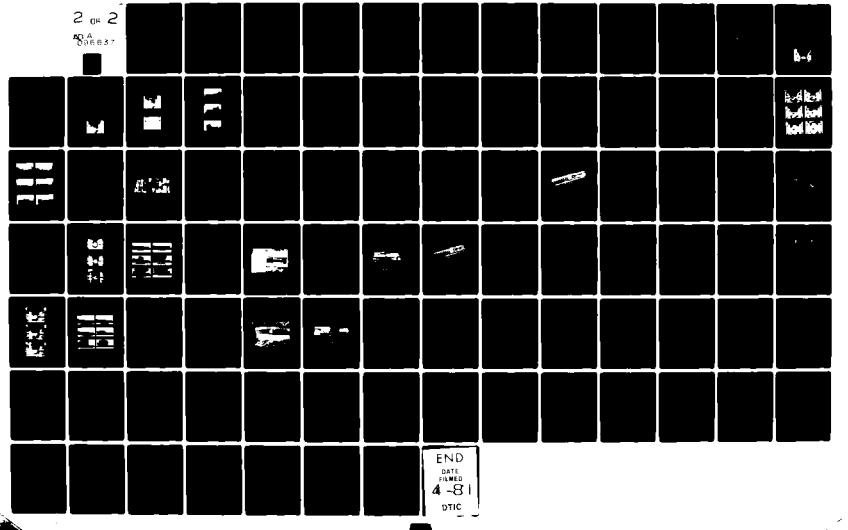

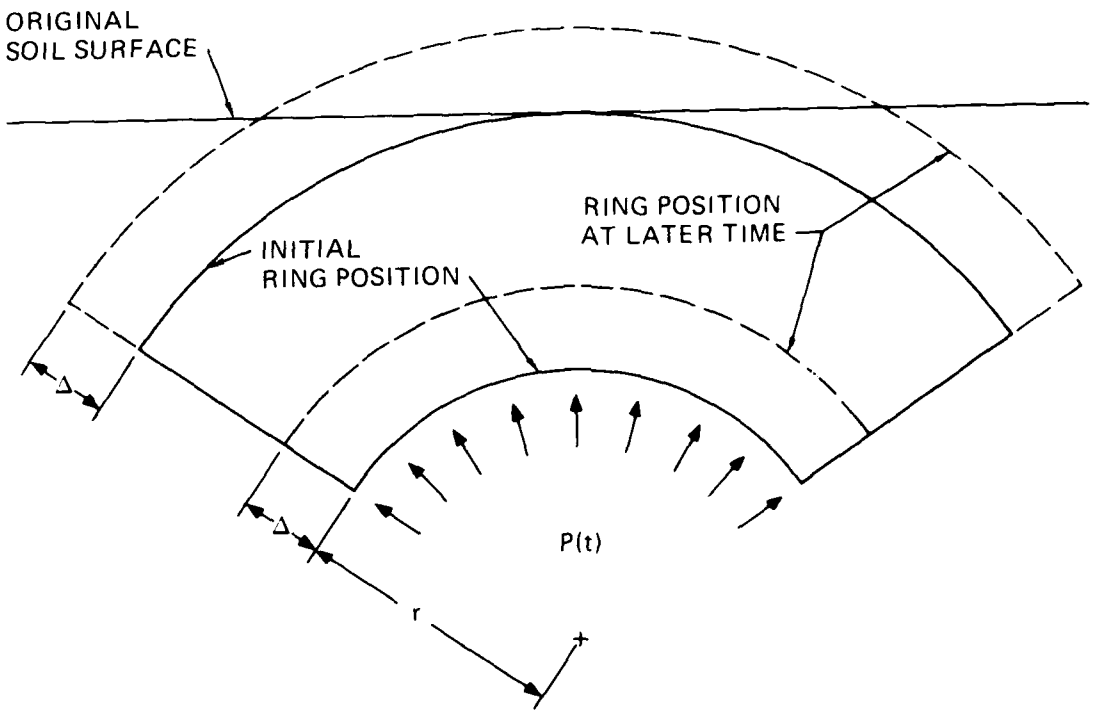

FIGURE 47 MODEL FOR PREDICTING ROOF DISPLACEMENT

to have a constant mass, and material strength is neglected. A kinematic constraint (consistent with observation) requires both the arc of the ring and the thickness to remain constant. Thus, as the inside radius grows, the loaded area increases and the mass density of the ring decreases. The equation of motion for this model is

$$2Pr = m \frac{d^2 r}{dt}$$

where P is the pressure, r is the inside ring radius, and m is the mass of the ring per unit length.

This model was used to calculate the roof displacement for each of the expansion and venting tests. Figure 48 compares the results of the calculations with roof displacement measurements taken from the Hycam movies for tests with peak reflected pressures of 700 psi (Test 17), 1100 psi (Test 18), and 2600 psi (Test 22). The soil displacement for Test 17 is also given, indicating that about 0.4 inch of compression was observed in the soil cover. The correlation of the calculations with the data enhances the reliability of the pressure and displacement measurements and indicates that the simple model for predicting roof motion is adequate.

4.2 SPRINGLINE AND INVERT DISPLACEMENT

The trench expansion into the surrounding soil was calculated to verify the consistency of the pressure and displacement data, and also to confirm the measurement of the soil wave speed from the movies of Test 16. The problem was formulated for an axisymmetric, plane strain analysis. Calculations were made with SRI PUFF, a finite difference computer code capable of analyzing two-dimensional continua undergoing large deformation (Reference 3).

The trench wall was modeled with typical concrete properties, allowing fracture at early time followed by rigid body translation of the trench fragments. The soil was modeled as a Mohr-Coulomb material without dilatancy. In this model the dilatational response is governed

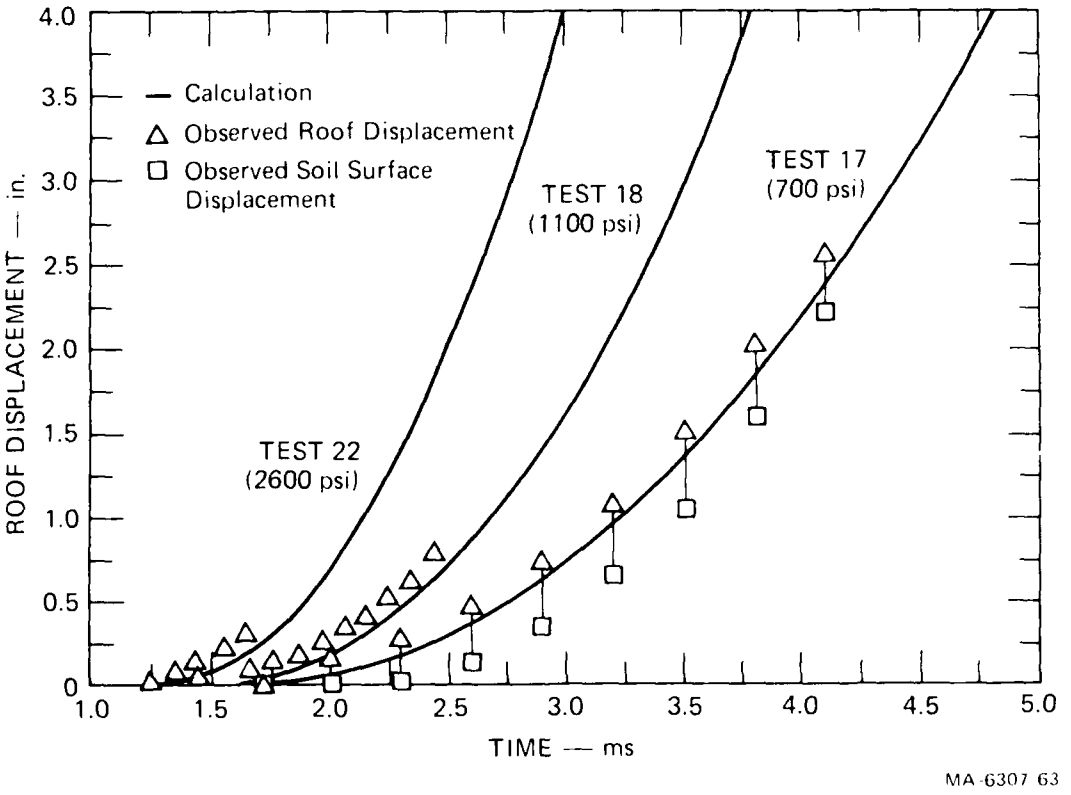

FIGURE 48 COMPARISON OF CALCULATED AND MEASURED ROOF DISPLACEMENT

by a variable bulk modulus (K). The distortional response is governed by two parameters, the cohesion c and the friction angle ϕ.

The soil properties were determined from WES's HAVE HOST backfill uniaxial strain test data (Reference 4), shown in Figure 49. (The soil used in the SRI experiments was also from the HAVE HOST site.) In the calculations, the loading pressure-volume path was made to follow the $\sigma_z - \varepsilon_z$ curves shown. For unloading, a bulk modulus equal to the maximum loading modulus shown was used. As shown below, a good correlation with the expansion test data was obtained using soil parameters computed from WES's lower bound curve for low density soil, the heavy curve in Figure 49(a), even though our measured wet soil density was 5% to 10% higher than WES's low density soil.

One reason for using the lower bound low density stress-strain curve is that the bulk modulus computed from that curve, up to about 4% vertical strain, agrees with the bulk modulus estimated from the observed wave speed by the elastic relation for a plane wave

$$\rho a^2 = 3K[(1 - \nu)/1 + \nu] \qquad (1)$$

where ρ is the mass density, a is the wave speed, and ν is Poisson's ratio. In Test 16 the measured wet soil density was 119 lb/ft^3, and the observed wave speed was 465 ft/s. For a Poisson's ratio of 0.35, the bulk modulus calculated from equation (1) is about 4000 psi. To compute the bulk modulus from the WES data, we first estimated the slope of the dynamic stress path for low density soil [Figure 49(b)] to be 2/3, providing the relation

$$(\sigma_z - \sigma_r) = 2/3[(\sigma_z + 2\sigma_r)/3] \qquad (2)$$

Next, defining the mean normal stress σ_m by $\sigma_m = (\sigma_z + 2\sigma_r)/3$ and eliminating σ_r, we can express σ_m in terms of σ_z

$$\sigma_m = 0.69\sigma_z \qquad (3)$$

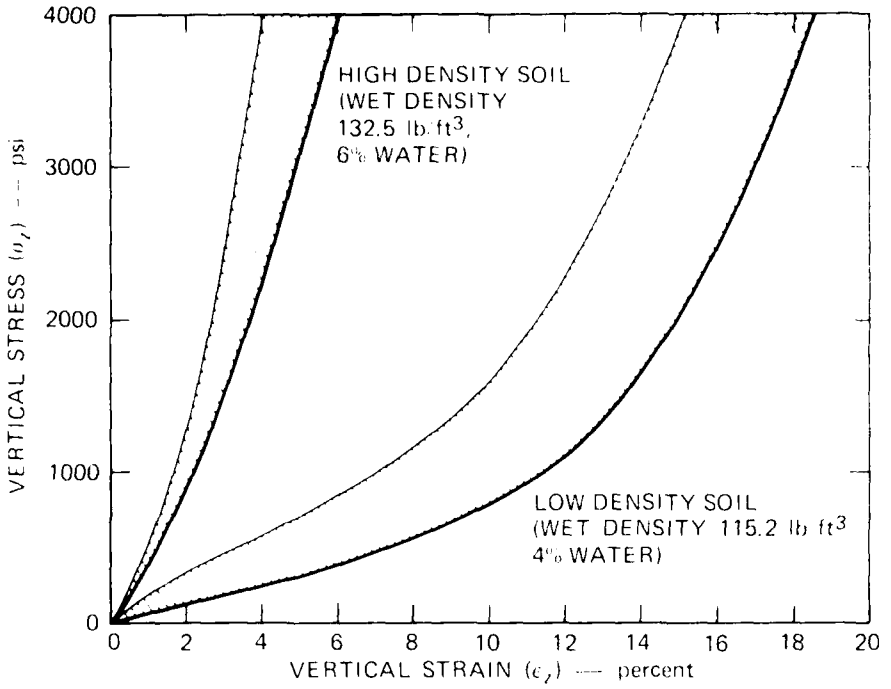

(a) BOUNDING UNIAXIAL STRESS-STRAIN RELATIONS

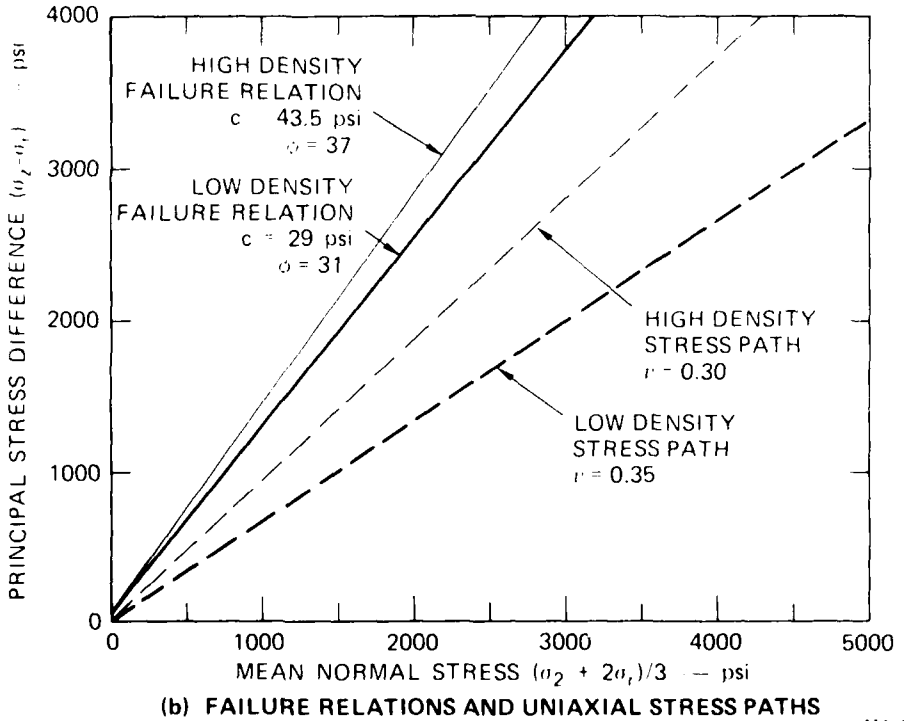

(b) FAILURE RELATIONS AND UNIAXIAL STRESS PATHS

MA 6307 64

FIGURE 49 WATERWAYS EXPERIMENTAL STATION'S UNIAXIAL STRAIN TESTS OF HAVE-HOST BACKFILL SOIL

We then used the stress-strain curve [Figure 49(a)] to obtain σ_m in terms of ε_z. Finally, we computed as the slope of the $\sigma_m - \varepsilon_z$ curve, since in this case ε_z is the total volumetric strain. Up to 4% strain, K has a constant value of about 4350 psi. This agrees to within 10% of the K value calculated from the wave speed measurement.

To further substantiate the choice of the low density soil data for computing our soil properties, we calculated the trench expansion due to the pressure measured in Test 17 (700 psi nominal) using both the lower bound low density soil data and the upper bound high density soil data. The values of ε and σ were taken directly from the WES data. The results of these two calculations are shown in Figure 50, along with the Test 17 results. Clearly, the low density soil data produce a more accurate expansion calculation.

We then made calculations of the wall motion using the pressures measured in Test 18 (1100 psi nominal) and Test 22 (2600 psi nominal) with the low density soil data. These calculations are also compared with the experimental results in Figure 50. Again, the calculations and the experiments correlate well enough to confirm the reliability of the pressure and expansion data and indicate that the computational model is adequate.

4.3 CALIBRATION PRESSURE AND SHOCK VELOCITY

The reflected shock pressure and the incident and reflected shock velocities were calculated for one of the load calibration tests (Test 13) to assure the reliability of those measurements. Reference 1 describes the theory used to calculate the pressures and velocities. Only the pertinent equations are repeated here.

The initial pressure in the test section p_1 is 14.7 psi and the particle velocity u_1 is zero. The measured incident pressure p_2 in Test 13 (Figure 3) is 200 psi. The shock strength p_{21} is given by the ratio of the pressures behind and in front of the shock front

$$p_{21} = p_2/p_1 = 13.6$$

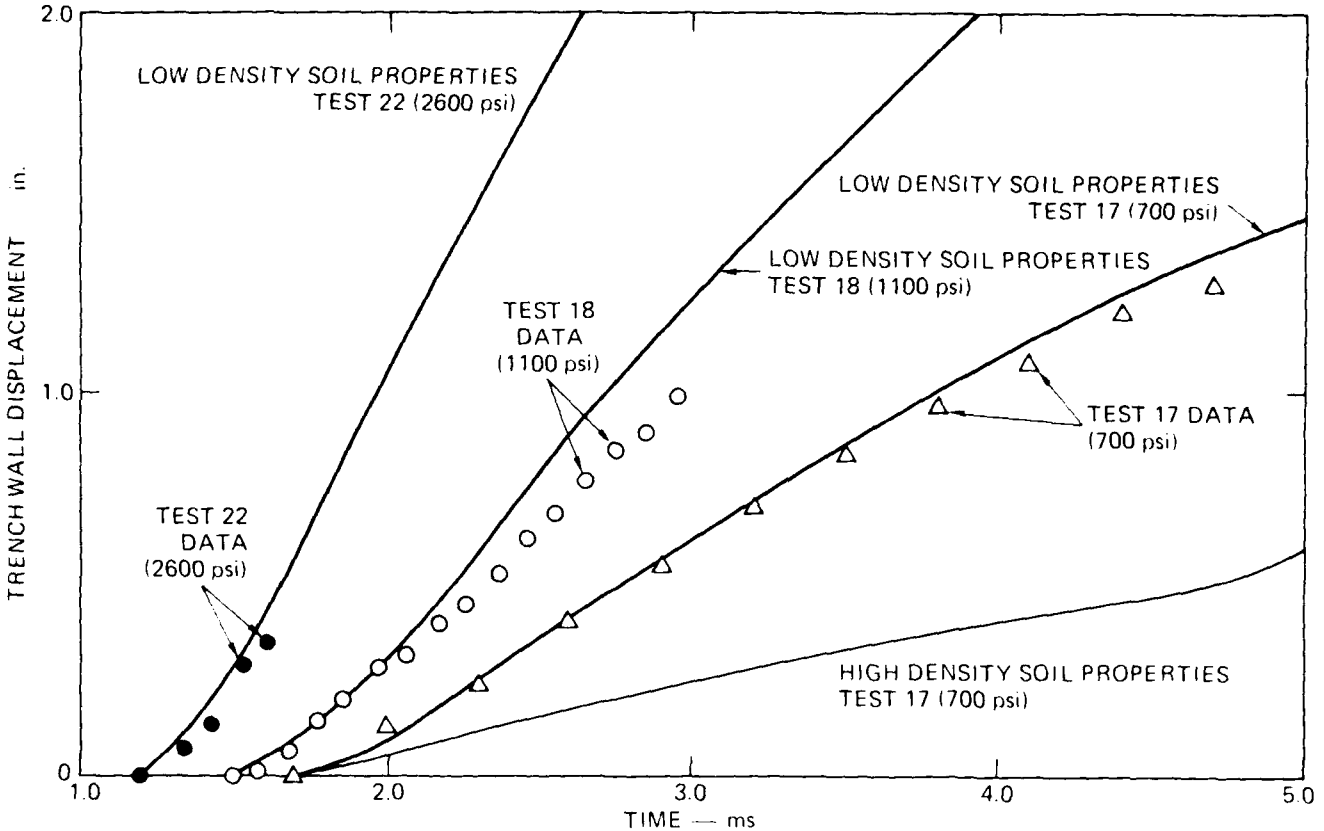

FIGURE 50 COMPARISON OF CALCULATED AND MEASURED SPRINGLINE AND INVERT DISPLACEMENTS

The ratio of specific heats γ for air at constant pressure and constant volume is taken to be 1.4. The sound speed a_1 in front of the shock is 1188 ft/s and the temperature T_1 is 90°F or 550°R.

The incident shock speed c_2 is given by

$$c_2 = \left(\frac{p_{21} + \gamma_1}{1 + \gamma_1}\right)^{\frac{1}{2}} a_1 = 4080 \text{ ft/s}$$

where $\gamma_1 = (\gamma - 1)/(\gamma + 1) = 0.167$

The particle velocity u_2 behind the incident shock front is

$$u_2 = \frac{a_1(p_{21} - 1)(1 - \gamma_1)}{[(p_{21} + \gamma_1)(1 + \gamma_1)]^{\frac{1}{2}}}$$

The temperature T_2 behind the incident shock front is

$$T_2 = p_{21} \frac{(1 + \gamma_1 p_{21})}{\gamma_1 + p_{21}} T_1 = 1777°R$$

The sound speed a_2 behind the incident shock front is

$$a_2 = a_1\sqrt{\frac{T_2}{T_1}} = 2130 \text{ ft/s}$$

The reflected pressure p_5 is given by

$$p_5 = \frac{(2\gamma_1 + 1)p_2 - \gamma_1}{\gamma_1 p_{21} + 1} p_2 = 1100 \text{ psi}$$

and $p_{52} = p_5/p_2 = 5.5$

the reflected shock velocity c_3 is given by

$$c_3 = \left(\frac{p_{32} + \gamma_2}{1 + \gamma_2} \right)^{\frac{1}{2}} \qquad a_2 = 4700 \text{ ft/s}$$

where $\gamma_2 = \gamma_1$.

Table 4 compares these calculations with the measurements of test 13. The experimental incident shock pressure is estimated from the records from gages P5 and P6 in the run-up section. The reflected shock pressure is the average over 2 ms of the record from gage P1 at the reflecting wall. The incident and reflected shock propagation velocities were determined from the times of arrival registered by gages P1 and P5. The good correlation between the calculations and the measurements indicates that the data are reliable.

Table 4

COMPARISON OF CALCULATED AND EXPERIMENTAL SHOCK PRESSURES AND VELOCITIES FOR CALIBRATION TEST 13

Quantity	Calculation	Experiment
Incident shock pressure	200 psi (p_2)	200 psi
Incident shock propagation velocity	4080 ft/s (c_3)	4380 ft/s
Reflected shock pressure	1100 psi (p_3)	1120 psi
Reflected shock propagation velocity	1590 ft/s ($c_3 - u_3$)	1580 ft/s

CALCULATION OF PRESSURE DECAY IN EXPANSION AND VENTING TESTS

In this analysis, we computed the decay in the expansion and venting test pressures at the reflecting wall from the corresponding calibration pressures and the trench expansion data. In particular, we investigated the effect of the expansion on the pressure.

Axial flow into the test section is taken to be zero and the expansion process is assumed to be adiabatic. With these assumptions the expansion and venting test pressure P(t) is given by

$$P(t) = P_c(t) \left[\frac{V_o}{V(t)} \right]^{\gamma}$$

where t is time, P_c is the corresponding calibration pressure, V_o is the original volume of the test section, V is the expanded test section volume, and γ is the ratio of specific heats for air. This expression was evaluated for the digitized calibration pressure records. The expanded volume V(t) was estimated from the roof, springline, and invert displacement data at the reflecting wall. A value of 1.4 was assumed for γ.

The results of this calculation for Test 17 are shown in Figure 51 along with the calibration pressure (Test 12) and the measured pressure in Test 17. The calculation was terminated at about 4.1 ms since venting was known to begin then. The comparison indicates that expansion accounts for the pressure drop for about 0.5 ms after the shock arrival. After that, the calculated pressure falls below the measured pressure, indicating that axial flow toward the reflecting wall must have occurred in the shock tube.

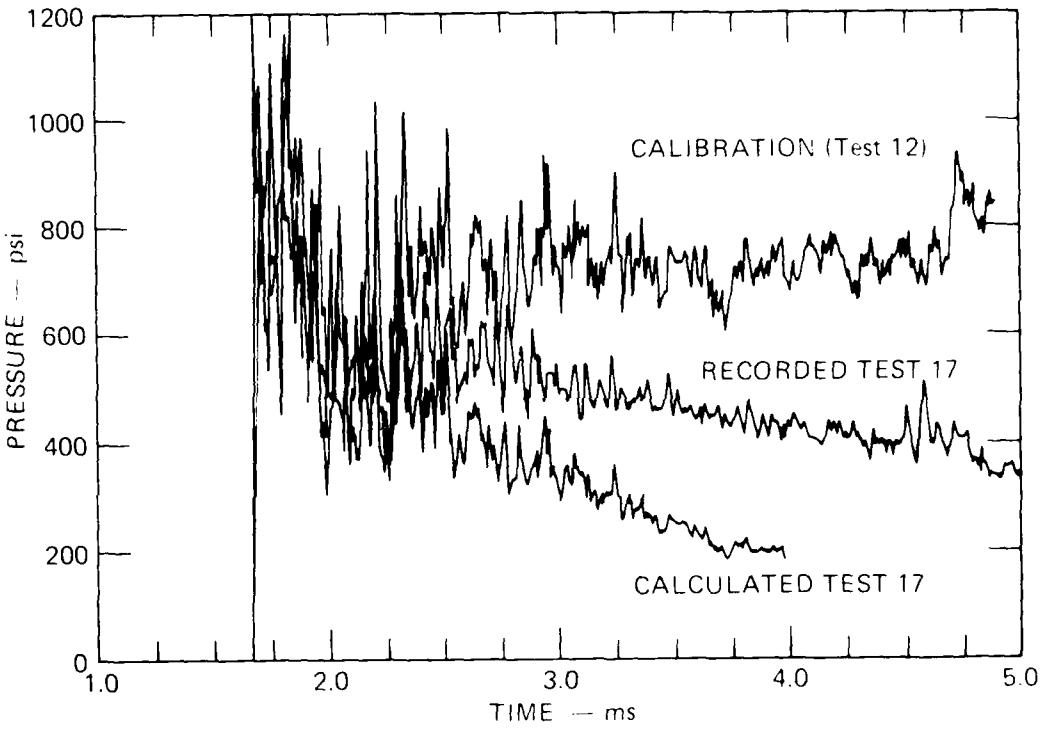

MA 6307 66

FIGURE 51 CALCULATION OF THE EXPANSION TEST PRESSURE AT THE REFLECTING WALL

(From the corresponding calibration pressure and the expansion data)

5. CONCLUSIONS FROM THE EXPANSION AND VENTING TESTS

The results of our scale model experiments and basic analyses suggest several conclusions regarding trench expansion dynamics and the effects of the pressure history, soil properties, and structural properties.

5.1 TRENCH EXPANSION DYNAMICS

The following general features of the response of the MX trench to internal pressure appear to be independent of loading, geometry, and material properties for the range of variables studied.

(1) Several longitudinal cracks form in a circumferentially symmetric distribution in the trench wall almost immediately (within 0.3 ms) after the arrival of the shock wave. Figure 52 shows the cracking patterns observed in Test 17.

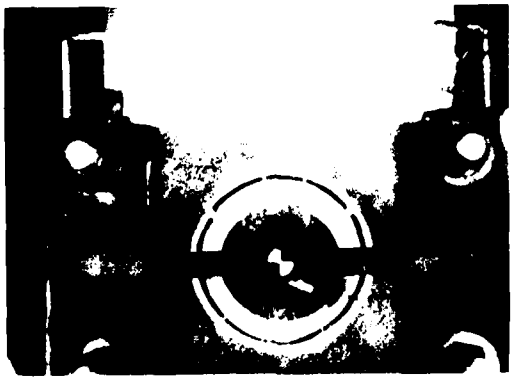

(t = 2.20 ms, Test 17)

MP-6307-15B

FIGURE 52 TRENCH CRACKING PATTERN

(2) The expansion of the trench into the soil is cylindrically symmetric until the rarefaction wave returns from the free soil surface to the trench roof. Figure 53 illustrates this phenomenon as observed in Test 17. In this illustration, the shock wave arrives at the reflecting wall at 1.7 ms, and the trench begins to expand symmetrically. Based on a soil wave speed of 465 ft/s (observed in Test 16), the pressure wave in the soil reaches the surface about 0.45 ms later, after which the soil surface begins to move also. After another 0.45 ms the relief wave from the soil surface reaches the crown, ending the symmetric phase of the expansion.

(3) After the symmetric expansion phase, the slug of roof fragments moves off in the vertical direction with little or no change of shape until venting occurs. The soil above the crown mounds up without much lateral flow. The expansion of the trench at the springlines and floor continues to be approximately symmetric. Figure 54 illustrates this phase of expansion in Test 17.

(4) Venting begins at the roof crack nearest the crown, when the trench roof has moved to about the level of the original soil surface. Initiation of venting in Test 17 is shown in Figure 55. In the cases where the roof did not crack, no venting was observed.

(5) Venting, even at late times, occurs only directly above the roof. The soil mounds up very steeply, forming a large opening for venting, but the surface is not broken anywhere else. This phenomenon is illustrated in Figure 56, again for Test 17.

(6) Once venting begins (near the reflecting wall), the soil surface unzips along the length of the trench at about the same rate as the propagation of the reflected shock wave. This phenomenon as observed in Test 17, is illustrated in Figure 57. (The unzipping phenomenon was difficult to observe with short test sections, especially at the higher pressures; tests with longer sections are needed to verify this response feature.)

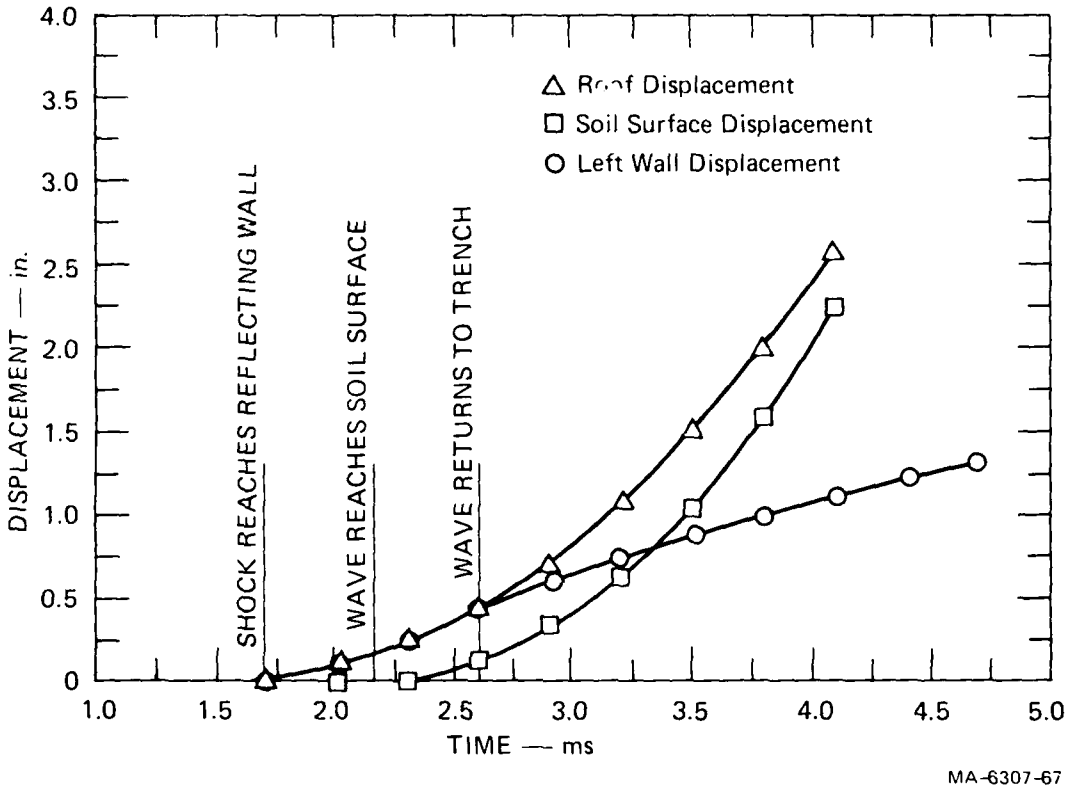

FIGURE 53 SYMMETRIC TRENCH EXPANSION PHASE (Test 17)

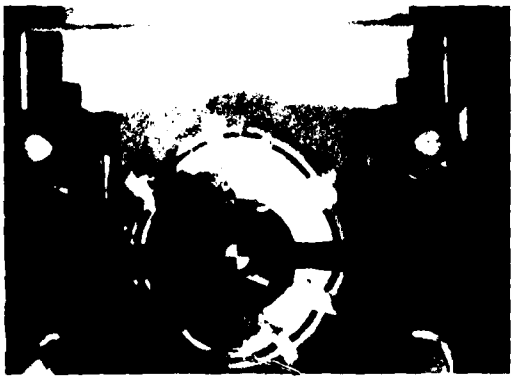

(t = 3.70 ms, Test 17)

MP-6307-15C

FIGURE 54 ASYMMETRIC EXPANSION PHASE

(t = 4.20 ms, Test 17)

MP-6307-15D

FIGURE 55 INITIATION OF VENTING AT CRACK NEAREST CROWN

(t = 6.30 ms, Test 17)

MP-6307-68

FIGURE 56 LATE-TIME VENTING

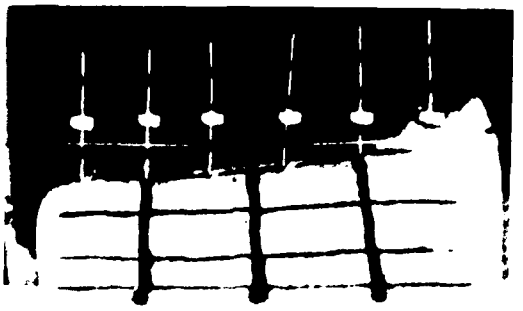

t = 4.10 ms

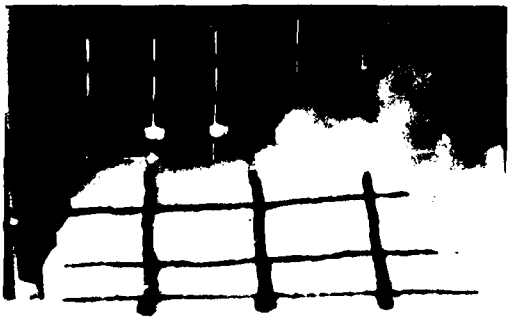

t = 4.50 ms

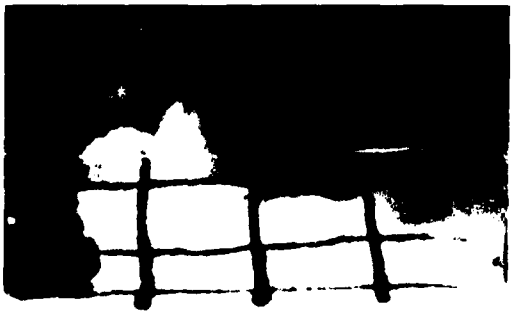

t = 4.95 ms

MP-6307 168

FIGURE 57 UNZIPPING PHENOMENON (Test 17)

5.2 EFFECT OF PRESSURE

The principal effect of higher pressure is to speed up the response. In addition, trends were noted with respect to trench fragmentation and venting.

The venting trend is illustrated in Figure 58, where the time of venting and roof displacement at time of venting are plotted against pressure for the expansion and venting tests (Tests 17, 18, 19, 20, 22, and 30) and the plug/trench interaction test (Test 21, described in Section 6). For this series of tests, a higher pressure caused venting to occur sooner and with less roof displacement. The pressure for Test 21 is only estimated since no gage existed at the plug face. The lines drawn through the data are not fitted curves; they only indicate the trend. The data from Tests 18 and 19 do not lie near the lines. Even though Tests 18 and 19 demonstrated repeatability of several measurements, the venting data from these tests are considered anomalous because venting initiated at a photo pin.

The effect of pressure on trench fragmentation is illustrated in Table 5, which lists the number of longitudinal cracks seen in both clay and reinforced concrete trench models at various pressures. These data suggest that slightly more cracking occurs at higher pressures.

Table 5

EFFECT OF PRESSURE ON LONGITUDINAL CRACKING

Nominal Peak Pressure	Number of Cracks	
	Clay	Reinforced Concrete
400		9 (Test 30, thin-wall ribbed)
800	6 (Test 11)	8 (Test 17)
800	5 (Test 15)	
1500		10 (Test 18)
1500		9 (Test 19)
1500		7 (Test 20)
2400	9 (Test 16)	
3000		12 (Test 22)

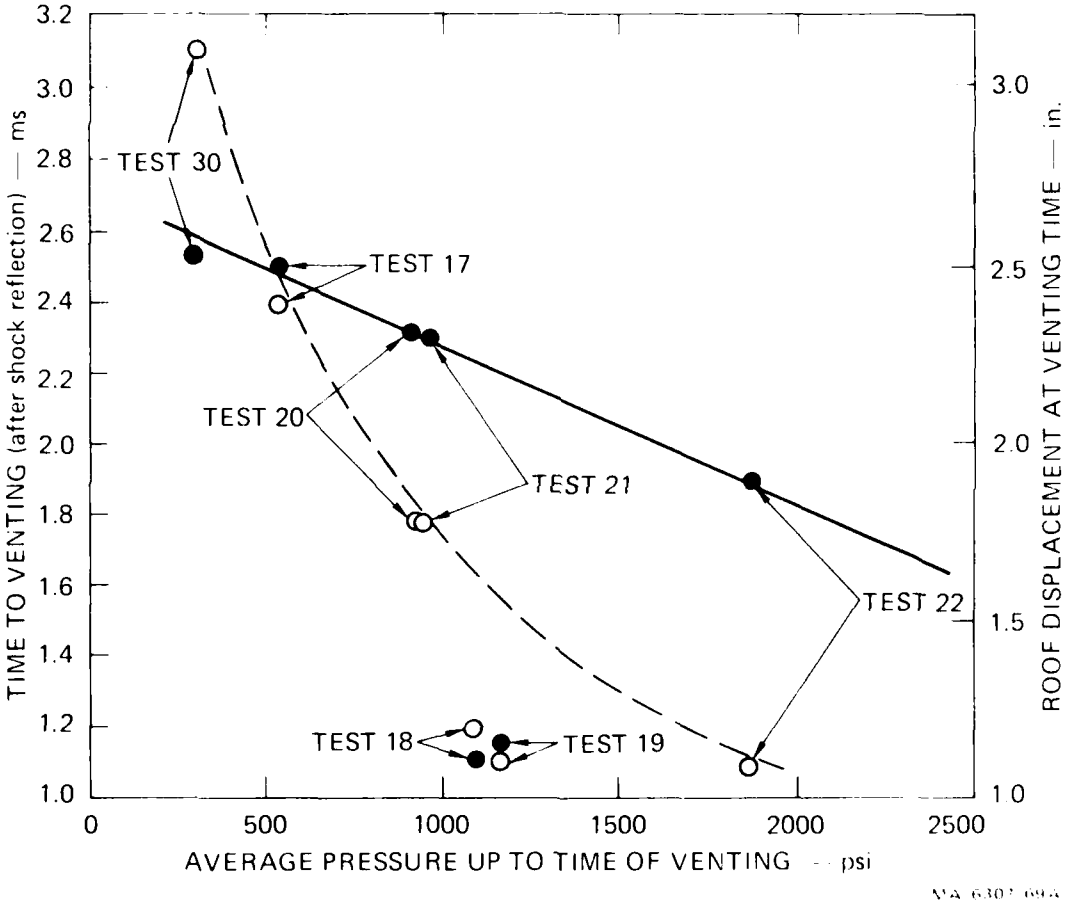

FIGURE 58 EFFECT OF PRESSURE ON VENTING TIME AND ROOF DISPLACEMENT AT VENTING TIME FOR REINFORCED CONCRETE TRENCHES
(○ venting time, ● roof displacement)

5.3 EFFECT OF SOIL PROPERTIES

For the range of soil properties of interest and for the range of pressures studied, analysis showed soil strength to significantly affect trench expansion below the springlines. Soil density has only a moderate effect except indirectly through the soil strength. That is, more compacted soil has a higher strength.

For a given pressure, the motion of the roof depends only on soil density. The trench expansion at the springlines and floor depends on soil strength. Using the analyses described in Section 4.1 and 4.2, and the pressure measured in Test 17 (700 psi), we calculated the trench expansion with the upper and lower bound soil properties provided by WES (Figure 49). The results of the calculations are plotted in Figure 59.

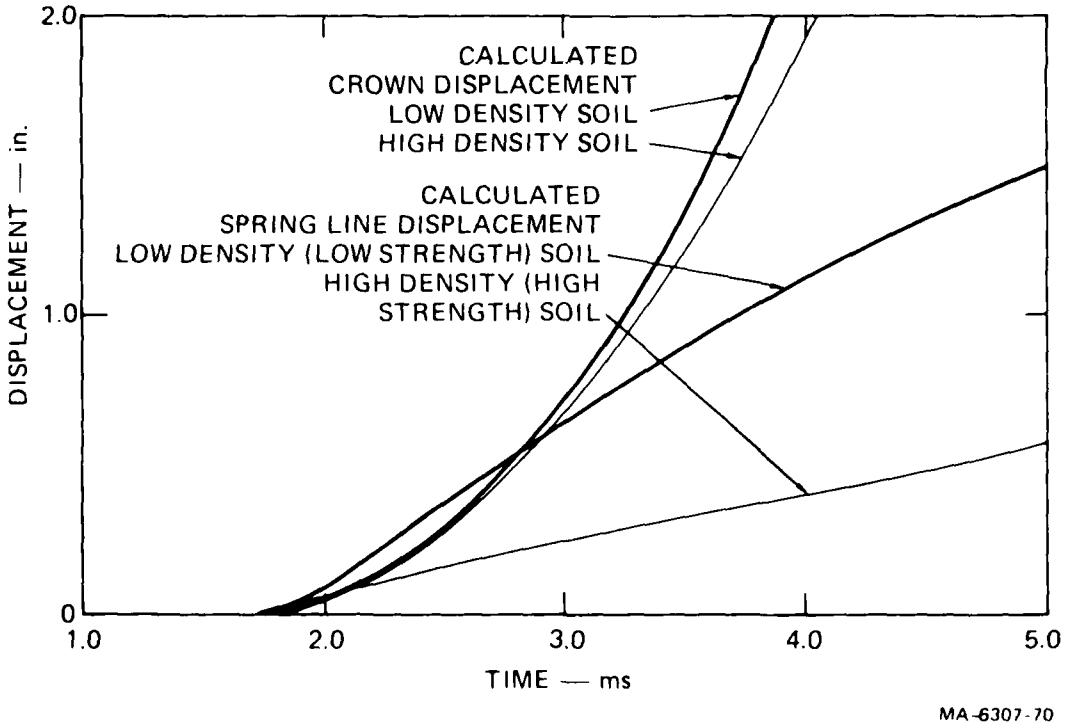

FIGURE 59 COMPARISON OF CALCULATED TRENCH EXPANSION FOR LOW DENSITY AND HIGH DENSITY BOUNDING SOIL PROPERTIES

The range of the calculated responses indicates the sensitivity of the expansion to soil compaction at this low pressure. Further study is necessary to determine this sensitivity at higher pressures.

The effect of moisture content on venting is thought to be minimal. In Test 20, where the soil was dried to about 1% water, venting occurred later than in Tests 18 and 19, which had the same loading. However, we attribute the early venting time in those two tests to the photo pins and not to the soil differences.

5.4 EFFECT OF TRENCH STRENGTH AND GEOMETRY

Differences in trench strength and geometry have only a small effect on trench expansion, but a larger effect on trench cracking and initiation of venting. This is seen by comparing the results of Tests 15 and 17. The soil used in both tests was from the HAVE HOST site, at approximately the same moisture content and density. The same explosive loading was used in both tests. The trench parameters for these tests are given in Table 6. The clay trench used in Test 15 had thicker walls and had a higher tensile strength than the fiber-reinforced concrete trench used in Test 17. The higher tensile strength of the clay is attributed to the fact it had been fired. Another difference between the two trenches was that the angle of the roof section was 90 degrees for Test 15 and 110 degrees for Test 17.

In Test 15, the roof section did not crack and venting did not occur. In Test 17, the roof cracked near the crown and venting began there about 2.4 ms after the shock arrived. In Test 15, five longitudinal cracks occurred; in Test 17, eight occurred. The expansion data for both tests are plotted in Figure 60. No appreciable difference is seen in the expansion of the two trenches at the springlines and invert. The difference in roof displacement is due to the greater mass (thicker wall, deeper soil) lifted in Test 15. Thus, the principal phenomena affected by trench strength and geometry appear to be trench cracking and venting initiation. However, further parameter testing is necessary to determine individually the effects of strength and geometry.

Table 6

TRENCH PARAMETERS FOR TESTS 15 AND 17

	Test 15	Test 17
Trench material	Clay	Reinforced concrete
Density	120 lb/ft³	120 lb/ft³
Ratio of inside radius to thickness	3	4
Roof section arc	90°	110°
Cover soil depth	2.5 in.	2.3 in.
Tensile strength	4120 psi*	930 psi* 1010 psi**

*Determined in three-point bending tests.

**Determined in split-cylinder tests.

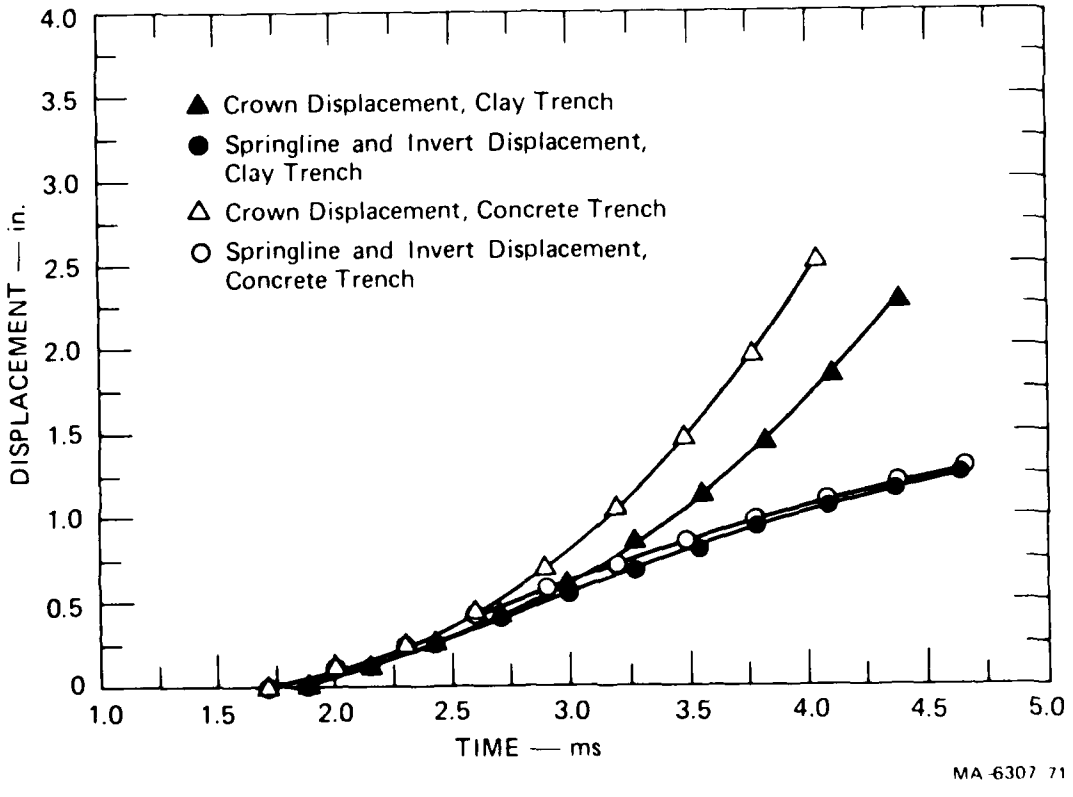

FIGURE 60 COMPARISON OF MEASURED TRENCH EXPANSION FOR CLAY AND REINFORCED CONCRETE TRENCH MODELS (Tests 15 and 17)

6. PLUG/TRENCH INTERACTION TESTS

Three plug/trench interaction tests were performed. The first test (Test 21) was performed with a simple 4-inch-long steel plug in a non-ribbed model trench. This experiment provided some initial data on leakage and crack propagation past a stationary plug.

The second and third tests (Tests 35 and 36) were performed on plug models that were simple, but more realistic. To simulate the design pressure and impulse for these plug tests, we performed an additional series of load calibration tests. Two of these load calibration tests (Tests 34 and 33), correspond to tests on plugs (Tests 35 and 36) and are described below.

6.1 SIMPLE PLUG/TRENCH INTERACTION TEST (TEST 21)

Test 21 was conducted for a nominal reflected pressure of 1100 psi using the same explosive configuration as calibration Test 13 (Section 2). Pressure records from calibration Test 13 are shown in Figure 3. As in the expansion and venting tests, the input pressure is a square wave (nondecaying) during the 5-ms test time.

The model trench used in Test 21 was the same as the models used in most expansion and venting tests (6-inch-ID, 12-inch-long, 0.75-inch-wall-thickness, and fabricated without internal ribs). Two longitudinal 0.56-inch-deep saw cuts offset 100 degrees from each other and two transverse 0.56-inch-deep saw cuts at the third points were used to separate the roof block.

The experiment setup is shown in Figure 61. (The complete small-scale shock tube assembly and loading technique were described in Sections 2 and 3.) A 6-inch-diameter, 4-inch-long steel plug was inserted at the reflecting wall end of the model trench. The clearance between the plug and the trench wall was 0.005 inch. The face of the

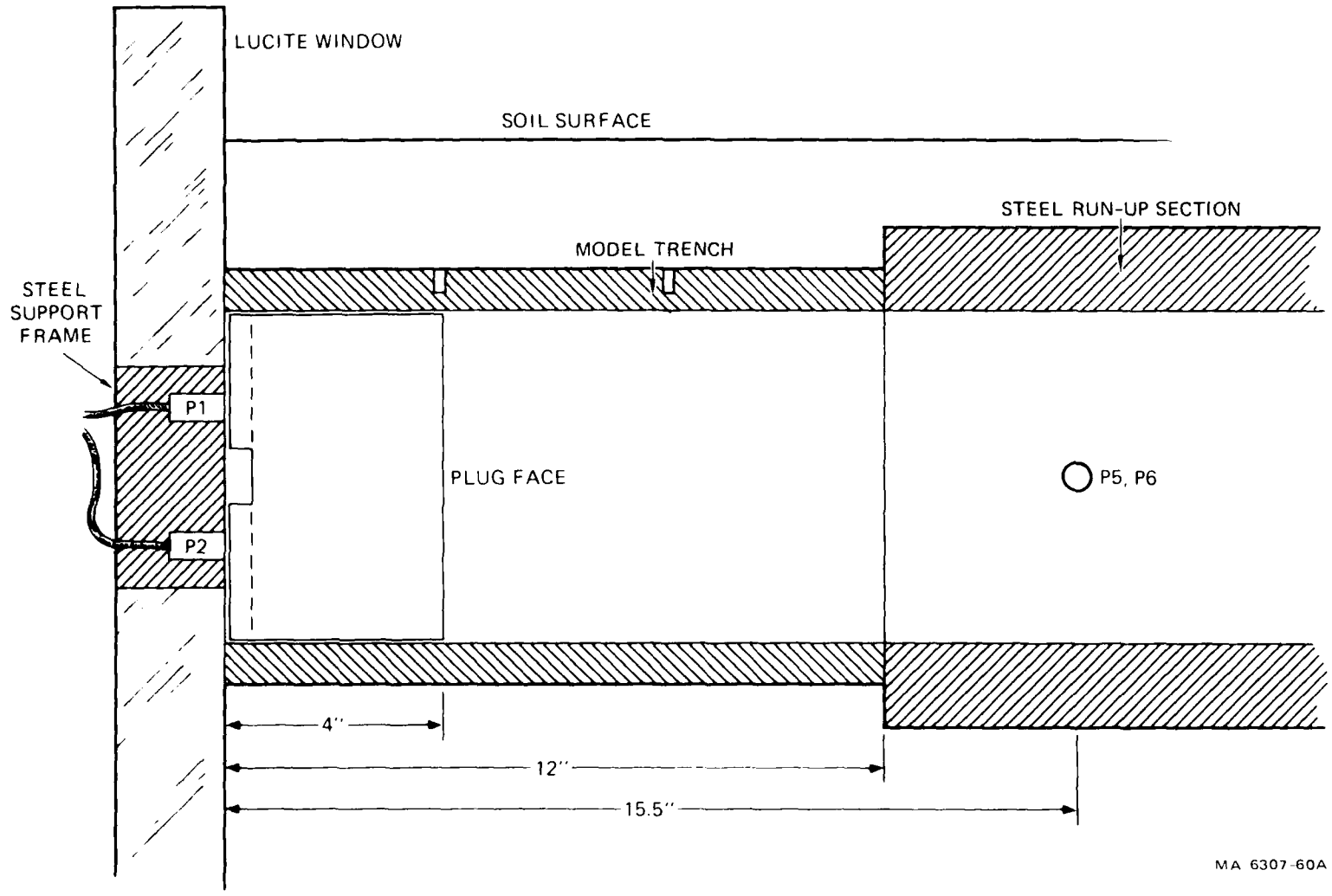

FIGURE 61 PLUG/TRENCH INTERACTION TEST

plug was aligned with the center of the transverse saw cut that formed the end roof block; the back of the plug rested against the reflecting wall.

As shown in Figure 61, the shock enters from the right, propagates into the model trench and reflects off the plug face. Three pressure gages measure the shock pressure in the steel run-up section. Two of these gages, P5 and P6 were located 11.5 inches upstream of the plug face. The third gage, P7, was located 34.5 inches upstream of the plug face (not shown in Figure 61). Two 1-inch-wide, 0.5-inch-deep grooves were machined in the back of the plug to provide a plenum for pressure gages P1 and P2 behind the plug.

As in the expansion and venting tests, the volume around the model trench was backfilled with HAVE HOST soil with a trench cover of 2.3 inches. The soil was compacted to 117 lb/ft^3, with a 3.9% moisture content.

The digitized pressure records from Test 21 are plotted in Figure 62. Gages P1 and P2 at the back of the plug registered over 1000 psi, indicating that considerable blow-by occurred. A comparison of these records with those from Test 18 at the same loading without a plug shows that, at the reflecting wall, the gross effect of the plug was to chop off the first 0.7 ms of reflected pressure [compare Figure 24(b) with Figure 62(b)]. At gages P5 and P6 (the open end of the trench), the effect was to simply reflect the incident wave about 0.7 ms earlier.

Two high-speed cameras (Hycams) were used to photograph the response; one was aimed at the Lucite window at the end of the test section and one was aimed at the soil surface from the side. Selected frames from the Hycam movies are shown in Figures 63 and 64. In the end view the film speed was 10,550 frames per second. In the side view the film speed was 10,730 frames per second. The films show that the trench expansion at the reflecting wall was nearly the same as in Test 18, but the entire process was delayed by the effect of the plug. Venting first occurred at the crown near the plug face at about t = 3.20 ms, 1.7 ms after the shock reflects off the plug face. This time is consistent with the time

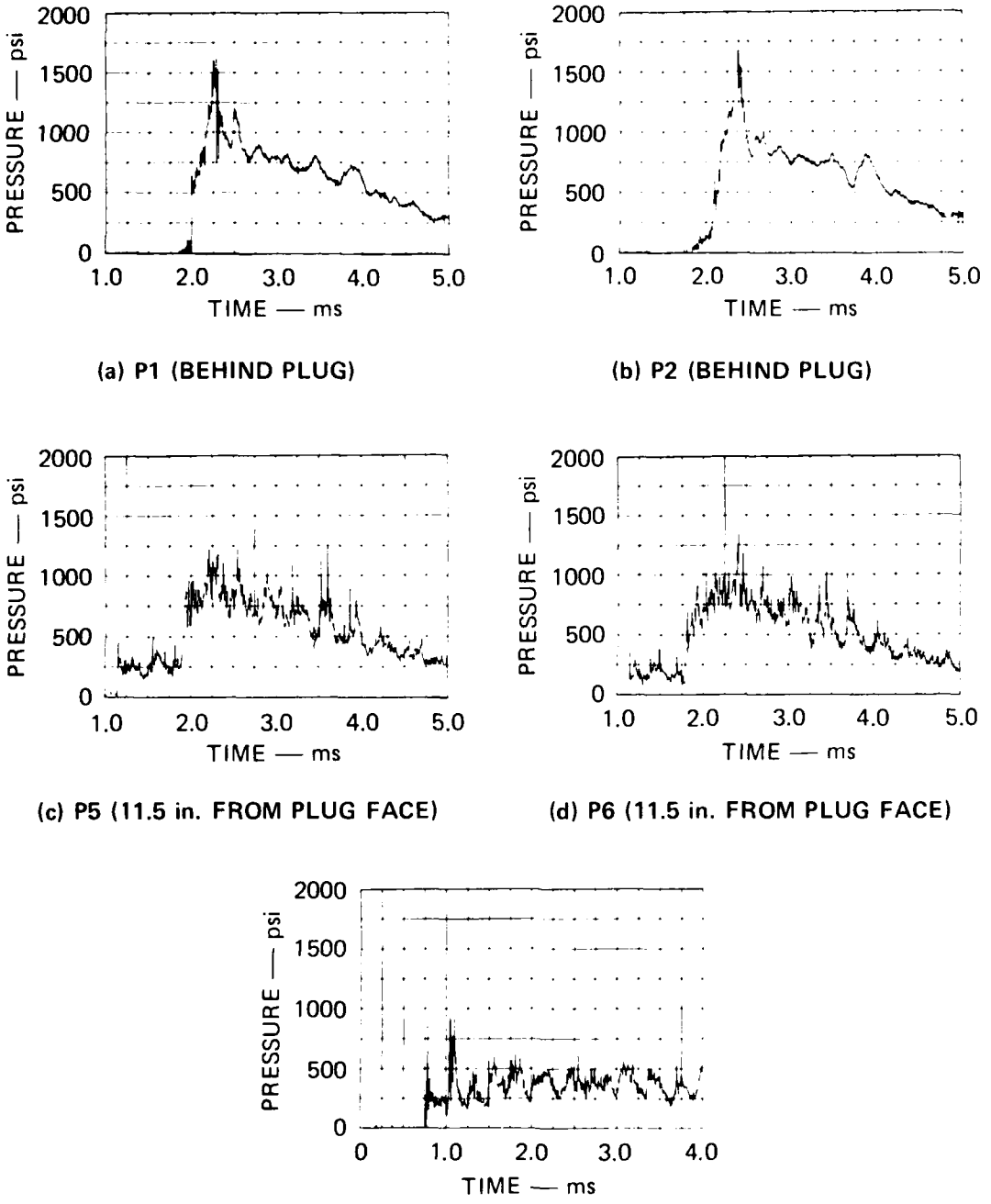

FIGURE 62 PRESSURE RECORDS FROM TEST 21

Explosive charge 800 gr/ft

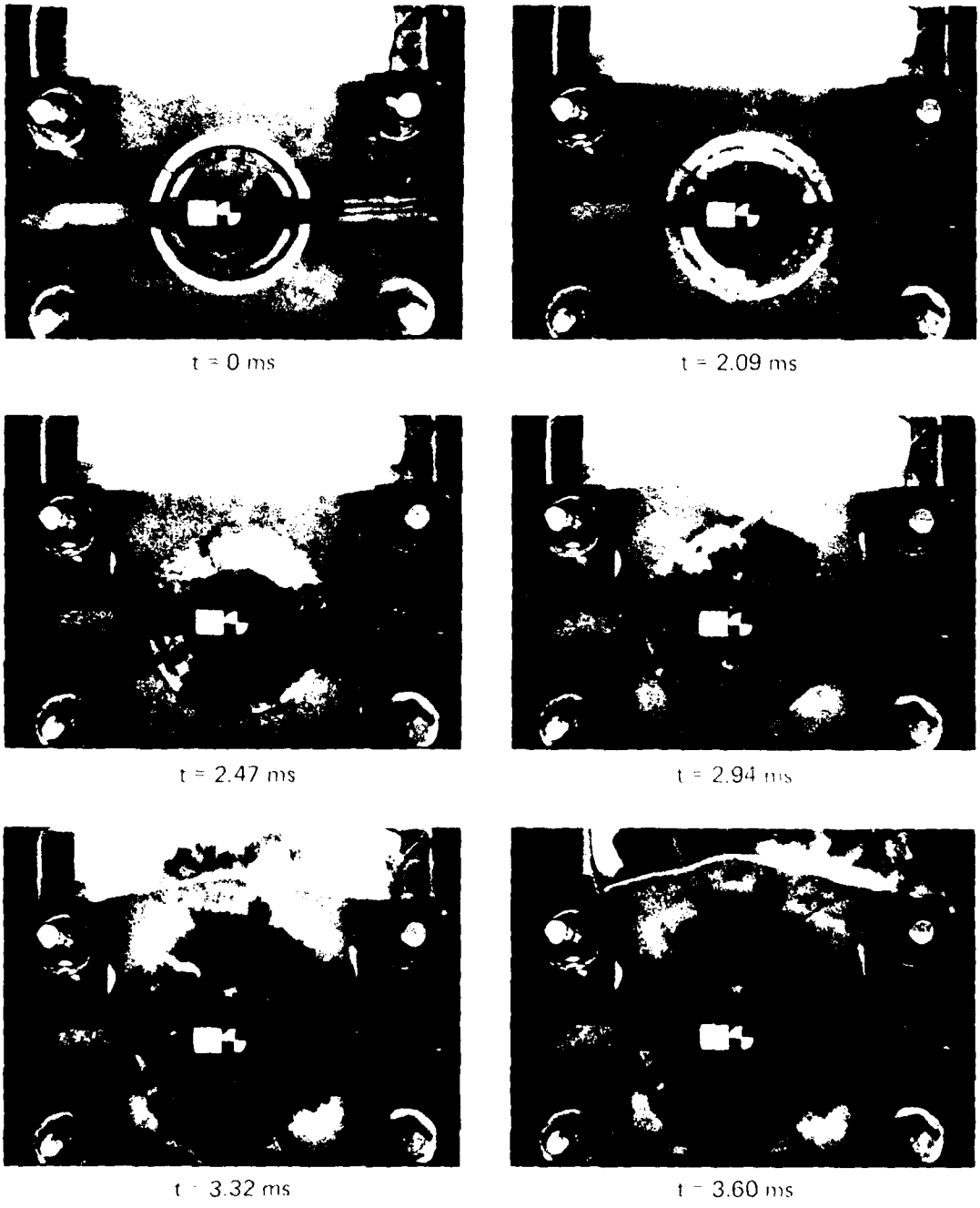

FIGURE 63 HYCAM PICTURES (End View, Test 21)

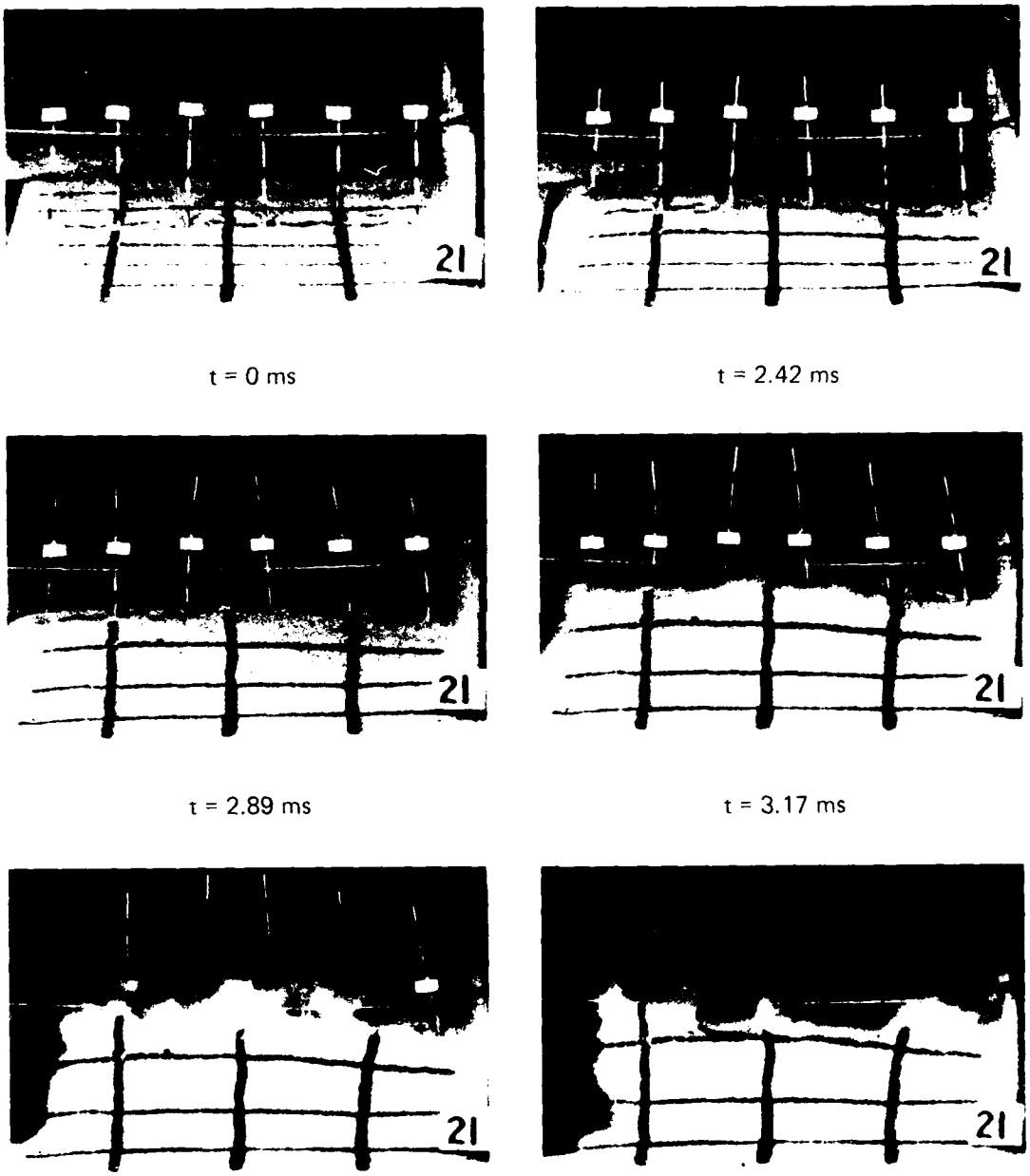

FIGURE 64 HYCAM PICTURES (Side View, Test 21)

of venting after shock reflection seen for the expansion and venting tests (Figure 58). The roof section at this location had moved about 2.3 inches. The recovered trench fragments, shown in Figure 65, indicated that longitudinal cracks in the roof, walls, and floor of the trench extended from end to end. That is, the portion of the trench surrounding the plug cracked and expanded with the rest of the trench, providing an open path for the high pressure gas to the back of the plug.

6.2 PLUG MODEL TESTS (TESTS 35 AND 36)

Current candidate plug designs combine the concepts of a leaky plug that allows blow-by and a solid plug downstream of the leaky plug that seals the trench to provide a "safe section." The concept is that the leaky plug reflects a portion of the air shock, causing the trench to open up and vent sooner thereby lowering the load on the solid plug. (The leaky plug in the Martin Marietta design consists of semirigid baffle plates; in the Boeing design, it is a flexible slotted drag seal.)

Our strategy was to study first the phenomenology of the plug/trench interaction with simple plug models. Our test series consisted of testing a simple leaky plug alone (Test 35) and then a simple solid plug alone (Test 36). This division leads to a clearer understanding of the phenomenology associated with each type of plug.

The MX plug design loading is an air shock with a 600-psi peak pressure and an exponential decay having a characteristic time of about 3 ms at 1/26-scale. This design loading was used as the desired upstream waveform for the leaky plug test. The desired upstream waveform for the solid plug test was chosen as a 200-psi peak pressure, again with an exponential decay having a characteristic time of about 3 ms. This lower pressure accounts for the absence of any load attenuation mechanisms (i.e., leaky plug) in front of our solid plug model.

Plug Load Calibration Tests

Calibration tests using a rigid steel test section were performed at loadings corresponding to both the leaky plug and solid plug tests.

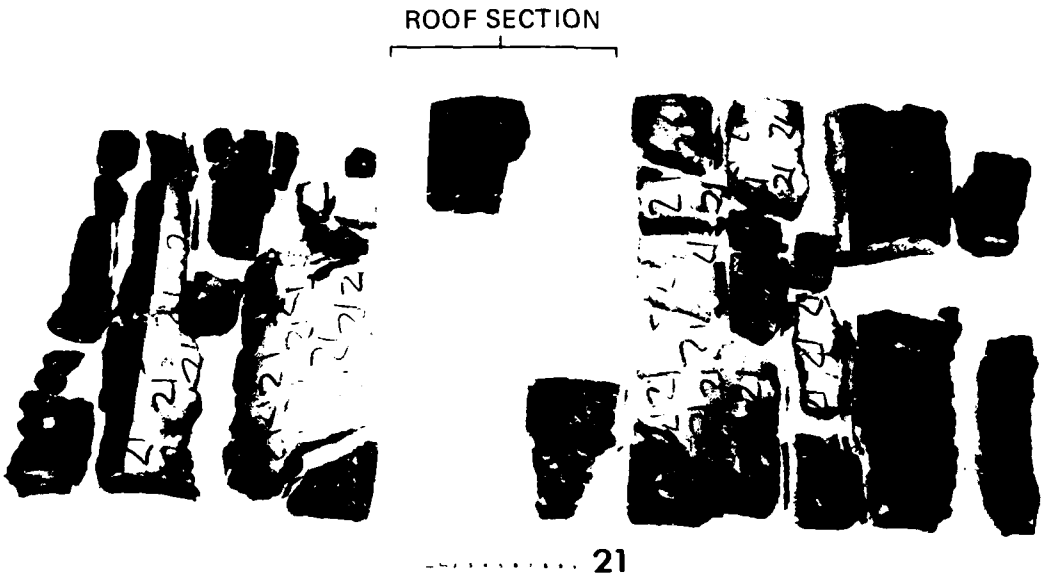

MP-6307-61

FIGURE 65 TRENCH FRAGMENTS RECOVERED FROM TEST 21
Front of trench is at bottom.

Figure 66 shows the shock tube assembly modified for the plug load calibration tests. For both wave forms, the explosive charge used was a mix of PETN and hollow glass microballoons in a 5-inch-diameter cylinder. (The microballoons lower the detonation pressure in the explosive, thereby lowering the stress in the driver section of the shock tube.) The charge was back-detonated in three places. To achieve the correct characteristic time, we increased the length of the driver section to 24 feet. The aft end of the shock tube was left open to prevent a second shock reflection.

In calibration Test 33, a 312-g, 5-inch-thick charge of PETN/microballoons was used. The charge standoff distance from the rigid reflecting wall was 20.5 feet. The pressure records for Test 33 are given in Figure 67. A 600-psi upstream waveform with a decay similar to the desired pressure-time history for the leaky plug test was generated. The upstream (indicent) waveform can be seen in the records from gages P3 through P7. At the wall, the reflected pressure was 3600 psi (gages P1 and P2).

In calibration Test 34, a 78-g, 1.25-inch-thick charge of PETN/microballoons was used. The charge standoff distance from the rigid reflecting wall was 20.5 feet. The pressure records for Test 34 are given in Figure 68. A 180-psi upstream waveform similar to the desired pressure-time history for the solid plug test was generated. The upstream (incident) waveform can be seen in the records from gages P3 through P7. At the wall, the reflected pressure was 1000 psi (gage P1 and P2).

Test 35 (Leaky Plug)

The simple leaky plug design is shown in Figure 69. It consists of three rigid aluminum cylinders: a 6-inch-long front cylinder with a 0.15-inch gap between the cylinder outside diameter and the trench rib inside diameter (the leaky plug), a 10.25-inch-long support shaft, and a 3-inch-long base. This base rested against the rigid end wall of the shock tube assembly. The plug assembly represents a simple leaky plug rigidly supported by an "ideal" solid plug. The weight of the entire plug assembly was 33.9 pounds.

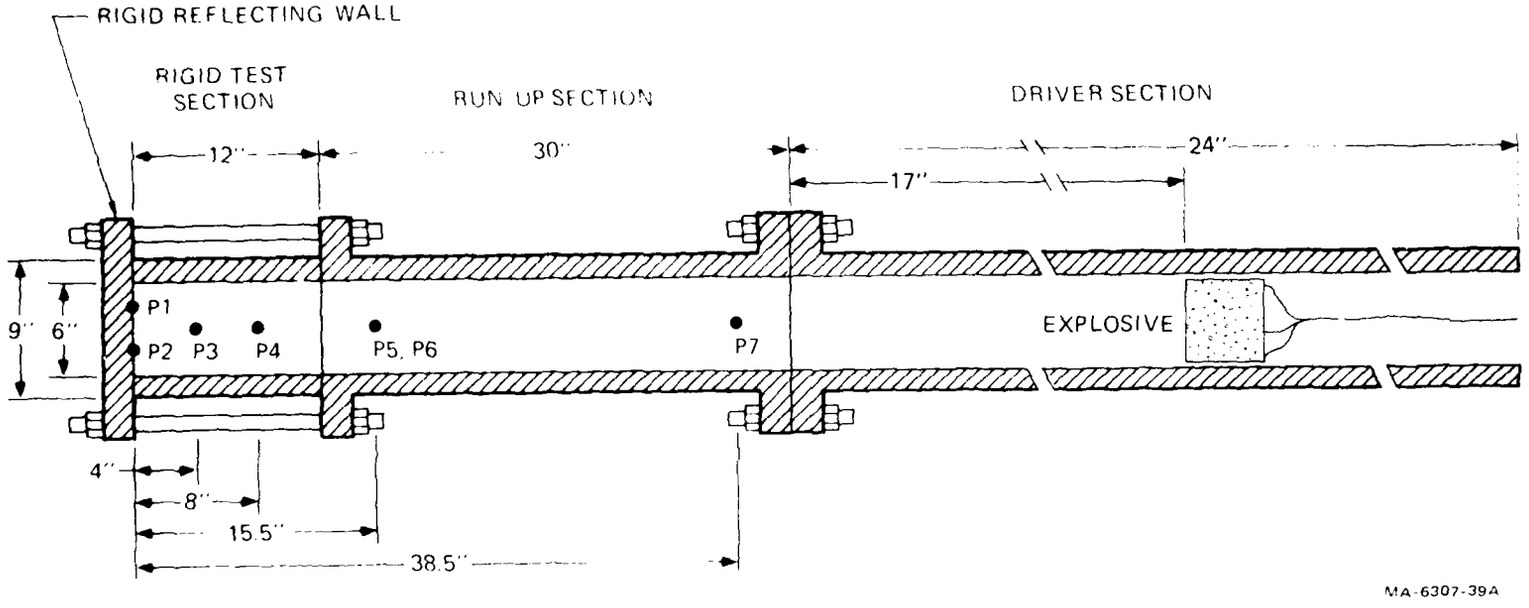

FIGURE 66 SHOCK TUBE ASSEMBLY FOR PLUG LOAD CALIBRATION TESTS

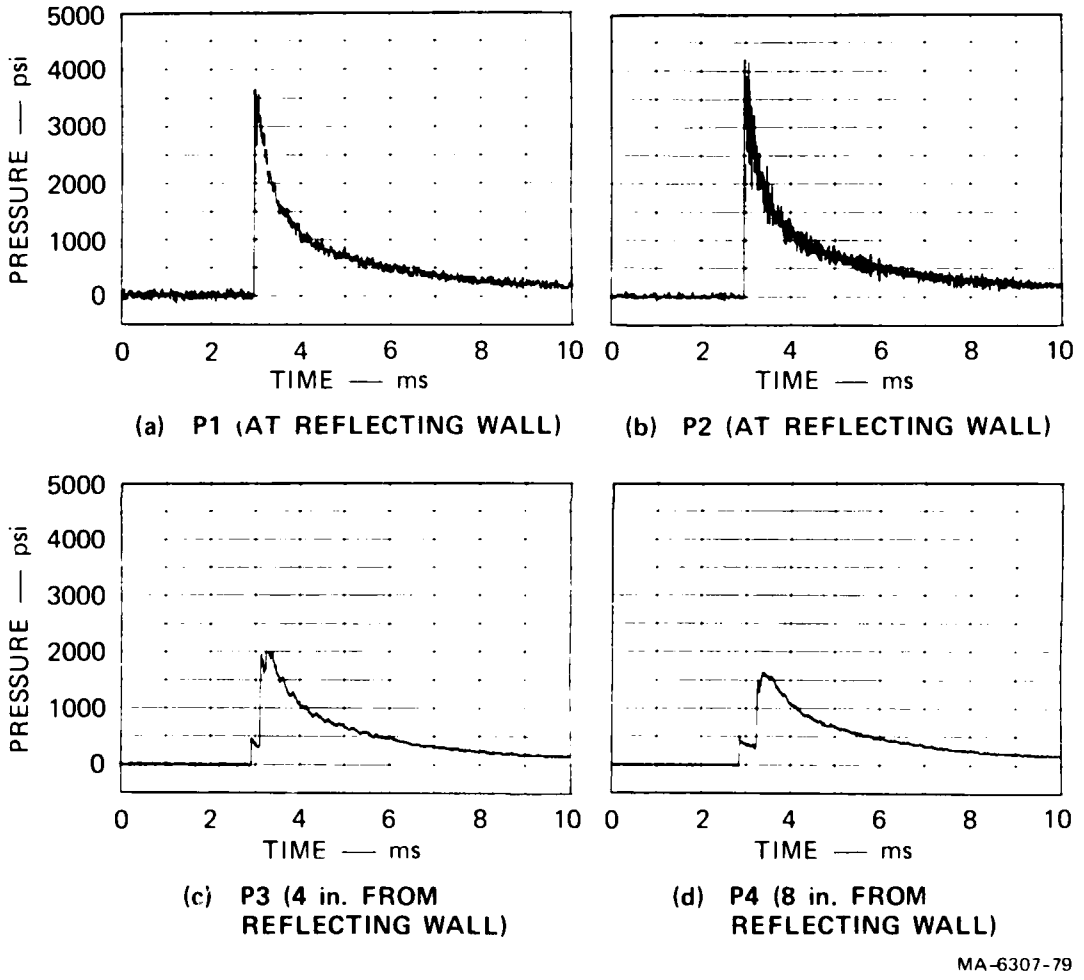

FIGURE 67 PRESSURE RECORDS FROM LOAD CALIBRATION TEST 33
312 g of PETN/microballoon at 20.5 ft standoff.

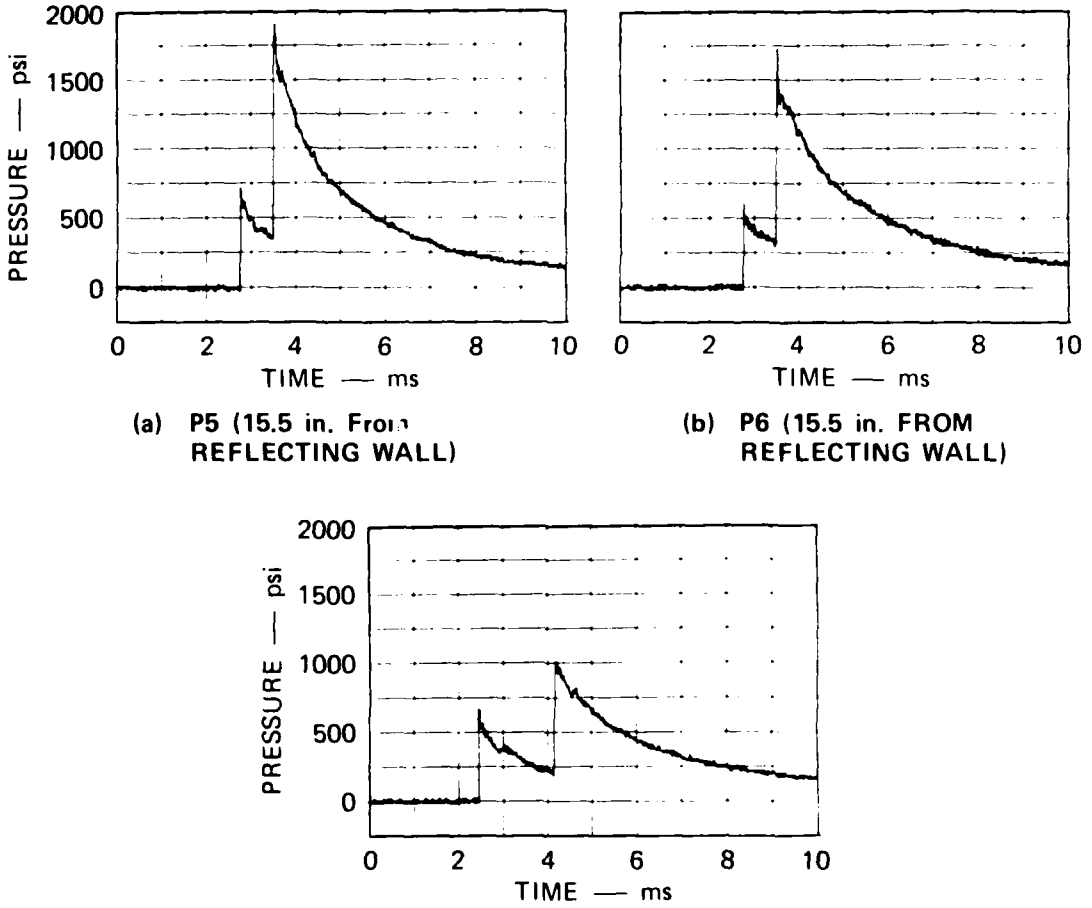

(a) P5 (15.5 in. From REFLECTING WALL)

(b) P6 (15.5 in. FROM REFLECTING WALL)

(c) P7 (38.5 in. FROM REFLECTING WALL)

MA-6307-80

FIGURE 67 PRESSURE RECORDS FROM LOAD CALIBRATION TEST 33 (Concluded)

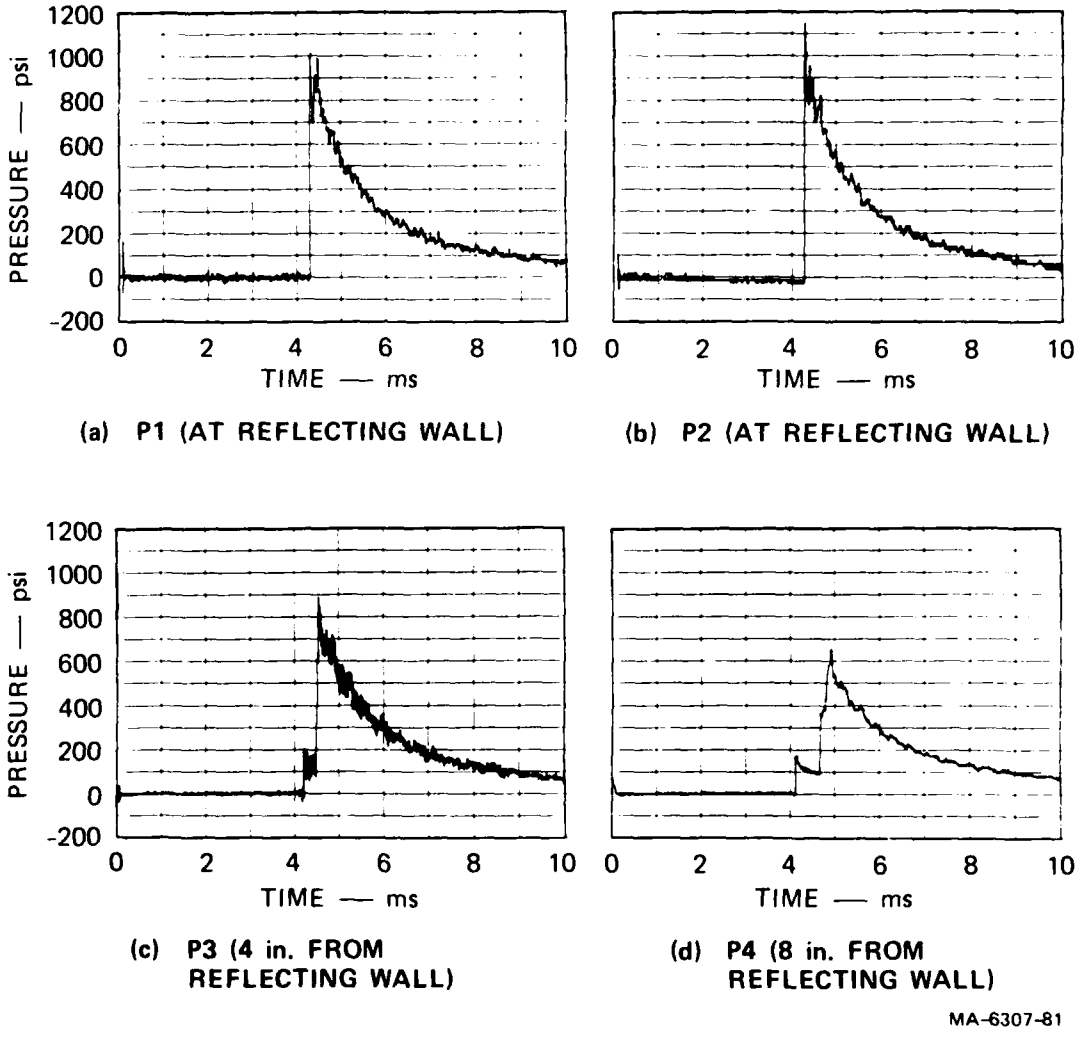

FIGURE 68 PRESSURE RECORDS FROM LOAD CALIBRATION TEST 34
78 g of PETN/microballoon at 20.5 ft standoff.

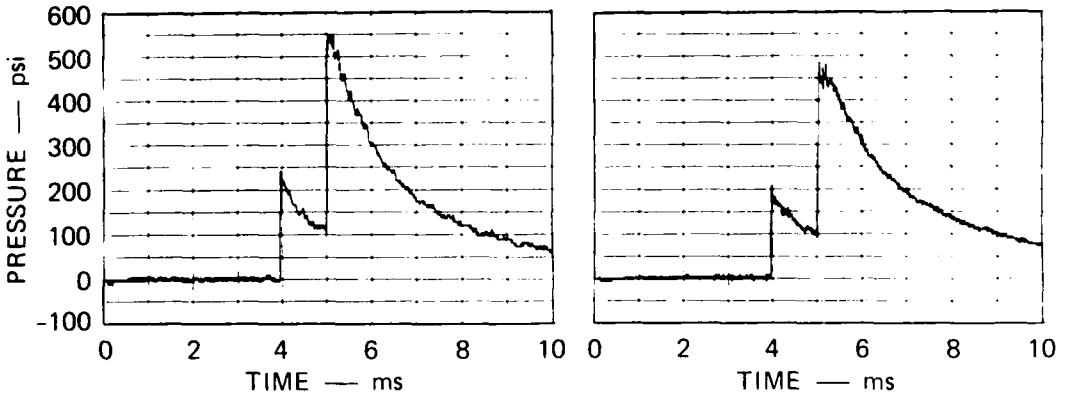

(a) P5 (15.5 in. FROM REFLECTING WALL)

(b) P6 (15.5 in. FROM REFLECTING WALL)

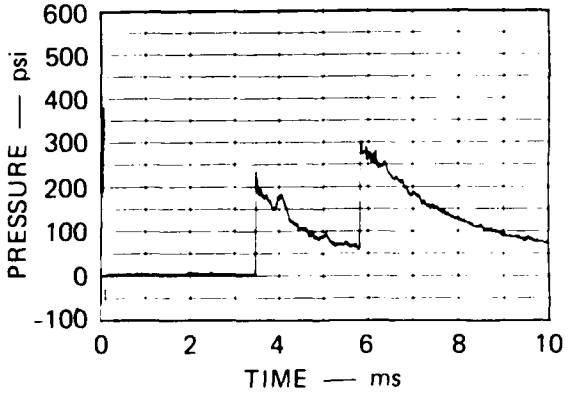

(c) P7 (38.5 in. FROM REFLECTING WALL)

MA-6307-82

FIGURE 68 PRESSURE RECORDS FROM LOAD CALIBRATION TEST 34 (Concluded)

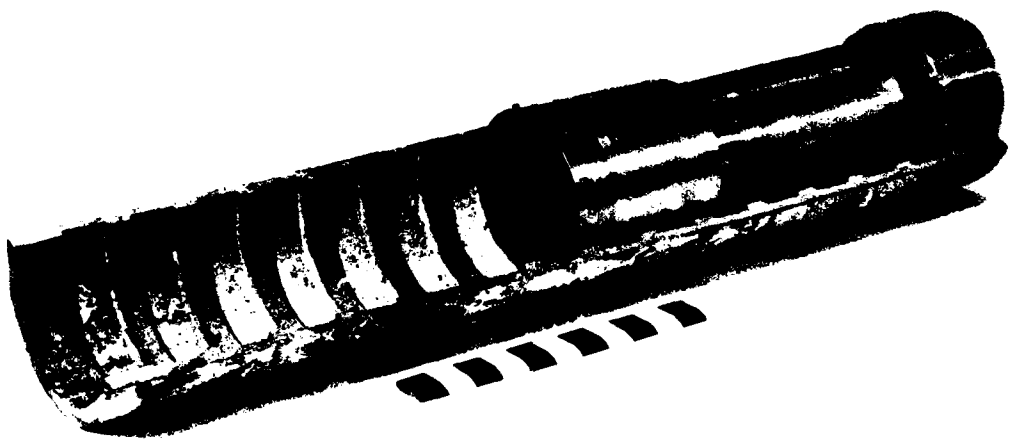

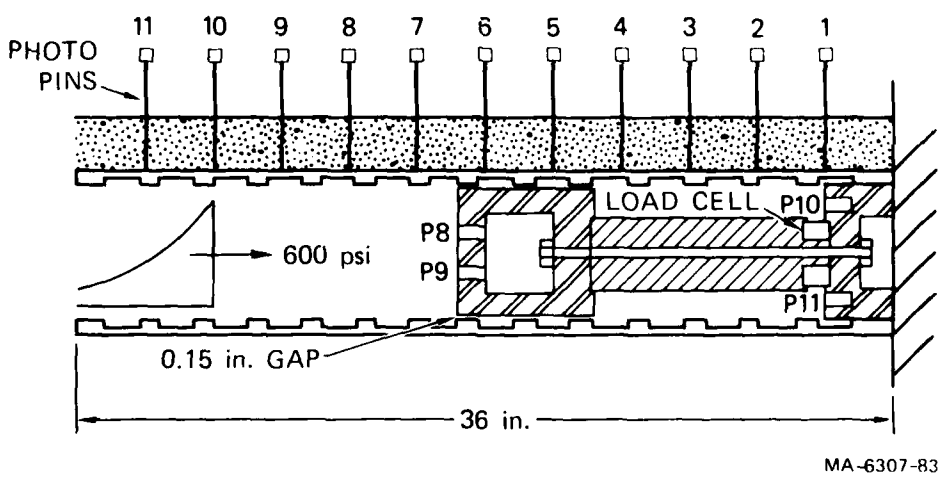

FIGURE 69 PLUG/TRENCH LAYOUT FOR LEAKY PLUG TEST 35

A 36-inch-long fiber-reinforced concrete ribbed trench was used for Test 35. The total length of the plug assembly was 19.25 inches, and the portion of the trench upstream of the plug face was 16.75 inches long. The model trench was constructed with scaled MX ribs. The trench wall was 0.375-inch thick (10-inch wall, full-scale); the rib spacing was 2.31 inches and the rib height was 0.25 inches. The rib face had a 18 degree cant. The inside diameter of the ribs was 6.00 inches. The trench roof was separated with two longitudinal saw cuts spaced 100 degrees apart. No transverse roof cuts were made. Two unconfined compression tests (ASTM C39-64) were performed on sample cylinders of the fiber-reinforced concrete mix 42 days after pouring. Compression strengths of 8580 psi and 8280 psi were obtained. (The trench was 56 days old at the time of the plug test).

The soil, obtained from the HAVE HOST site, was compacted to a wet density of 130 lb/ft^3 at a water content of 9.5 percent. The soil cover was 2.3 inches thick. Photo pins protruding through the soil and resting on the trench roof were used to measure roof motion. The pins were spaced every 3 inches and for future reference were numbered consecutively starting from the rigid end wall of the test section (Figure 69).

The explosive charge for Test 35 was identical to that used in calibration Test 33 (312-g of PETN/microballoons in a 5-inch-diameter, 5-inch-long cylinder). The charge standoff distance from the plug face was 20.5 feet, the same as the standoff distance from the reflecting wall in the load calibration test.

Figure 70 shows the pressure in the steel run-up section for Test 35. Two pressure gages (P5 and P6) are located 20 inches upstream from the plug face, 180 degrees apart. One pressure gage (P7) is located 43 inches upstream from the plug face. Comparison of these gage records with those from load calibration Test 33 (Figure 67) shows very good agreement in the incident waveforms. (The run-up distances between gages P5, P6, and P7 and the plug face or reflecting wall differ slightly between Tests 33 and 35 because the inserted rigid steel tube used for the load calibration tests did not match the length of the trench run-up to the plug face).

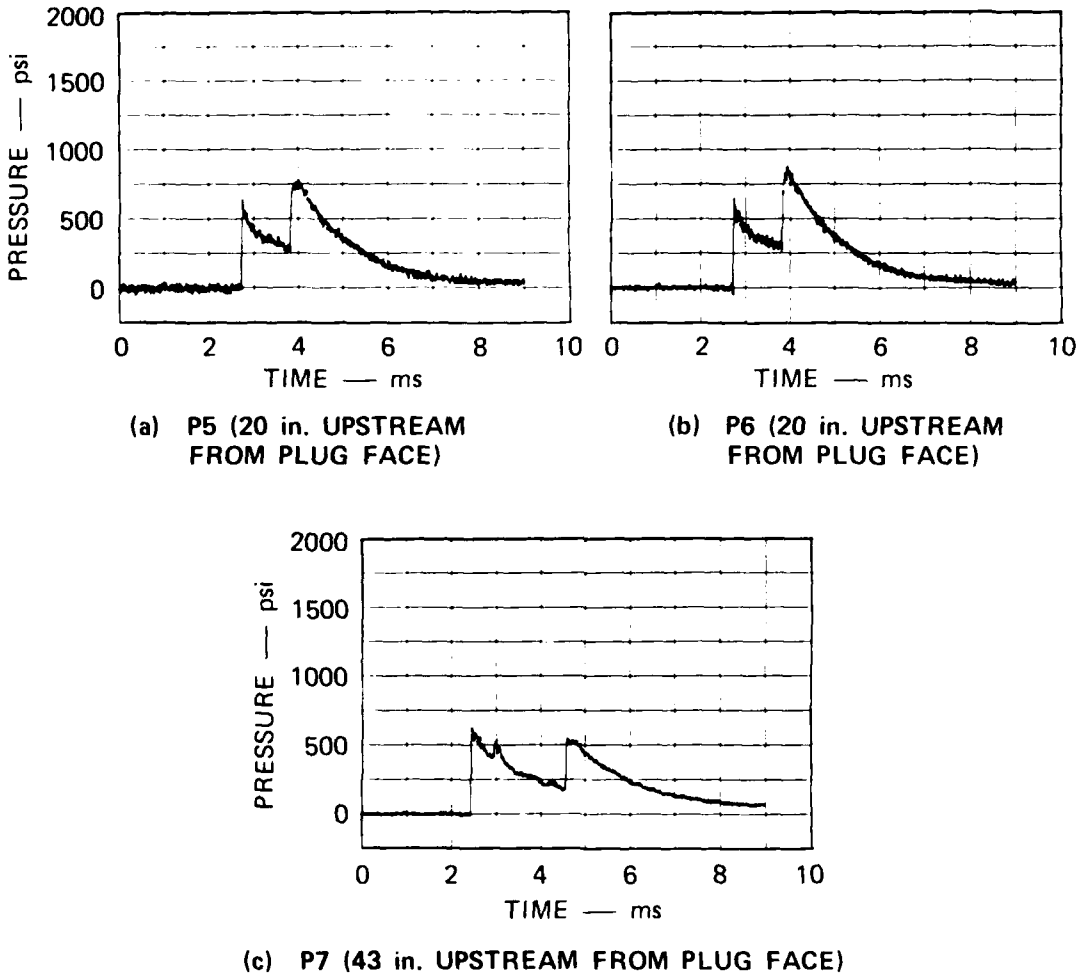

FIGURE 70 PRESSURE IN RUNUP SECTION FOR LEAKY PLUG TEST 35
312 g of PETN/microballoon at 20.5 ft standoff.

Two pressure gages (P8 and P9) were located on the leaky plug face, 1.25 inches above and below the plug centerline. Two pressure gages (P10 and P11) were located on the support base, 2.0 inches above and below the plug centerline. A load cell was fitted between the plug support shaft and the base to measure the load transmitted to the base.

Figure 71 shows the pressure and load cell records from Test 35. Comparison of P8 and P9 on the plug face for Test 35 with P1 and P2 on the reflecting wall in the corresponding load calibration Test 33 (Figure 67) shows the initial reflected pressure in Test 35 to be a few hundred psi lower and to have a faster decay rate. The initially lower relected pressure is probably due to rib drag in the last 16.75 inches of run-up to the plug face (no ribs were present in the calibration test). We attribute the faster decay time to expansion and then venting of the trench run-up section.

Poor records were obtained with both P10 and P11 in the plug base (Figure 71). Post-test examination showed that the cable to P10 had been pinched, probably at t = 3.85 ms, as indicated in Figure 71, resulting in a large baseline shift. The pressure record for P11 also shows a baseline shift, as indicated by the negative pressure after t = 8 ms. The apparent precursor in P11, seen at t = 3.13 ms, was not observed in P10. It is probably not a real pressure signal but, rather, a baseline shift caused by structural ringing through the aluminum plug assembly. On the basis of these observations, a shock of about 300 psi appears to have arrived at the plug base at t = 3.45 ms, or 0.45 ms after the shock reached the leaky plug face. An interesting observation is that 300 psi is 10 percent of the pressure on the leaky plug face; also the 0.15-inch gap between the leaky plug outside diameter and the rib inside diameter accounts for 10 percent of the cross sectional area of the trench. Better cable protection and a method for vibration isolation of P10 and P11 should improve the records of these gages in future tests.

The load cell record (Figure 71) shows an initial peak load of 71,000 pounds in the support shaft (the 3000-psi pressure on the plug face times plug face area is 76,000 pounds). The later "ringing" of the load

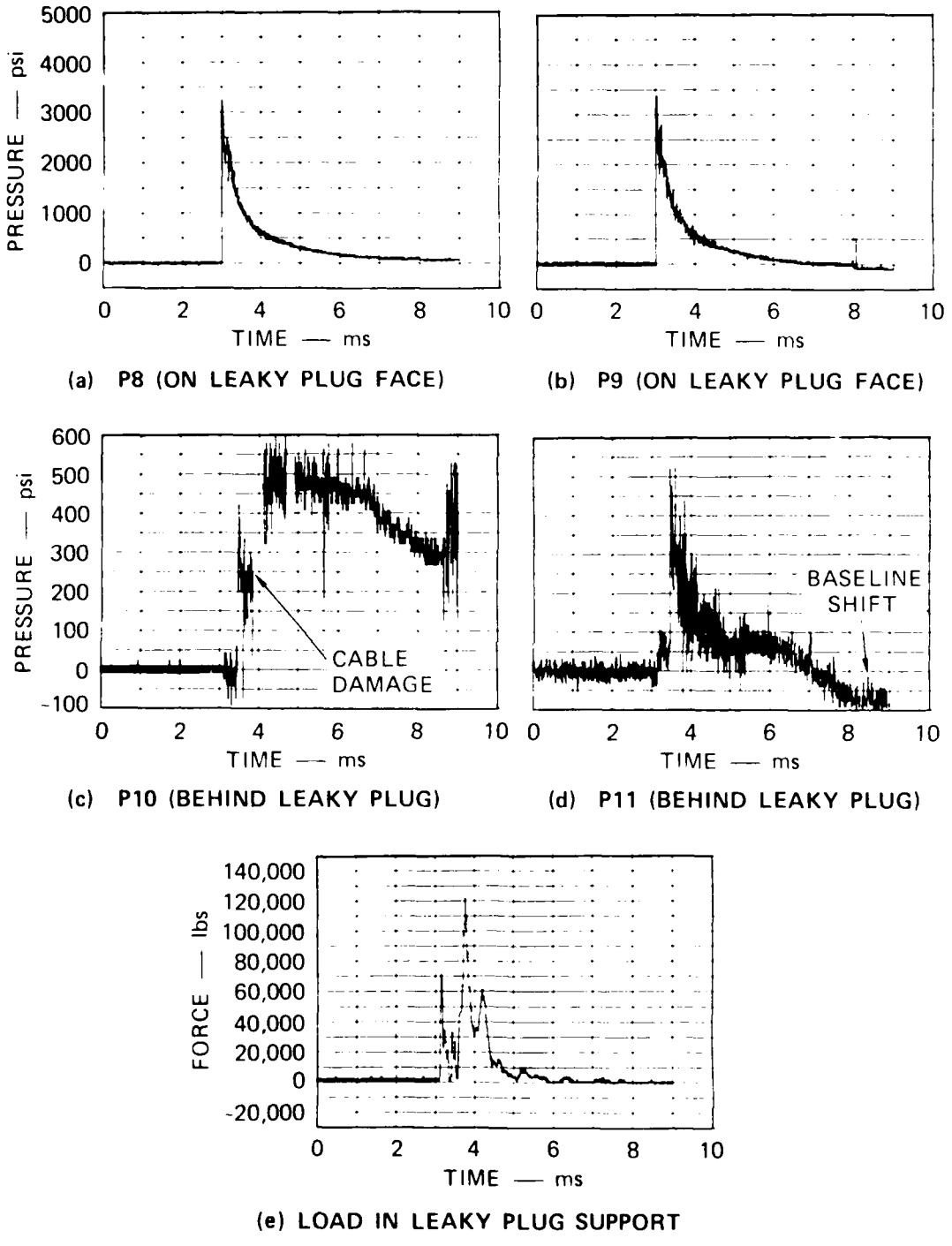

FIGURE 71 PRESSURE AND LOAD CELL RECORDS FROM LEAKY PLUG TEST 35
312 g of PETN/microballoon at 20.5 ft standoff.

is caused by stress waves propagating up and down the length of the plug assembly (at approximately 0.2 ms round trip transit time) and by the fact that the plug assembly was not tied down to the rigid end wall of the shock tube assembly.

Photographic coverage consisted of two high-speed movie cameras (Hycams), one viewing the soil surface from the side and one viewing the end of the trench from behind the Lucite reflecting wall. Selected Hycam frames are shown in Figures 72 and 73. In the end view, the film speed was 10,660 frames per second; in the side view, the film speed was 10,390 frames per second. The accuracy of the times presented in Figures 72 and 73 is ±0.05 ms, mainly because of errors in determining an exact zero time.

The shock hits the leaky plug face at t = 3.00 ms. By t = 3.66 ms, the roof in front of the plug has lifted 0.4 inch (Figure 72), whereas no significant expansion has taken place past the plug (note photo pin 5). As seen in the end view (Figure 72), the first longitudinal cracks have propagated past the 3-inch-thick plug base by t = 4.41 ms, which is 0.96 ms after the shock has reached the face of the plug base. At t = 4.71 ms, the first venting is seen above the face of the leaky plug (Figure 73). At this time the trench roof has lifted 2.05 inches at the leaky plug face. By t = 6.06 ms, the section of the trench upstream of the leaky plug face has vented along its entire length, whereas downstream of the leaky plug no venting is seen even at t = 14.14 ms, although by then (Figure 73), significant downstream expansion is apparent.

Figure 74 shows a plot of the displacement of the trench roof versus time for Test 35 from the photo pin data. Comparison of the data for photo pins 6 and 7 shows the roof displacement directly in front of and behind the plug face (over the leaky plug) to be similar, whereas the roof displacement behind the leaky plug lags behind (photo pin 2).

Figure 75 is a post-test photo of Test 35. After the test, the loose soil was blown away with an air hose to expose the trench fragments and plug for observation. As seen in the figure, the entire plug assembly has rebounded 2.0 inches from the end wall of the shock tube assembly.

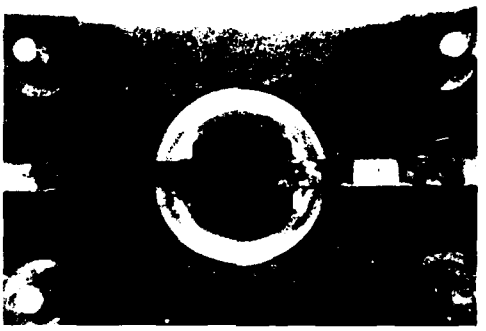

t = 4.41 ms

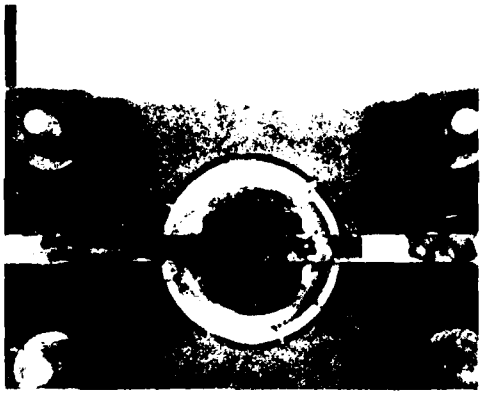

t = 4.88 ms

t = 8.73 ms

MP-6307-86

FIGURE 72 HYCAM PICTURES FROM LEAKY PLUG TEST 35 (End View)

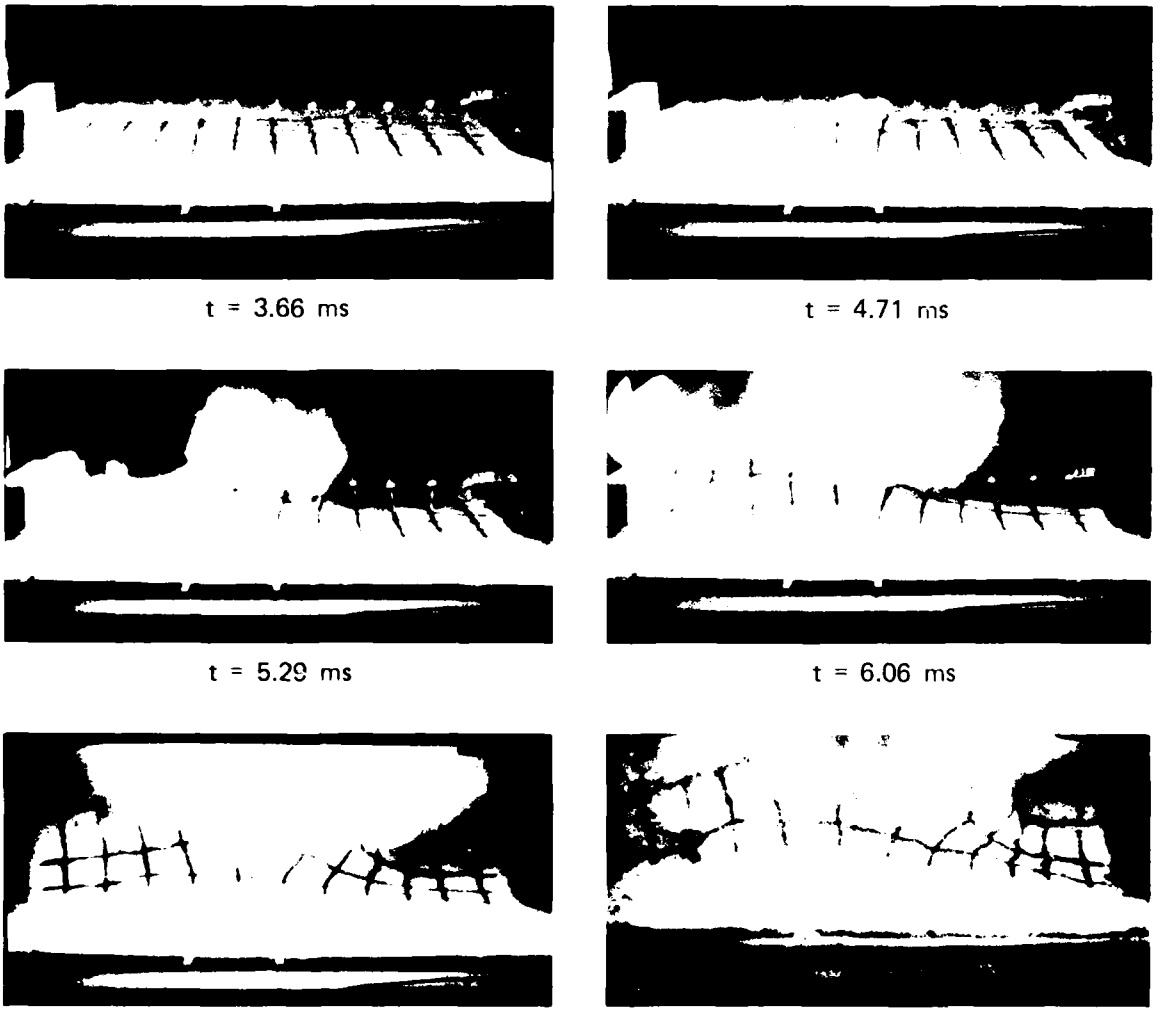

FIGURE 73 HYCAM PICTURES FROM LEAKY PLUG TEST 35 (Side View)

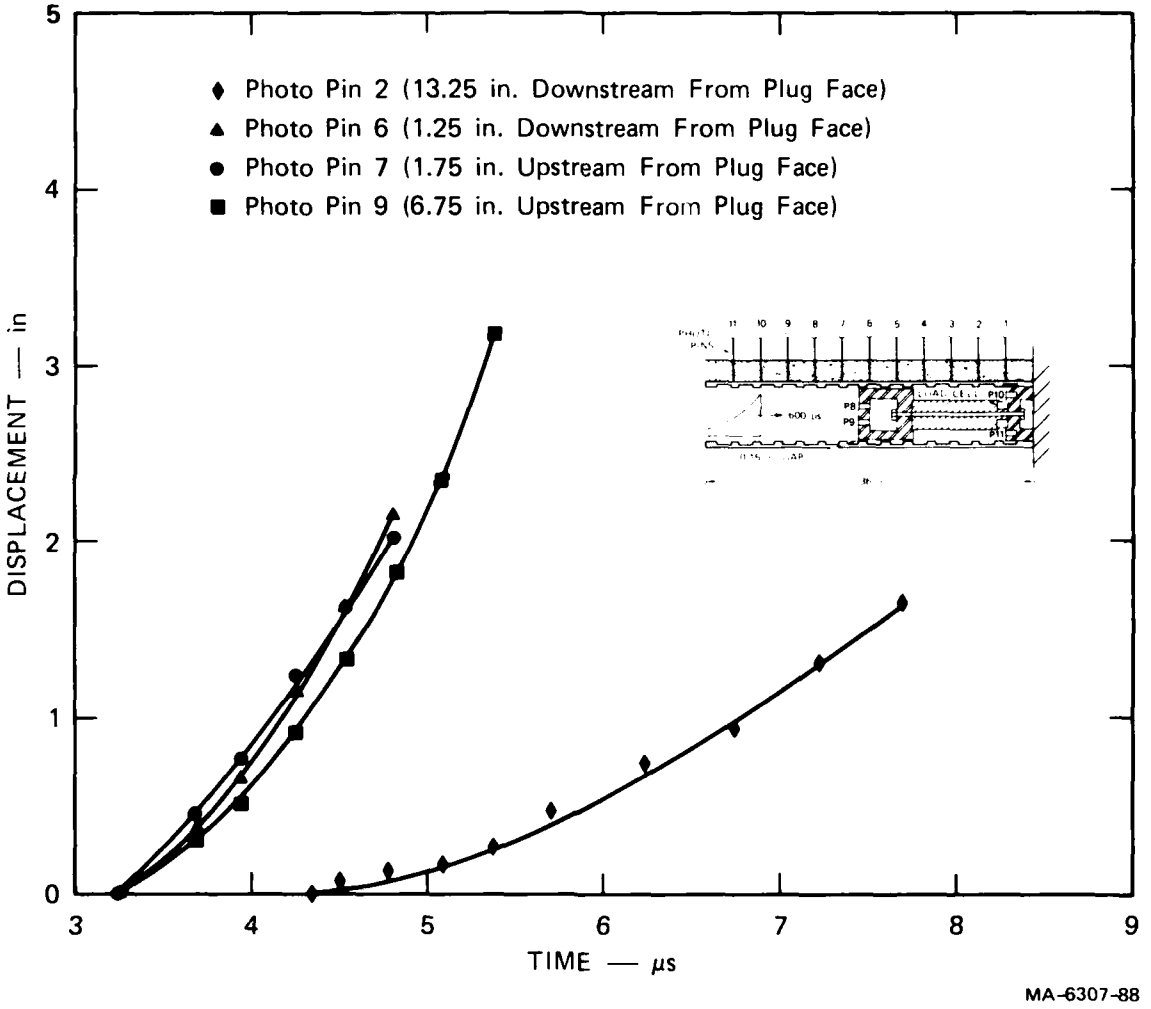

FIGURE 74 PHOTO PIN DISPLACEMENTS FOR LEAKY PLUG TEST 35

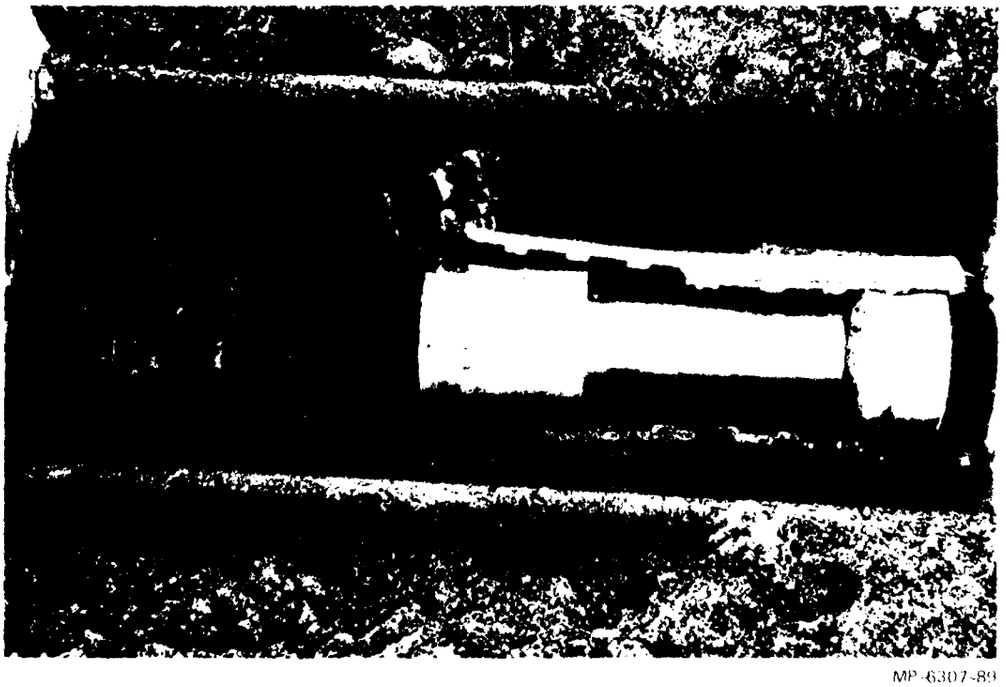

MP-6307-89

FIGURE 75 POSTTEST PHOTOGRAPH FROM LEAKY PLUG TEST 35 (After Soil Removal)

Figure 76 shows the recovered trench fragments from Test 35. Most of the roof in front of and over the leaky plug was not recovered. Longitudinal cracks run the entire length of the trench section. A major circumferential crack is located between the eighth and ninth rib. For reference, the face of the leaky plug aligns with the upstream face of the ninth rib (see Figure 69).

Test 36 (Solid Plug)

The simple solid plug design and plug/trench layout is shown in Figure 77. It consists of five aluminum cylinders sandwiching three rib-bearing plates. A 0.063-inch-thick neoprene ring is bonded to the rib-bearing plates, and when the plug is in place, the neoprene bears on the rib face providing a seal. Unlike the leaky plug model, the solid plug is assembled inside the trench. The rib-bearing plates are segmented into 120 degree sections to facilitate assembly. The entire plug assembly is held together by seven 1/2-inch bolts connecting the front and back cylinders. The entire plug assembly weighs 33.5 pounds and is 12.55 inches long.

A 36-inch-long fiber-reinforced concrete ribbed trench was used for Test 36. The model trench was constructed with scaled MX ribs. The trench wall was 0.375 inch thick, the rib spacing was 2.31 inches, and the rib was 0.25 inch high. The rib face had an 18 degree cant. The inside diameter of the ribs was 6.00 inches. The trench roof was not saw-cut, to match the monolithic trench designs for the plug section of Tests T-3 and T-5 of the HAVE HOST Program. Two unconfined compression tests (ASTM C39064) were performed on samples of the fiber-reinforced concrete mix after 15 days. Compression strengths of 11,870 psi and 13,930 psi were obtained. At the time of Test 36, the trench was 29 days old.

For Test 36 the plug was supported by the fourth, sixth, and eighth ribs. As the plug was assembled in the trench, an epoxy filler was placed on the face of the three bearing ribs. The plug was pushed against these ribs, and the epoxy filled any gaps between plug and trench

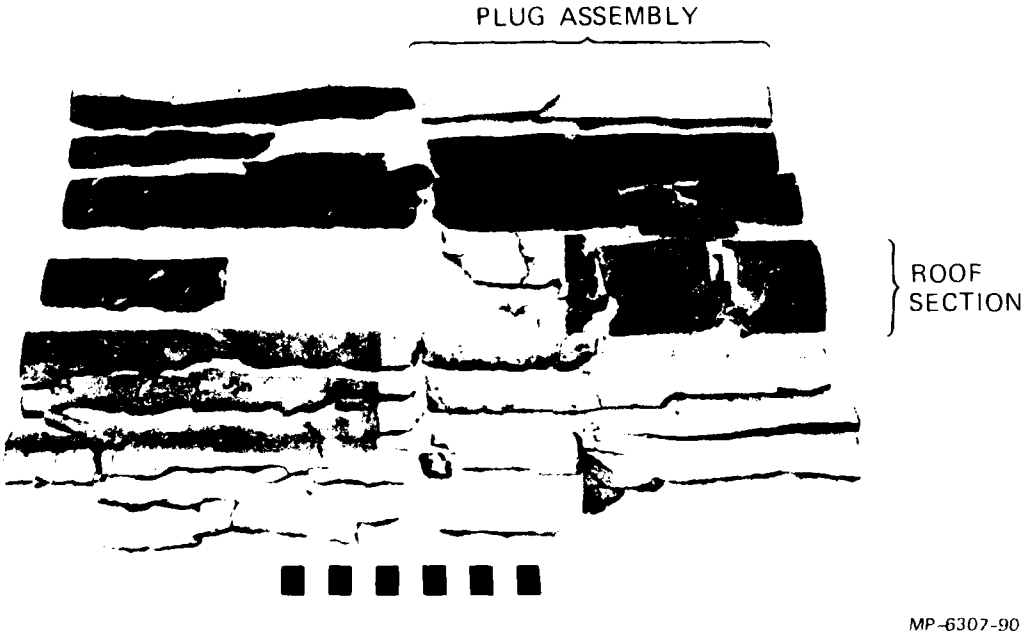

FIGURE 76 TRENCH FRAGMENTS RECOVERED FROM LEAKY PLUG TEST 35

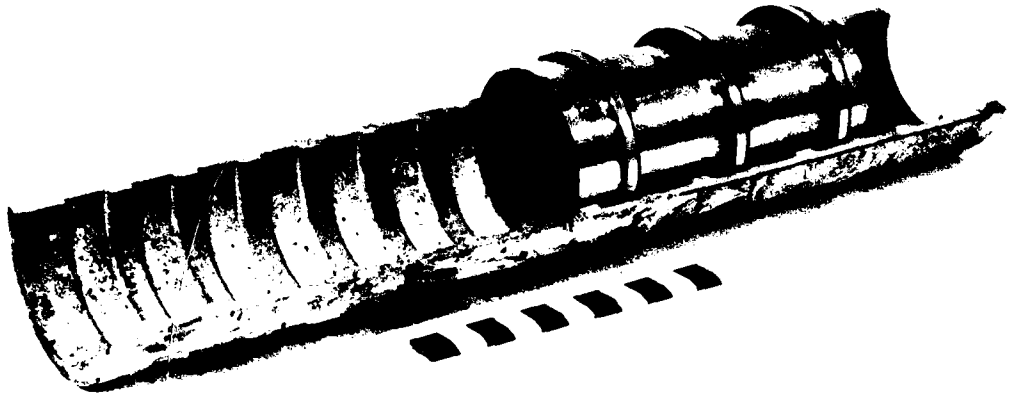

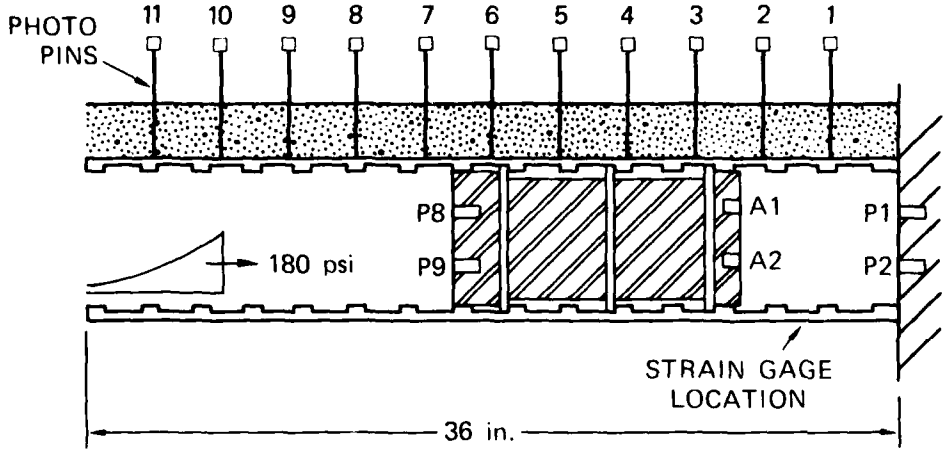

MP-6307-91

FIGURE 77 PLUG/TRENCH LAYOUT FOR SOLID PLUG TEST 36

created by the tolerances on plug and trench dimensions. Therefore, when the epoxy had set, we knew that the plug was bearing equally on all three ribs. A release agent was placed on the plug so that the plug and trench were not bonded together. The face of the solid plug was aligned with the upstream face of the ninth rib (see Figure 77). Thus, 16.25 inches of trench separated the plug face and the steel run-up section.

The soil used was from the HAVE HOST site and was compacted to a wet density of 128 lb/ft^3 at a water content of 8.9 percent. The soil cover was 2.3 inches thick. As in Test 35, photo pins were used to measure roof motion. Again, the pins were spaced 3 inches apart and were numbered consecutively starting from the rigid end wall of the test section (Figure 77).

The explosive charge for Test 36 was identical to that used in load calibration Test 34 (78-g of PETN/microballoons in a 5-inch-diameter, 1.25-inch-thick cylinder). The charge standoff distance from the plug face was 20.5 feet. Three pressure gages were located in the steel run-up section of the shock tube. Two of these gages (P5 and P6) were located 20 inches upstream from the plug face, spaced 180 degrees apart, and one gage (P7) was located 43 inches upstream from the plug face.

Two pressure gages (P8 and P9) were located on the solid plug face, 2.0 inches above and below the plug centerline. Two pressure gages (P1 and P2) were located behind the solid plug in the rigid end wall of the shock tube assembly, 1.25 inches above and below the plug centerline.

Figure 78 shows the pressure records from Test 36. No records are shown here for gages P5 and P7 in the steel run-up section. Gage P5 was recorded on an oscilloscope only (due to lack of an available tape channel) and showed no difference in pressure from the symmetrically located gage P6. Because of a damaged cable, no record was obtained for gage P7. Comparison of the record from P6 with load calibration Test 34 shows very good agreement in incident pressure.

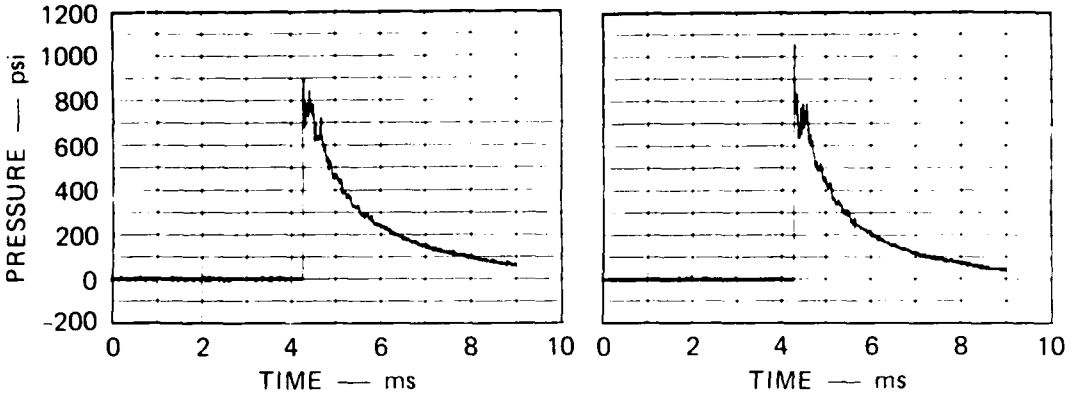

(a) P8 (ON PLUG FACE)

(b) P9 (ON PLUG FACE)

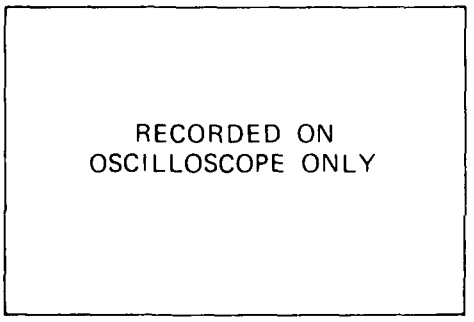

(c) P5 (20 in. UPSTREAM FROM PLUG FACE)

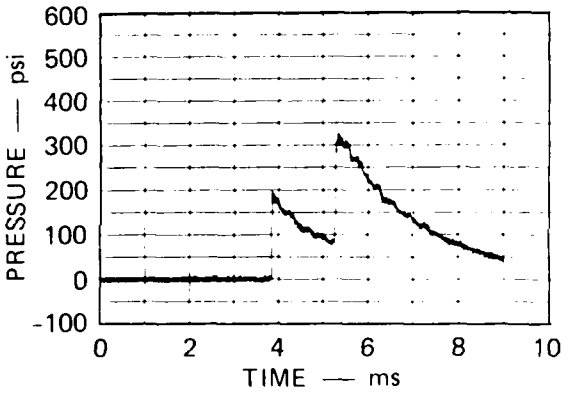

(d) P6 (20 in. UPSTREAM FROM PLUG FACE)

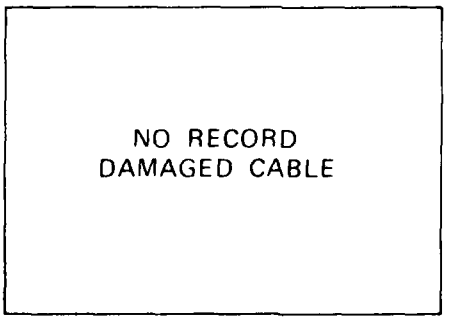

(e) P7 (43 in. UPSTREAM FROM PLUG FACE)

MA-6307-92

FIGURE 78 PRESSURE RECORDS FROM SOLID PLUG TEST 36
78 g PETN/microballoon at 20.5 ft standoff

Comparison of P8 and P9 on the plug face for Test 36 with P1 and P2 on the reflecting wall in the corresponding load calibration Test 34 (Figure 68) shows the reflected pressure in Test 36 to be lower initially and to have a slightly faster decay rate. Again, the initially lower reflected pressure is attributed to the rib drag in the last 16.25 inches of run-up to the plug face (no ribs were present in the calibration test): the slightly faster decay time is probably a result of expansion and then venting of the trench run-up section. There was no significant leakage past the solid plug, and gages P1 and P2 behind the plug registered no measurable pressure (less than 5 psi). Therefore, the records for P1 and P2 were not included in this report.

Four strain gages were located downstream of the plug on the outer trench wall between the second and third rib locations. As viewed from downstream, SG1 was located 45 degrees counterclockwise from the invert; SG2, 45 degrees clockwise from the invert; SG3, 45 degrees counterclockwise from the crown; and SG4, 45 degrees clockwise from the crown. Figure 79 shows the records from these gages (compression is positive). Comparison of the strains between symmetrically located gages SG1 and SG2 or SG3 and SG4 shows good agreement. The initial strain in SG1 and SG2 is due to a slight preload in the trench caused by the bolts holding the end wall of the shock tube assembly in place. This indicates that the lower portion of the trench is carrying the load that clamps the trench in place, which is a possible reason why SG1 and SG2 registered higher strains during the test.

The shock hit the plug face at t = 4.25 ms, and the first strain occurred in the concrete at t = 4.30 ms, the peak strain occurred at t = 4.85 ms, and a second smaller peak occurred at t = 6.60 ms. The second peak may be due to vibration of the plug on the neoprene seal which cushions the plug on the trench ribs. The peak strain in the trench obtained by averaging the four strain records was 410 . In order to relate this strain to the force in the trench a posttest static compression test was performed on the trench section behind the plug. This test showed that at 410 microstrain the concrete is still in the

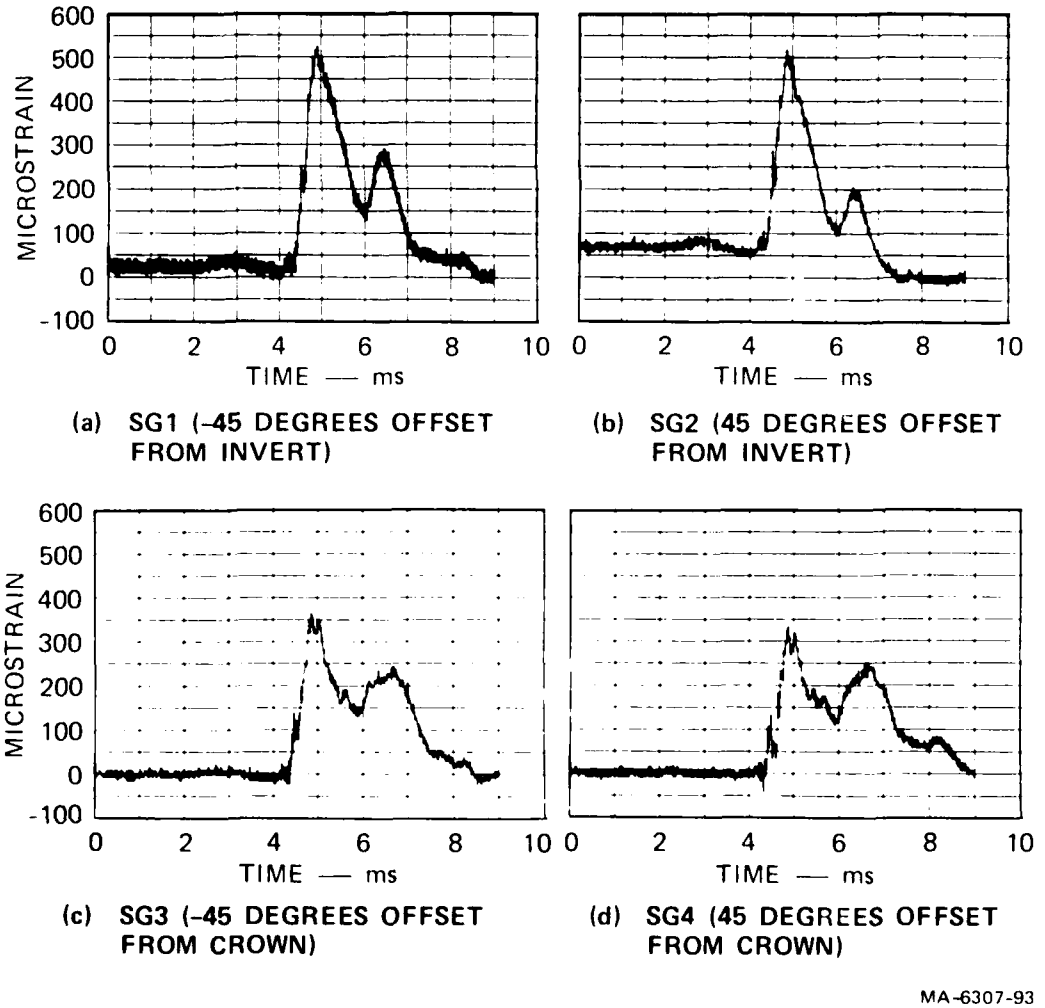

FIGURE 79 LONGITUDINAL STRAIN IN TRENCH WALL BEHIND SOLID PLUG (TEST 36)

elastic range and the force in the trench section is 23,500 pounds, corresponding to a stress in the trench wall of 2900 psi. This peak force of 23,500 pounds agrees closely with the peak force on the plug face of 22,600 pounds (a peak pressure of 800 psi times the 28.3 in.^{2} area of the plug face), indicating all load on the plug face was transferred to the trench. It is also of importance to note that the peak stress in the trench of 2900 psi is well below the specified design strength for the concrete trench, which for the various trench designs, ranged from 6000 psi to 10,000 psi.

Two accelerometers (A1 and A2) were located in the back plate of the plug, 1.0 inch above and below the plug centerline. Figure 80 shows the records from these accelerometers along with velocity and displacement records obtained by numerical integration of the accelerometer records. Although there is substantial ringing in the records, realistic velocity and displacement records were obtained at least up through the first positive peak (the positive direction is downstream). A peak velocity of 50 in./s was reached at t = 4.70 ms and a peak displacement of 0.030 inch was reached at t = 5.40 ms. (A slight baseline correction is necessary for A1 as seen by the early time shift of the velocity and displacement records.) The later time negative velocity and displacements are not as accurate as the positive peaks due to the greater effect of small baseline shifts at later times.

Again, two high-speed movie cameras (Hycams) were used. Selected Hycam frames are shown in Figures 81 and 82. In the end view, the film speed was 10,330 frames per second; in the side view, the film speed was 10,390 frames per second. The times presented in Figures 81 and 82 are accurate to ±0.05 ms.

The shock arrives at the solid plug face at t = 4.25 ms. By t = 5.99 ms, a uniform roof displacement can be seen in the upstream portion of the trench (photo pins 7 through 10, Figure 82). Photo pin 6, downstream of the plug face, yet upstream of the first rib support, shows a displacement similar to that of the upstream pins. No displacement is seen in photo pins 1 through 5, downstream of the first rib support.

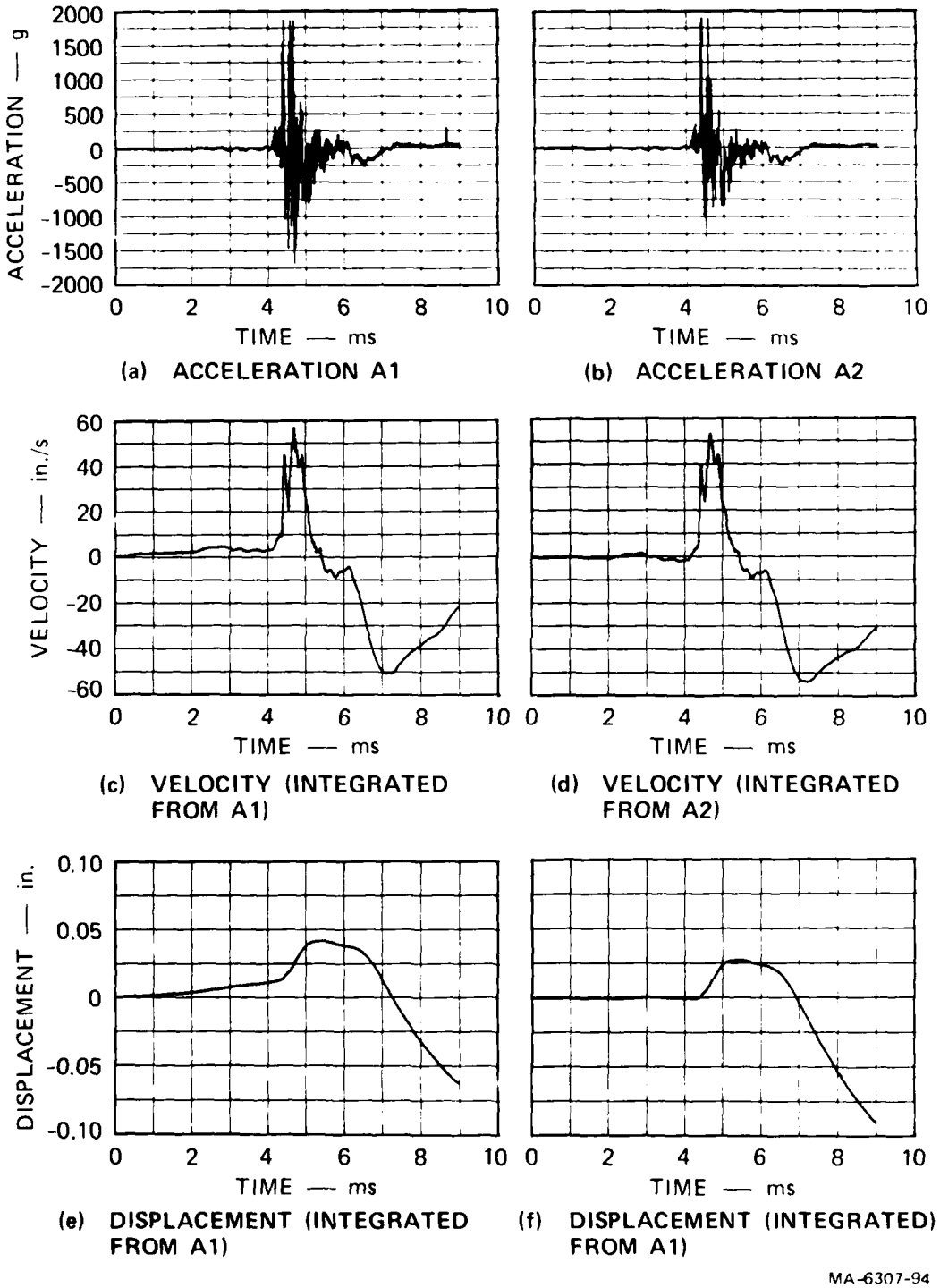

FIGURE 80 PLUG MOTION FOR SOLID PLUG TEST 36

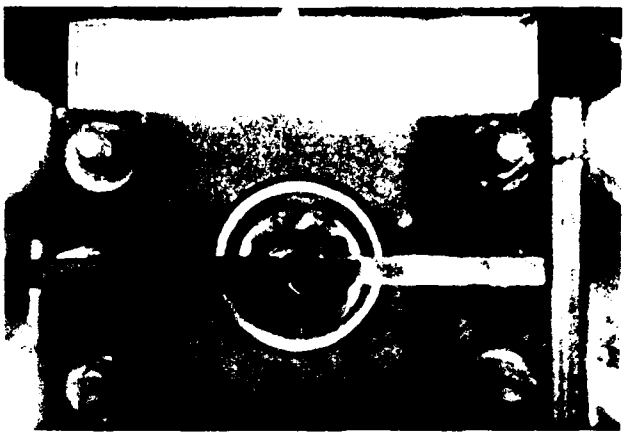

t = 8.04 ms

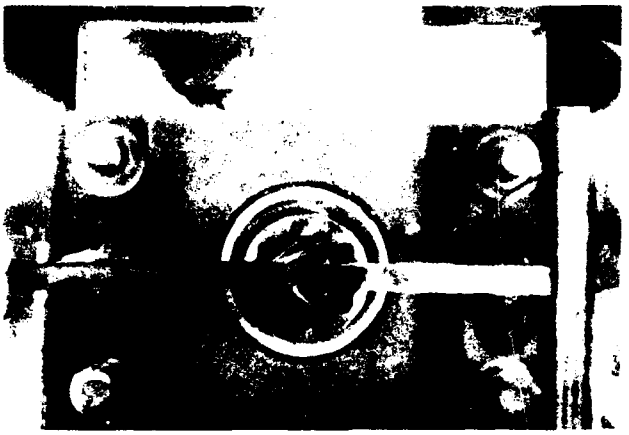

t = 10.36 ms

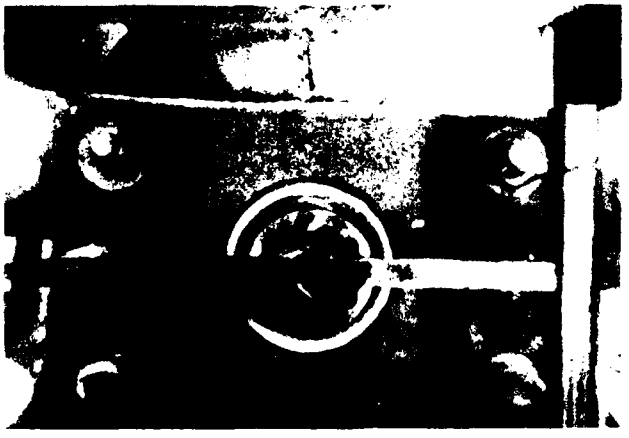

t = 20.53 ms

MP 6307 95

FIGURE 81 HYCAM PICTURES FROM SOLID PLUG TEST 36 (End View)

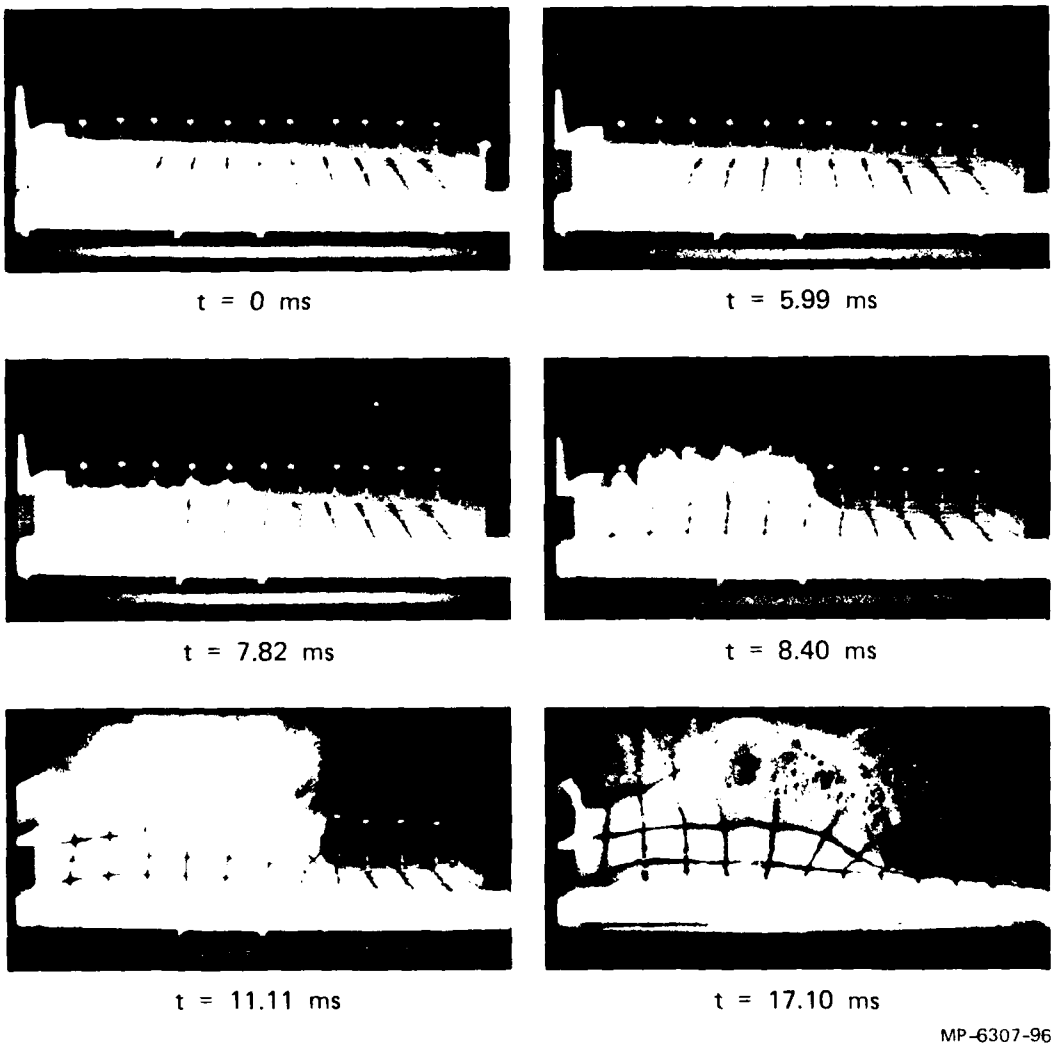

FIGURE 82 HYCAM PICTURES FROM SOLID PLUG TEST 36 (Side View)

(The cause of the lesser displacement of photo pin 11 is not known.) At t = 7.82 ms, venting appears along the entire upstream portion of the trench almost simultaneously (Figure 82). At this time, the roof at the plug face has displaced vertically 2.4 inches and the soil downstream of the first rib support has displaced horizontally about one inch downstream, as noted by the position of the base of photo pin 5 (Figure 82). At t = 8.04 ms, the vented gas has risen high enough to be seen in the end view (Figure 81). Both the soil and the trench downstream of the plug remain intact, as seen in the end view at t = 20.63 ms (Figure 81).

Figure 83 shows the displacement of the trench roof for Test 36 determined from photo pin data. The data are given for photo pins 4, 6, 7, and 9. Pins 1 through 4 showed no displacement, and pin 5 showed only a small displacement due to soil motion since, as described below, the trench did not fail at the location of pin 5.

Figure 84 shows a posttest photo of Test 36. After the test, the loose soil was blown away with an air hose to expose the trench fragments and plug for observation. The lower 180 degrees of the upstream portion of the trench was approximately in its original position. The soil above the plug section of the trench was for the most part ejected during the test. The soil behind the plug was still undisturbed, with photo pins 1 and 2 still in place.

Figure 85 shows the recovered trench fragments from Test 36. A major circumferential crack occurred at the upstream face of the eighth rib (the first bearing rib). Longitudinal cracks in the upstream section of the trench extend past the face of the plug (aligned with the upstream face of the ninth rib) and stop at this circumferential crack. The trench downstream of the eighth rib was intact.

Although Test 36 was conducted at a relatively low pressure, it demonstrated that a solid plug can seal the trench and that the longitudinal cracking that accompanies the trench breakup can be stopped at a sealed, loaded rib. A future test at a higher pressure would be useful to bound the upper limit of survival for a solid plug/trench system and to determine the mode of failure.

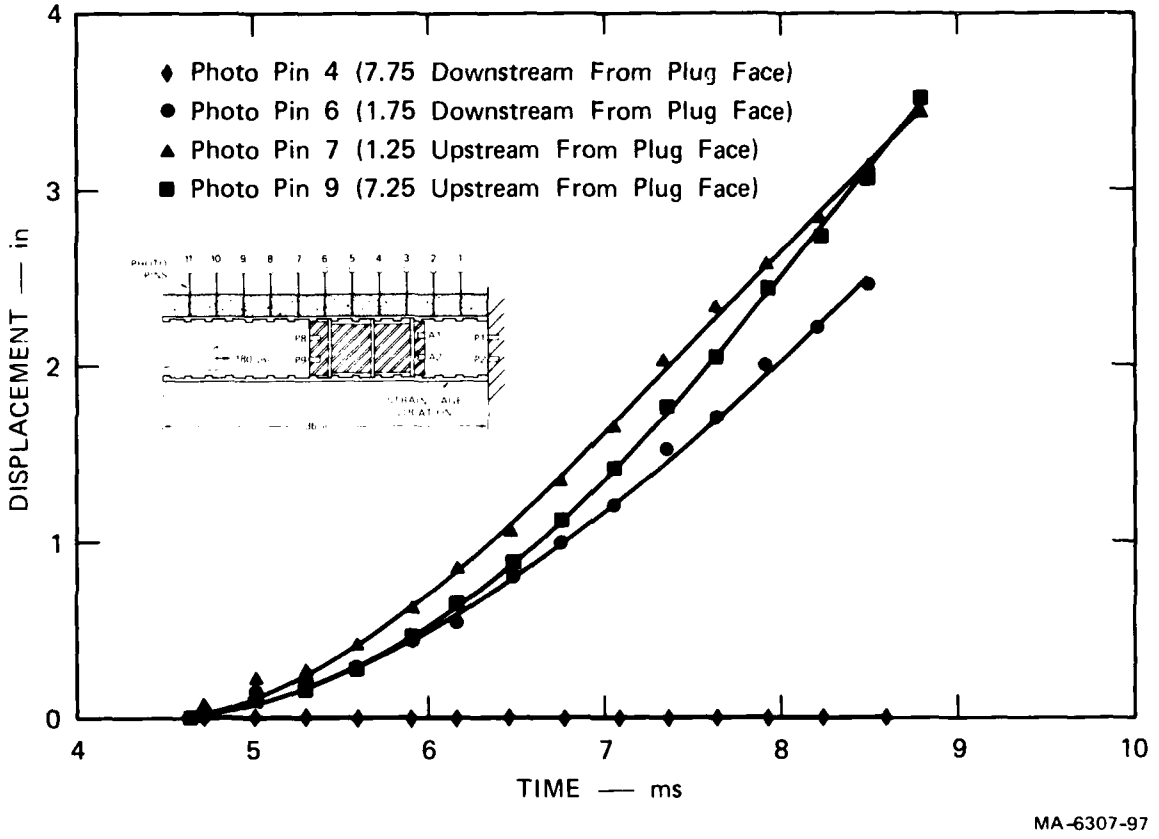

FIGURE 83 PHOTO PIN DISPLACEMENT FOR SOLID PLUG TEST 36

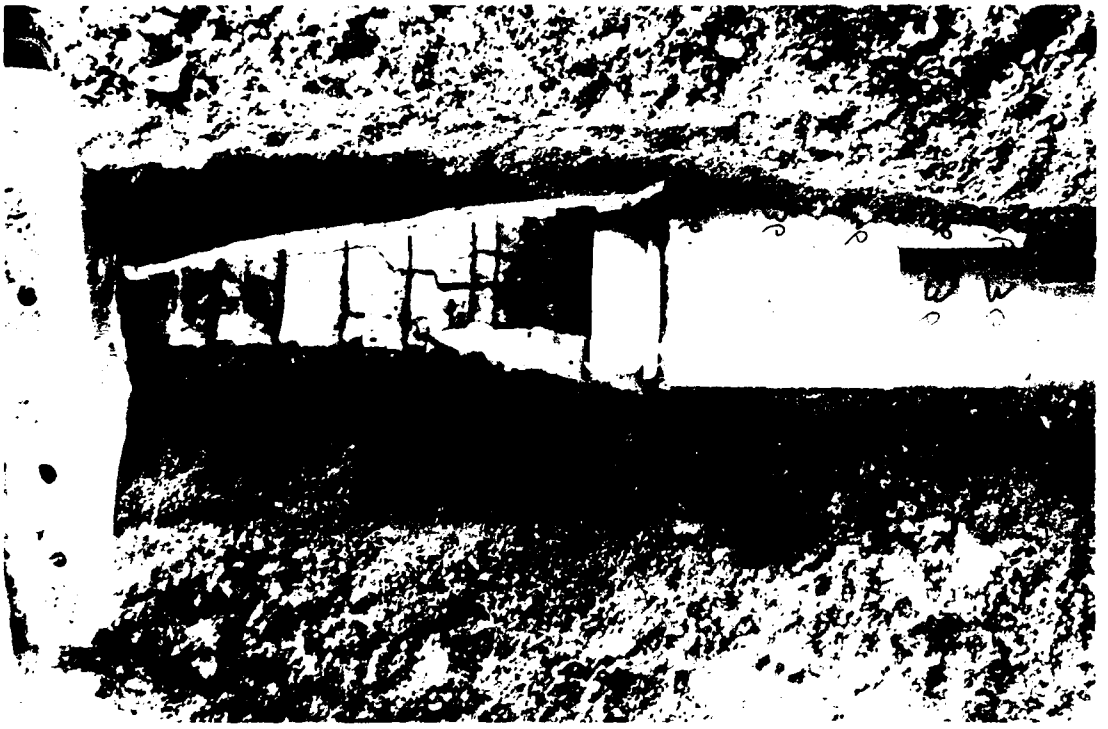

MP 6307-98

FIGURE 84 POSTTEST PHOTOGRAPH FROM SOLID PLUG TEST 36 (After Soil Removal)

MP-6307-99

FIGURE 85 TRENCH FRAGMENTS RECOVERED FROM SOLID PLUG TEST 36

6.3 CONCLUSIONS

The three experiments described in this section were an initial step in the study of plug/trench interaction using scale models. The results of these experiments suggest some conclusions regarding plug/trench interaction.

The response in the plug tests strongly suggests that longitudinal cracking of the trench walls is a very important phenomenon. In the test of the simple 4-inch-long plug (Test 21), the portion of the trench surrounding the plug cracked and expanded with the rest of the trench, providing an open path for the high pressure gas to the back of the short plug. This same phenomenon was seen in the leaky plug test (Test 35) with cracks propagating past the plug base. In the solid plug test (Test 36) the longitudinal cracks stopped at a major circumferential crack at the upstream face of the first bearing rib, allowing the plug to hold and seal the trench. This phenomenon of longitudinal cracking should be considered in future plug and trench designs.

The results of the solid plug test showed that a solid plug can seal the trench at a reflected pressure of at least 800 psi. The results of the leaky plug test showed that for a 600-psi incident pressure (3600 psi reflected) the pressure behind the leaky plug was around 300 psi. To seal the trench at the prescribed 600-psi incident pressure design loading a leaky plug could be connected to a solid plug using a load-limiting, energy-absorbing material of reasonable dimensions.

REFERENCES

1. H. E. Lindberg et al., "Response of Reentry Vehicle-Type Shells to Blast Loads," prepared for Lockheed Missiles and Space Company, Sunnyvale, California, Contract AF 04(694)-655, SRI Project FGD-5228, Stanford Research Institute, Menlo Park, California (30 September 1965).

2. S. J. Ayala et al., "HAVE HOST T-1 Quick Look," Preliminary Report prepared by AFWL/DEP for the Space and Missile Systems Organization (SAMSO), Project 627A, Program Element 63305F under DNA Contract, Subtask H35HAXSX355, Program Element 62710H (25 August 1977).

3. L. Seaman, "SRI PUFF 3 Computer Code for Stress Wave Propagation," prepared for Air Force Weapons Laboratory, Air Force Systems Command, Kirtland AFB, New Mexico, Technical Report No. AFWL-TR-70-51, Stanford Research Institute, Menlo Park, California (September 1970).

4. J. G. Jackson, Jr., Waterways Experiment Station, Vicksburg, Mississippi, "Recommended Calculational Properties for HAVE HOST High-Density Backfill," letter to AFWL, Kirtland AFB, New Mexico (7 July 1977); "Recommended Calculational Properties for HAVE HOST Low-Density Backfill," letter to AFWL, Kirtland AFB, New Mexico (5 April 1977).

Appendix A

TEST SUMMARY

Test No.	Test Type	Nominal Peak Reflected Pressure (psi)	Total Charge	Charge Configuration	Soil Type	Density (lb/ft³)	Water Content (%)	Concrete Compressive Strength (psi)	Concrete Split Cylinder Tension Strength (psi)	Comments
1	Load Calibration	300	100 (gr/ft)	1 strand 100 gr/ft-7 ft centered						
2	Load Calibration	450	200 (gr/ft)	4 strands 50 gr/ft-7 ft outer edge			-	-		
3	Load Calibration	800	400 (gr/ft)	8 strands 50 gr/ft-7 ft outer edge	-	-	-		-	
4	Load Calibration	1600	800 (gr/ft)	4 strands 200 gr/ft-7 ft outer edge		-	-	-	-	
5	Load Calibration	1900	800 (gr/ft)	4 strands 200 gr/ft-11 ft outer edge	-		-	-		
6	Load Calibration	2600	1200 (gr/ft)	6 strands 200 gr/ft-9 ft outer edge	-		-	-	-	
7	Clay Trench Model	50	400 (gr/ft)	4 strands 100 gr/ft-9 ft outer edge	Dolomite	102	0.0	-		[illegible] failed to detonate; pressure from det cord only [illegible]
8	Clay Trench Model	800	400 (gr/ft)	4 strands 100 gr/ft-9 ft outer edge	Dolomite	102	0.0	-		Did not vent
9	Load Calibration	1000	400 (gr/ft)	4 strands 100 gr/ft-9 ft outer edge	-	-	-	-	-	
10	Load Calibration	800	400 (gr/ft)	8 strands 50 gr/ft-11 ft Distributed	-	-	-	-	-	
11	Clay Trench Model	800	400 (gr/ft)	8 strands 50 gr/ft-11 ft Distributed	Monterey Sand	100	0.0	-	-	Did not vent
12	Load Calibration	800	400 (gr/ft)	8 strands 50 gr/ft-11 ft Distributed			-		-	
13	Load Calibration	1600	800 (gr/ft)	8 strands 100 gr/ft-11 ft Distributed		-	-	-	-	
14	Load Calibration	2400	1200 (gr/ft)	8 strands 150 gr/ft-11 ft Distributed		-				
15	Clay Trench Model	800	400 (gr/ft)	8 strands 50 gr/ft-11 ft Distributed	Yuma Soil	118	[illegible]			Flash bulbs did not trigger [illegible] Did not vent
16	Clay Trench Model	1600	[illegible] (gr/ft)	8 strands 100 gr/ft-11 ft Distributed	Yuma Soil	119	[illegible]			Vented when roof displaced 1.2 inches
17	F.R. Concrete Trench Model	800	400 (gr/ft)	8 strands 50 gr/ft-11 ft Distributed	Yuma Soil	122	[illegible]	8000		Vented when roof displaced [illegible] inches
18	F.R. Concrete Trench Model	1600	800 (gr/ft)	8 strands 100 gr/ft-11 ft Distributed	Yuma Soil	[illegible]	[illegible]	[illegible]		Vented when roof displaced 1.1 inches
19	F.R. Concrete Trench Model	1600	800 (gr/ft)	8 strands 100 gr/ft-11 ft Distributed	Yuma Soil	[illegible]	[illegible]	[illegible]	[illegible]	Vented when roof displaced 1.1 inches
20	F.R. Concrete Trench Model	2500	800 (gr/ft)	8 strands 200 gr/ft-11 ft Distributed	Yuma Soil	120	[illegible]	7800		Vented when roof displaced 2.3 inches
21	4" Plug and F.R. Concrete Trench Model	1600	800 (gr/ft)	8 strands 100 gr/ft-11 ft Distributed	Yuma Soil	117	[illegible]	6800	850	Pressure behind plug of [illegible] psi
22	F.R. Concrete Trench Model	4000	1600 (gr/ft)	16 strands 100 gr/ft-11 ft Distributed	Yuma Soil	118	[illegible]	6800	850	Vented when roof displaced 1.9 inches
23	Load Calibration	4000	1600 (gr/ft)	16 strands 100 gr/ft-11 ft Distributed						

PRECEDING PAGE BLANK-NOT FILMED

APPENDIX A (Continued)

TEST SUMMARY

Test No.	Test Type	Nominal Peak Reflected Pressure (psi)	Total Charge	Charge Configuration	Soil Type	Density lb/ft^3	Water Content (%)	Concrete Compressive Strength (psi)	Concrete Split Cylinder Tension Strength (psi)	[illegible]
24	Load Calibration	400	200 (gr/ft)	8 strands 25 gr/ft-11 ft Distributed	-	-	-	-	-	Field test [illegible] [illegible]
25	Load Calibration	6000	3200 (gr/ft)	40 strands 80 gr/ft-11 ft Distributed	-	-	-	-	-	Field test [illegible] [illegible]
26	Load	400	200 (gr/ft)	8 strands 25 gr/ft-11 ft Distributed	-	-	-	-	-	
27	Plug Load Calibration	4500	156 (2)	5-in.-dia. 2.5-in. thick 8-ft standoff	-	-	-	-	-	
28	Plug Load Calibration	3600	156 (2)	5-in.-dia. 2.5-in.-thick 12-ft standoff	-	-	-	-	-	
29	Plug Load Calibration	2600	78 (2)	5-in.-dia. 1.25-in.-thick 8-ft standoff	-	-	-	-	-	
30	F. R. Concrete Trench Model (Ribbed)	400	200 (gr/ft)	8 strands 25 gr/ft-11 ft Distributed	Yuma Soil	126	6.0	8,500	-	[illegible]
31	F. R. Concrete Trench Model	800	400 (gr/ft)	8 strands 50 gr/ft-11 ft Distributed	Yuma Soil	125	6.6	-	-	[illegible]
32	Plug Load Calibration	4500	312 (2)	5-in.-dia. 5-in.-thick 25-ft standoff	-	-	-	-	-	
33	Plug Load Calibration	3600	312 (2)	5-in.-dia. 5-in.-thick 29.5-ft standoff	-	-	-	-	-	
34	Plug Load Calibration	1000	78 (2)	5-in.-dia. 1.25-in.-thick 29.5-ft standoff	-	-	-	-	-	
35	Leaky Plug Test	3600	312 (2)	5-in.-dia. 5.0-in.-thick 29.5-ft. standoff	Yuma Soil	130	9.5	8400	-	400-psi pressure behind plug, [illegible]
[illegible]	Solid Plug Test	800	78 (2)	5-in.-dia. 1.25-in.-thick 29.5-ft standoff	Yuma Soil	128	8.9	12,000	-	[illegible]

Appendix B

DISPLACEMENT DATA

TEST 11 TRENCH EXPANSION - END VIEW

Time (s)	Displacement (in) Soil Surface	Crown	Right Wall	Invert	Left Wall
0.000000	0.00	0.00	0.00	0.00	0.00
.001703	0.00	0.00	0.00	0.00	0.00
.002203	.03	.09	.09	.04	.13
.002504	.07	.19	.23	.17	-
.002804	.23	-	.29	.26	.53
.003105	.43	.66	.48	.40	.65
.003405	.70	1.00	.59	.56	.84
.003706	1.01	1.28	.78	.78	-
.004006	1.36	1.58	.93	.97	-
.004507	2.18	-	-	-	-
.005008	3.43	-	-	-	-
.005308	4.64	-	-	-	-

TEST 15 TRENCH EXPANSION - END VIEW

Time (s)	Displacement (in) Soil Surface	Crown	Right Wall	Invert	Left Wall
0.000000	0.00	0.00	0.00	0.00	0.00
.001869	0.00	0.00	0.00	0.00	0.00
.002150		.11	.05	.13	.12
.002430	.06	.25	.07	.25	.32
.002710	.06	.42	.10	.36	.41
.002991	.33	.59	.26	.53	.54
.003271	.52	.84	.43	.64	.61
.003551	.76	1.13	.56	.77	.62
.003832	1.11	1.44	.59	.95	.87
.004112	1.50	1.85	.76	1.09	.90
.004393	2.02	2.26	.79	1.18	
.004673	2.47		1.05	1.25	

TEST 16 TRENCH EXPANSION - END VIEW

Time (s)	Displacement (in) Soil Surface	Crown	Right Wall	Invert	Left Wall
0.000000	0.00	0.00	0.00	0.00	0.00
.001565	0.00	0.00	0.00	0.00	0.00
.001841	.01	.22	.17	.26	.22
.002117		.48	.55	.61	.44
.002393	.33	.94	.63	.86	.75
.002670	.91		1.08	1.22	1.09
.002946	1.83	1.50		1.48	1.26

TEST 17 TRENCH EXPANSION - END VIEW

Time (s)	Displacement (in) Soil Surface	Crown	Right Wall	Invert	Left Wall
0.000000	0.00	0.00	0.00	0.00	0.00
.001704	0.00	0.00	0.00	0.00	0.00
.002004	-.00	.11	.07	.12	.12
.002305	-.00	.25	.23	.29	.25
.002605	.11	.45	.38	.48	.43
.002906	.33	.70	.53	.68	.57
.003207	.62	1.06	.70	.88	.70
.003507	1.03	1.49	.83	1.09	.86
.003808	1.55	1.99	.99	1.28	.95
.004109	2.21	2.55	1.09	1.39	1.08
.004409			1.18	1.51	1.22
.004710				1.64	1.29
.005011				1.70	1.17
.005311				1.82	1.45
.005612				1.87	1.37

TEST 17 TRENCH CROWN DISPLACEMENT - SIDE VIEW

	Displacement (in)					
Time (s)	Pin 1	Pin 2	Pin 3	Pin 4	Pin 5	Pin 6
0.000000	0.00	0.00	0.00	0.00	0.00	0.00
.001905	0.00	0.00	0.00	0.00	0.00	0.00
.002190	.13	.10	.09	.08	.05	.04
.002476	.30	.26	.21	.18	.15	.11
.002762	.49	.47	.41	.35	.32	.25
.003048	.79	.74	.68	.60	.55	.51
.003333	1.18	1.11	.99	.89	.83	.75
.003619	1.61	1.52	1.38	1.26	1.17	1.12
.003905	2.14	2.02	1.85	1.68	1.55	1.50
.004190	2.77	2.62	2.38	2.18	1.99	1.98
.004476		3.22	2.94	2.65	2.51	2.55
.004762						

Pin 1 - 1 inch from reflecting wall
Pin 2 - 3 inches from reflecting wall
Pin 3 - 5 inches from reflecting wall
Pin 4 - 7 inches from reflecting wall
Pin 5 - 9 inches from reflecting wall
Pin 6 -11 inches from reflecting wall

TEST 17 SOIL SURFACE DISPLACEMENT - SIDE VIEW

	Displacement (in)					
Time (s)	Pin 1	Pin 2	Pin 3	Pin 4	Pin 5	Pin 6
0.000000	0.00	0.00	0.00	0.00	0.00	0.00
.001905	0.00	0.00	0.00	0.00	0.00	0.00
.002190	.00	.00	-.03	.01	-.01	.01
.002476	.14	.10	.09	.11	.05	.08
.002762	.36	.29	.24	.30	.20	.24
.003048	.63	.53	.53	.55	.39	.41
.003333	1.01	.89	.78	.82	.64	.65
.003619	1.44	1.36	1.15	1.13	.95	.92
.003905	1.96	1.83	1.59	1.51	1.33	1.32
.004190		2.42	2.17	2.00	1.83	1.82
.004476				2.57	2.50	2.52
.004762						

Pin 1 - 1 inch from reflecting wall
Pin 2 - 3 inches from reflecting wall
Pin 3 - 5 inches from reflecting wall
Pin 4 - 7 inches from reflecting wall
Pin 5 - 9 inches from reflecting wall
Pin 6 -11 inches from reflecting wall

TEST 18 TRENCH EXPANSION - END VIEW

Time (s)	Displacement (in) Soil Surface	Crown	Right Wall	Invert	Left Wall
0.000000	0.00	0.00	0.00	0.00	0.00
.001473	0.00	0.00	0.00	0.00	0.00
.001572	.00	-.01	-.04	.02	.01
.001670	.02	.08	.05	.02	.07
.001768	.02	.11	.13	.13	.15
.001866	.01	.17	.18	.23	.20
.001965	-.01	.25	.22	.28	.28
.002063	.01	.32	.32	.35	.32
.002161	.03	.38	.38	.44	.40
.002259	.10	.51	.46	.50	.45
.002358	.16	.61	.56	.60	.53
.002456	.28	.76		.65	.62
.002554	.41			.80	.69
.002652	.54			.85	.78
.002750	.76			.85	.86
.002849	.87			.98	.90
.002947	1.14			1.11	1.00

TEST 18 TRENCH CROWN DISPLACEMENT - SIDE VIEW

	Displacement (in)					
Time (s)	Pin 1	Pin 2	Pin 3	Pin 4	Pin 5	Pin 6
0.000000	0.00	0.00	0.00	0.00	0.00	0.00
.001543	0.00	0.00	0.00	0.00	0.00	0.00
.001639	.02	.03	.01	.03	.04	.02
.001736	.06	.06	.03	.05	.05	.02
.001832	.10	.10	.06	.07	.07	.05
.001928	.16	.15	.10	.09	.08	.05
.002025	.23	.19	.13	.13	.13	.07
.002121	.30	.28	.20	.20	.19	.12
.002218	.40	.39	.28	.27	.23	.17
.002314	.49	.47	.36	.33	.29	.22
.002411	.61	.58	.47	.44	.38	.29
.002507	.76	.71	.58	.54	.46	.37
.002603	.91	.83	.67	.64	.55	.47
.002700	1.08	1.00	.80	.75	.66	.58
.002796	1.27	1.18	.95	.88	.78	.67
.002893	1.49	1.40	1.08	1.02	.92	.83
.002989		1.58	1.22	1.18	1.03	.94
.003086			1.38	1.35	1.17	1.11
.003182				1.52	1.30	1.24
.003278					1.43	1.40
.003375					1.59	1.57
.003471						1.77

Pin 1 - 1 inch from reflecting wall
Pin 2 - 3 inches from reflecting wall
Pin 3 - 5 inches from reflecting wall
Pin 4 - 7 inches from reflecting wall
Pin 5 - 9 inches from reflecting wall
Pin 6 -11 inches from reflecting wall

TEST 18 SOIL SURFACE DISPLACEMENT - SIDE VIEW

	Displacement (in)					
Time (s)	Pin 1	Pin 2	Pin 3	Pin 4	Pin 5	Pin 6
0.000000	0.00	0.00	0.00	0.00	0.00	0.00
.001543	0.00	0.00	0.00	0.00	0.00	0.00
.001639	-.03	.01	.01	.11	.01	-.03
.001736	.05	.01	.01	.03	.01	-.02
.001832	-.03	-.00	.01	.06	.01	-
.001928	.03	.02	.02	.12	-.00	-.01
.002025	.05	.06	.07	.15	.01	-.03
.002121	.16	.14	.14	.19	.05	0.01
.002218	.26	.22	.22	.26	.11	.12
.002314	.33	.36	.36	.29	.18	.12
.002411	.48	.43	.41	.46	.24	.24
.002507	____	.64	.53	.56	.32	.25
.002603	____	.76	.63	.68	.37	.28
.002700	____	.79	.78	.80	.48	.42
.002796	____	1.04	.92	.90	.66	.50
.002893	____	1.22	1.18	1.14	.79	.64
.002989	____	____	____	1.30	.94	.81
.003086	____	____	____	1.56	1.13	.97
.003182	____	____	____	____	1.45	1.12
.003278	____	____	____	____	____	1.34
.003375	____	____	____	____	____	1.79
.003471	____	____	____	____	____	____

Pin 1 - 1 inch from reflecting wall
Pin 2 - 3 inches from reflecting wall
Pin 3 - 5 inches from reflecting wall
Pin 4 - 7 inches from reflecting wall
Pin 5 - 9 inches from reflecting wall
Pin 6 -11 inches from reflecting wall

TEST 19 TRENCH EXPANSION - END VIEW

Time (s)	Displacement (in) Soil Surface	Crown	Right Wall	Invert	Left Wall
0.000000	0.00	0.00	0.00	0.00	0.00
.001382	0.00	0.00	0.00	0.00	0.00
.001481	.02	.02	.03	.02	0.00
.001579	.01	.05	.07	.07	.05
.001678	.04	.12	.10	.12	.12
.001777	.02	.17	.16	.25	.16
.001875	.01	.24	.22	.33	.23
.001974	.01	.33	.31	.42	.30
.002073	.04	.42	.37	.53	.38
.002172	.11	.53	.48	.64	.46
.002270	.20	.66	.59	.76	.55
.002369	.31	.80	.65	.83	.59
.002468	.47		.71	.94	.70
.002566	.66		.80	1.03	
.002665	1.03		.88	1.15	
.002764			.91	1.25	
.002863			1.01	1.36	
.002961			1.10	1.43	
.003060			1.14	1.52	

TEST 19 TRENCH CROWN DISPLACEMENT - SIDE VIEW

	Displacement (in)					
Time (s)	Pin 1	Pin 2	Pin 3	Pin 4	Pin 5	Pin 6
0.000000	0.00	0.00	0.00	0.00	0.00	0.00
.001517	0.00	0.00	0.00	0.00	0.00	0.00
.001612	.00	.02	.01	.01	.01	.00
.001706	.05	.04	.01	.00	.02	-.01
.001801	.08	.08	.03	.04	.04	.01
.001896	.14	.13	.07	.06	.07	.02
.001991	.22	.18	.12	.09	.09	.04
.002086	.28	.25	.19	.14	.12	.08
.002181	.39	.35	.27	.22	.18	.12
.002275	.50	.47	.37	.31	.25	.17
.002370	.63	.59	.49	.41	.35	.24
.002465	.78	.72	.60	.51	.43	.31
.002560	.96	.87	.74	.64	.54	.40
.002655	1.20	1.01	.89	.77	.65	.49
.002749	1.46	1.17	1.04	.91	.78	.62
.002844	1.70	1.32	1.21	1.08	.93	.73
.002939		1.48	1.33	1.26	1.07	.84
.003034			1.48	1.46	1.25	.94
.003129				1.67	1.40	1.06
.003223				1.85	1.50	1.20

Pin 1 - 1 inch from reflecting wall
Pin 2 - 3 inches from reflecting wall
Pin 3 - 5 inches from reflecting wall
Pin 4 - 7 inches from reflecting wall
Pin 5 - 9 inches from reflecting wall
Pin 6 -11 inches from reflecting wall

TEST 19 SOIL SURFACE DISPLACEMENT - SIDE VIEW

Displacement (in)

Time (s)	Pin 1	Pin 2	Pin 3	Pin 4	Pin 5	Pin 6
0.000000	0.00	0.00	0.00	0.00	0.00	0.00
.001517	0.00	0.00	0.00	0.00	0.00	0.00
.001612	.05	.01	.01	.00	.00	.02
.001706	.03	.01	.03	.01	-.01	.04
.001801	.03	.02	.02	.00	.03	.04
.001896	.04	.03	.05	.06	.04	.00
.001991	.10	.05	.08	.06	.06	.03
.002086	.14	.09	.09	.06	.09	.06
.002181	.24	.19	.17	.14	.13	.05
.002275	.34	.28	.27	.22	.20	.10
.002370	.48	.39	.37	.33	.27	.18
.002465	.64	.52	.48	.43	.35	.24
.002560	.94	.69	.61	.54	.46	.35
.002655	1.28	.91	.74	.67	.57	.44
.002749		1.12	.95	.83	.70	.56
.002844		1.50	1.26	1.04	.85	.61
.002939			1.72	1.32	1.00	.79
.003034						1.05
.003129						1.39

Pin 1 - 1 inch from reflecting wall
Pin 2 - 3 inches from reflecting wall
Pin 3 - 5 inches from reflecting wall
Pin 4 - 7 inches from reflecting wall
Pin 5 - 9 inches from reflecting wall
Pin 6 -11 inches from reflecting wall

TEST 20 TRENCH EXPANSION - END VIEW

Time (s)	Displacement (in) Soil Surface	Crown	Right Wall	Invert	Left Wall
0.000000	0.00	0.00	0.00	0.00	0.00
.001460	0.00	0.00	0.00	0.00	0.00
.001557	.04	.04	.06	.08	.07
.001654	.03	.07	.12	.13	.15
.001751	.04	.12	.17	.21	.21
.001849	.09	.18	.25	.31	.27
.001946	.12	.25	.30	.41	.32
.002043	.20	.37	.35	.52	.43
.002141	.30	.48	.48	.65	.51
.002238	.41	.61	.54	.77	.59
.002335	.51	.74	.61		.66
.002433	.62			.98	.75
.002530	.80				.85
.002627	.96				.92
.002725	1.19				.98
.002822	1.35				1.00
.002919	1.58				1.09
.003016	1.81				1.16
.003114	2.12				1.23
.003211	2.36				1.28
.003308	2.58				1.34

TEST 20 SOIL SURFACE DISPLACEMENT - SIDE VIEW

	Displacement (in)		
Time (s)	Pin 1	Pin 2	Pin 3
0.000000	0.00	0.00	0.00
.001608	0.00	0.00	0.00
.001703	0.00	0.00	.01
.001797	.01	.02	.03
.001892	.06	.04	.06
.001987	.11	.10	.09
.002081	.21	.17	.14
.002176	.27	.22	.20
.002270	.39	.31	.27
.002365	.61	.50	.42
.002460	.75	.63	.54
.002554	.90	.76	.64
.002649	1.08	.92	.77
.002743	1.28	1.11	.93
.002838	1.49	1.32	1.07
.002933	1.74	1.62	1.29
.003027	2.03	1.94	1.53
.003122	2.34	2.34	1.82

Pin 1 - 3 inches from reflecting wall
Pin 2 - 6 inches from reflecting wall
Pin 3 - 9 inches from reflecting wall

TEST 21 TRENCH EXPANSION - END VIEW

Time (s)	Displacement (in) Soil Surface	Crown	Right Wall	Invert	Left Wall
0.000000	0.00	0.00	0.00	0.00	0.00
.001706	0.00	0.00	0.00	0.00	0.00
.001801	.00	.03	.02	.02	-.01
.001896	.00	.02	.03	.09	.06
.001991	.02	.04	.08	.15	.10
.002086	.02	.09	.18	.20	.17
.002180	.02	.16	.22	.28	.24
.002275	.04	.26	.30	.32	.32
.002370	.12	.35	.38	.44	.36
.002465	.15	.40	.44	.49	.51
.002559	.24	.52		.65	.57
.002654	.34	.62			.62
.002749	.47	.74			
.002844	.60				
.002939	.79				
.003033	.94				
.003128	1.14				
.003223	1.37				
.003318	1.54				
.003413	1.79				
.003507	1.99				
.003602	2.27				

TEST 21 TRENCH CROWN DISPLACEMENT - SIDE VIEW

	Displacement (in)					
Time (s)	Pin 1	Pin 2	Pin 3	Pin 4	Pin 5	Pin 6
0.000000	0.00	0.00	0.00	0.00	0.00	0.00
.001397	0.00	0.00	0.00	0.00	0.00	0.00
.001491	.01	0.00	0.00	0.00	0.00	0.00
.001584	.01	0.00	.06	.01	0.00	.03
.001677	.01	.03	.10	.03	.03	.04
.001770	0.00	.06	.16	.10	.09	.10
.001863	0.00	.10	.20	.15	.13	.14
.001956	.03	.16	.26	.22	.18	.18
.002050	.10	.24	.34	.30	.25	.24
.002143	.15	.32	.44	.42	.36	.35
.002236	.21	.41	.55	.52	.45	.43
.002329	.28	.50	.65	.62	.55	.50
.002422	.38	.63	.80	.77	.68	.63
.002515	.52	.77	.95	.92	.81	.74
.002609	.63	.91	1.11	1.08	.95	.87
.002702	.74	1.05	1.27	1.25	1.10	1.00
.002795	.88	1.21	1.47	1.44	1.24	1.13
.002888	1.03	1.41	1.66	1.65	1.41	1.27
.002981	1.21	1.59	1.86	1.85	1.56	1.42
.003074	1.40	1.80	2.09	2.08	1.74	1.57
.003168	1.56	1.97	2.31	2.28	1.92	1.74
.003261	1.79	2.20	2.55	2.53	2.12	1.96
.003354	2.00	2.41	2.78	2.75	2.31	2.15

Pin 1 - over plug (3 inches back from plug face)
Pin 2 - over plug (1 inch back from plug face)
Pjn 3 - 1 inch from plug face
Pin 4 - 3 inches from plug face
Pin 5 - 5 inches from plug face
Pin 6 - 7 inches from plug face

TEST 21 SOIL SURFACE DISPLACEMENT - SIDE VIEW

	Displacement (in)					
Time (s)	Pin 1	Pin 2	Pin 3	Pin 4	Pin 5	Pin 6
0.000000	0.00	0.00	0.00	0.00	0.00	0.00
.001397	0.00	0.00	0.00	0.00	0.00	0.00
.001491	.02	.02	.02	0.00	0.00	0.00
.001584	.03	.02	.02	.02	0.00	0.00
.001677	.03	.02	.02	.00	0.00	.03
.001770	.06	.02	.03	.03	.01	.08
.001863	.03	.01	.06	.06	.02	.13
.001956	.00	.00	.12	.15	.08	.15
.002050	.05	.06	.22	.25	.19	.24
.002143	.10	.12	.33	.39	.27	.30
.002236	.15	.21	.41	.49	.35	.39
.002329	.26	.30	.47	.63	.41	.53
.002422	.37	.39	.69	.82	.59	.60
.002515	.49	.56	.79	.93	.69	.71
.002609	.63	.65	1.01	1.15	.76	.82
.002702	.72	.78	1.11	1.23	.88	.97
.002795	.84	.91	1.29	1.44	1.05	1.10
.002888	.96	1.17	1.47	1.62	1.22	1.25
.002981	1.22	1.36	1.59	1.78	1.35	1.33
.003074	1.50	1.63	1.86	2.04	1.58	1.56
.003168	1.46	1.76	2.08	2.25	1.84	1.84

Pin 1 - over plug (3 inches back from plug face)
Pin 2 - over plug (1 inch back from plug face)
Pin 3 - 1 inch from plug face
Pin 4 - 3 inches from plug face
Pin 5 - 5 inches from plug face
Pin 6 - 7 inches from plug face

TEST 22 TRENCH EXPANSION - END VIEW

	Displacement (in)				
Time (s)	Soil Surface	Crown	Right Wall	Invert	Left Wall
0.000000	0.00	0.00	0.00	0.00	0.00
.001143	0.00	0.00	0.00	0.00	0.00
.001238	0.00	0.00	0.00	0.00	0.00
.001333	.04	.06	.01	.08	.07
.001429	.05	.15	.12	.20	.13
.001524	.05	.25	.24	.34	.29
.001619	.05	.30	.27	.46	.34
.001714	.07				
.001810	.13				
.001905	.24				
.002000	.37				
.002095	.58				
.002190	.76				
.002286	1.04				

TEST 22 TRENCH CROWN DISPLACEMENT - SIDE VIEW

	Displacement (in)		
Time (s)	Pin 1	Pin 2	Pin 3
0.000000	0.00	0.00	0.00
.001308	0.00	0.00	0.00
.001402	0.00	0.00	.02
.001495	.03	.03	.06
.001589	.05	.03	.01
.001682	.15	.09	.08
.001776	.22	.17	.13
.001869	.34	.25	.17
.001963	.45	.32	.26
.002056	.62	.48	.41
.002150	.75	.59	.50
.002243	.93	.71	.57
.002336	1.12	.87	.74
.002430	1.33	1.06	.89
.002523	1.53	1.22	1.06
.002617		1.40	1.25
.002710		1.56	1.46
.002804			1.71
.002897			1.92

Pin 1 - 3 inches from reflecting wall
Pin 2 - 6 inches from reflecting wall
Pin 3 - 9 inches from reflecting wall

TEST 22 SOIL SURFACE DISPLACEMENT - SIDE VIEW

	Displacement (in)		
Time (s)	Pin 1	Pin 2	Pin 3
0.000000	0.00	0.00	0.00
.001308	0.00	0.00	0.00
.001402	.02	.01	.03
.001495	.03	.03	.03
.001589	.00	0.00	-.05
.001682	.02	.00	-.03
.001776	.07	.07	.01
.001869	.18	.12	.05
.001963	.27	.21	.08
.002056	.46	.36	.23
.002150	.59	.47	.30
.002243	.75	.58	.40
.002336	.99	.72	.46
.002430	1.24	.93	.63
.002523	1.66	1.13	.78
.002617		1.35	.95
.002710		1.65	1.18
.002804			1.45
.002897			1.72

Pin 1 - 3 inches from reflecting wall
Pin 2 - 6 inches from reflecting wall
Pin 3 - 9 inches from reflecting wall

Appendix C

FABRICATION OF TRENCH MODELS

The Air Force Weapons Laboratory (AFWL) provided drawings of the half-scale AFWL models from which dimensions for our 6-inch-ID (1/26-scale) trench models were determined. Most of the expansion and venting tests were performed using 6-inch-ID fiber-reinforced concrete trench models fabricated without internal ribs. One expansion and venting test and two of the plug tests were performed with fiber-reinforced concrete models fabricated with internal ribs.

The formula used for the riber-reinforced concrete was similar to that used by AFWL for its 13-inch-diameter model. The mixture contains 31.8% cement (by weight), 25.1% No. 20 sand, 25.1% No. 60 sand, 1.7% steel fiber (U.S. Steel Fibercon), 16.3% water, and a trace of CFR2 (0.1%). A Type III cement was used to give a 14-day cure time. Unconfined compression tests (ASTM C39-64) performed on 3-inch-diameter, 6-inch-long samples of the mixture after 14 days gave compressive strengths between 6600 and 8400 psi (7400-psi average).

The method for fabricating the trench models without ribs was as follows: Two coaxial thin-walled Plexiglass tubes formed the mold for the trench wall. The tubes were held in alignment by fixtures at the top and bottom; the end fixtures were held together with a threaded rod down the center. The concrete was poured through openings in the top end fixture. Since the concrete mixture was relatively dry, we found it necessary to place the concrete mix in a vacuum chamber (approximately 30 torr) for a few minutes after pouring it into the mold to remove trapped air bubbles. Use of a shake table to remove trapped air and facilitate proper settling of the concrete mix was discontinued early in the project because it tended to settle the steel fiber to the bottom of the mold. After approximately 18 hours of curing in the mold, the

end fixtures were removed and the Plexiglass tubes were withdrawn from the trench in a hydraulic press. The trenches were then cured in water for 14 days. After curing, the roof sections were sawed out. Typically, the dimensions of the trench models were held to within ±0.010 inch.

The method of fabricating a ribbed trench model was similar. Segmented rings were attached to the Plexiglass tubes that formed the inside trench wall. The rings were attached using screws from the inside of the tube. After the concrete had cured for 18 hours, the screws were removed and the tubes were withdrawn as before. The segmented rings were then removed one at a time.

Our ribbed trenches were made using the alternative thin-wall design (10-inch-thick-wall, full-scale). The baseline trench design is for a 17-inch-thick wall, full-scale. The thin-wall design specifies a 9000 to 10,000 psi concrete strength. To achieve this high strength without sacrificing concrete fluidity, we added a fluidizing agent (Melment) to the mix and lowered the percentage of water to 10%. This mix gave a compressive strength of 12,500 psi, higher than desired. In future mixes, a water content of around 13% is suggested to achieve 9000 to 10,000 psi concrete strength.

DISTRIBUTION LIST

DEPARTMENT OF DEFENSE

Assistant to the Secretary of Defense
Atomic Energy
ATTN: Executive Assistant

Defense Advanced Rsch Proj Agency
ATTN: TIO

Defense Intelligence Agency
ATTN: RDS-3A

Defense Nuclear Agency
ATTN: SPSS, G. Ullrich
ATTN: SPSS, T. Deevy
4 cy ATTN: TITL

Defense Technical Information Center
12 cy ATTN: DD

Field Command
Defense Nuclear Agency
ATTN: FCPR
ATTN: FCTMD

Field Command
Defense Nuclear Agency
Livermore Branch
ATTN: FCPRL

Joint Strat Tgt Planning Staff
ATTN: NRI-STINFO Library
ATTN: XPFS

Undersecretary of Def for Rsch & Engrg
ATTN: Strategic & Space Systems (OS)

DEPARTMENT OF THE ARMY

BMD Advanced Technology Center
Department of the Army
ATTN: ATC-T

BMD Systems Command
Department of the Army
ATTN: BMDSC-HW

Chief of Engineers
Department of the Army
ATTN: DAEN-MPE-T, D. Reynolds

Harry Diamond Laboratories
Department of the Army
ATTN: DELHD-I-TL
ATTN: DELHD-N-P

U.S. Army Ballistic Research Labs
ATTN: DRDAR-BLT, J. Keefer
ATTN: DRDAR-TSB-S

U.S. Army Cold Region Res Engr Lab
ATTN: Library

U.S. Army Construction Engrg Res Lab
ATTN: Library

U.S. Army Engineer Center
ATTN: Technical Library

U.S. Army Material & Mechanics Rsch Ctr
ATTN: Technical Library

DEPARTMENT OF THE ARMY (Continued)

U.S. Army Engr Waterways Exper Station
ATTN: WESSD, J. Jackson
ATTN: J. Zelasko
ATTN: Library
ATTN: WESSA, W. Flathau

U.S. Army Materiel Dev & Readiness Cmd
ATTN: DRXAM-TL

U.S. Army Nuclear & Chemical Agency
ATTN: J. Simms
ATTN: Library

DEPARTMENT OF THE NAVY

Naval Construction Battalion Center
ATTN: Code L53, J. Forrest
ATTN: Code L08A
ATTN: Code L51, J. Crawford

Naval Postgraduate School
ATTN: G. Lindsay
ATTN: Code 1424 Library

Naval Research Laboratory
ATTN: Code 2627
ATTN: Code 4040, J. Boris

Naval Surface Weapons Center
ATTN: Code F31
ATTN: Code X211
ATTN: R44, H. Glaz

Naval Surface Weapons Center
ATTN: Tech Library & Info Svcs Br

DEPARTMENT OF THE AIR FORCE

Air Force Institute of Technology
ATTN: Library

Air Force Systems Command
ATTN: DLWM

Air Force Weapons Laboratory
Air Force Systems Command
ATTN: NTE, M. Plamondon
ATTN: NTES-G
ATTN: SUL
ATTN: NTYV, D. Payton
ATTN: NTED-1
ATTN: NTED-A
ATTN: NTES-S
ATTN: NTEO
ATTN: DEY

Assistant Chief of Staff
Intelligence
ATTN: IN

Assistant Secretary of the Af
Research, Development & Logistics
ATTN: SAFALR/DEP for Strat & Space Sys

Ballistic Missile Office
Air Force Systems Command
ATTN: MNNXH, D. Gage
ATTN: MNN, W. Crabtree
ATTN: MNNXH, M. Delvecchio

DEPARTMENT OF THE AIR FORCE (Continued)

Strategic Air Command
ATTN: J. McKinney

Deputy Chief of Staff
Research, Development, & Acq
ATTN: AFRDQI, N. Alexandrow
ATTN: AFRDQI
ATTN: AFRDPN
ATTN: AFRDQA

Strategic Air Command
ATTN: XPFS
ATTN: NRI-STINFO Library

Vela Seismology Center
ATTN: G. Ullrich

OTHER GOVERNMENT AGENCY

Central Intelligence Agency
ATTN: OSWR/NED

DEPARTMENT OF ENERGY CONTRACTORS

Lawrence Livermore National Lab
ATTN: D. Glenn

Los Alamos National Scientific Lab
ATTN: C. Keller
ATTN: R. Sanford

Sandia National Lab
ATTN: ORG 1250, W. Brown
ATTN: A. Chabai

DEPARTMENT OF DEFENSE CONTRACTORS

Acurex Corp
ATTN: K. Triebes
ATTN: J. Stockton
ATTN: C. Wolf

Aerospace Corp
ATTN: Technical Information Services
ATTN: H. Mirels

Agbabian Associates
ATTN: M. Agbabian

Applied Research Associates, Inc
ATTN: J. Bratton
ATTN: H. Auld
ATTN: N. Higgins

Applied Theory, Inc
2 cy ATTN: J. Trulio

Artec Associates, Inc
ATTN: S. Gill

Astron Research & Engineering
ATTN: J. Huntington

Boeing Co
ATTN: Aerospace Library
ATTN: S. Strack

Weidlinger Assoc., Consulting Engineers
ATTN: I. Sandler

DEPARTMENT OF DEFENSE CONTRACTORS (Continued)

California Research & Technology, Inc
ATTN: Library
ATTN: M. Rosenblatt

University of Denver
ATTN: J. Wisotski

Eric H. Wang
Civil Engineering Rsch Fac
University of New Mexico
ATTN: P. Lodde
ATTN: J. Lamb
ATTN: J. Kovarna

General Electric Company—TEMPO
ATTN: DASIAC

H-Tech Labs, Inc
ATTN: B. Hartenbaum

IIT Research Institute
ATTN: Documents Library

J.H. Wiggins Co., Inc
ATTN: J. Collins

Kaman AviDyne
ATTN: R. Ruetenik

Kaman Sciences Corp
ATTN: D. Sachs

Martin Marietta Corp
ATTN: G. Freyer

McDonnell Douglas Corp
ATTN: D. Dean
ATTN: R. Halprin

Merritt Cases, Inc
ATTN: Library

Mission Research Corp
ATTN: C. Longmire
ATTN: G. McCartor

Nathan M. Newmark Consult Eng Svcs
ATTN: W. Hall
ATTN: N. Newmark

Pacific-Sierra Research Corp
ATTN: H. Brode

Pacifica Technology
ATTN: Tech Library

Patel Enterprises, Inc
ATTN: M. Patel

Physics International Co
ATTN: J. Thomsen
ATTN: F. Sauer
ATTN: Technical Library

Science Applications, Inc
ATTN: D. Hove

Weidlinger Assoc., Consulting Engineers
ATTN: J. Isenberg

DEPARTMENT OF DEFENSE CONTRACTORS (Continued)

R & D Associates
ATTN: Technical Information Center
ATTN: J. Lewis
ATTN: A. Kuhl
ATTN: R. Port
ATTN: J. Carpenter
ATTN: P. Haas

Science Applications, Inc
ATTN: R. Schlaug
ATTN: H. Wilson
ATTN: Technical Library

Science Applications, Inc
ATTN: J. Cockayne
ATTN: W. Layson
ATTN: B. Chambers III

SRI International
ATTN: J. Colton
ATTN: G. Abrahamson
ATTN: Library
ATTN: D. Johnson

Systems, Science & Software, Inc
ATTN: Library
ATTN: J. Barthel
ATTN: K. Pyatt
ATTN: C. Dismikes

DEPARTMENT OF DEFENSE CONTRACTORS (Continued)

Systems, Science & Software, Inc
ATTN: J. Murphy

Systems, Science & Software, Inc
ATTN: C. Hastings

Teledyne Brown Engineering
ATTN: J. McSwain

Terra Tek, Inc
ATTN: Library
ATTN: A. Abou-Sayed

TRW Defense & Space Sys Group
ATTN: Technical Information Center
ATTN: T. Mazzola
ATTN: N. Lipner

TRW Defense & Space Sys Group
ATTN: P. Dai
ATTN: G. Hulcher
ATTN: E. Wong

Systems, Science & Software, Inc
ATTN: C. Needham

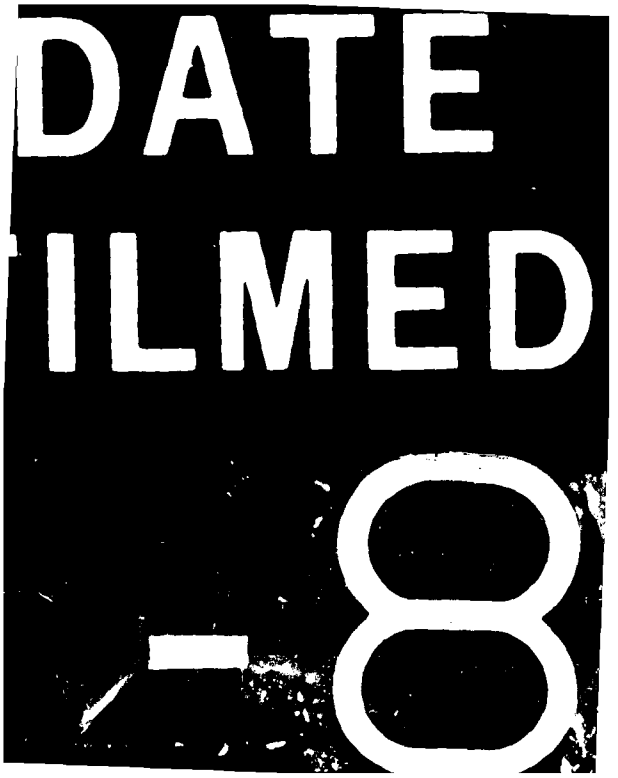
DATE
ILMED
-8